Measurement of wide-angle elastic scattering of pions and protons off protons

K. A. Jenkins* and L. E. Price†
Columbia University, New York, New York 10027

R. Klem, R. J. Miller,‡ and P. Schreiner
Argonne National Laboratory, Argonne, Illinois 60439

M. L. Marshak, E. A. Peterson, and K. Ruddick
University of Minnesota, Minneapolis, Minnesota 55455

(Received 13 November 1979)

A comprehensive measurement of the differential cross section for $\pi^{\pm}p$ and pp elastic scattering has been made at large center-of-mass angles. $\pi^{-}p$ and pp scattering were measured with incident laboratory momenta ranging from 2 to 9.5 GeV/c. $\pi^{+}p$ scattering was measured with momenta from 2 to 6.3 GeV/c. Scattering angles were in the range $-0.3 \lesssim \cos\theta_{\text{c.m.}} \lesssim 0.4$. The results of the experiment are compared to constituent models and statistical models.

I. INTRODUCTION

Large-momentum-transfer scattering processes have had an important role in providing information about the structure of hadrons. Inelastic lepton scattering, Drell-Yan production of lepton pairs, electron-positron annihilation to hadrons, and inclusive hadrons from hadron collisions, all with $|q^2| > 1$ GeV^2 form the main body of experimental data on which the quark-parton model rests. High-quality elastic-scattering data for electrons and protons from protons also exist and generally support the model. Notably lacking have been detailed measurements of pion-proton elastic scattering at large momentum transfers, except for the region near $\theta_{\text{c.m.}} = 180°$ where coherent processes dominate. The pion-proton channels are particularly interesting because of the presence of resonances and the resulting opportunity to compare the data with predictions of statistical models as well as constituent models of hadron scattering.

This paper reports the results from an experiment which measured large-angle elastic scattering of positive and negative pions and protons from protons with high statistics and good resolution in both s (square of c.m. energy) and t (four-momentum transfer squared). Measurements were made for the range of incident laboratory momenta from 2 to 9.5 GeV/c (to 6.3 GeV/c for π^{+}) and for $\cos\theta_{\text{c.m.}}$ from -0.3 to $+0.4$. The angular range was chosen to be well away from the forward and backward peaks in the differential cross section. Figure 1 shows the kinematic region covered by this experiment.

It has been shown by Brodsky and Farrar[1] and by Matveev *et al.*[2] that models with fermion constituents in general lead to the dimensional-counting rule, which predicts that $d\sigma/dt \propto s^{-n}$, where n is predictable. The data presented here allow the first sensitive test of the rule for $\pi^{\pm}p$ elastic scattering. They also allow a search for the effects of large numbers of resonances as predicted by statistical models. We have looked especially for evidence of Ericson fluctuations, as discussed by Frautschi[3] in analogy with nuclear physics.

In Sec. II of this paper we present a short discussion of the theoretical predictions. The details of the experimental method are given in Sec. III. Section IV contains discussion of the results and comparison with models. Partial results from this experiment have been published earlier.[4]

II. THEORETICAL MODELS

A. Constituent models

1. Dimensional-counting rule

Brodsky and Farrar[1] and Matveev *et al.*[2] have shown that in a two-body collision $a + b \to c + d$, the

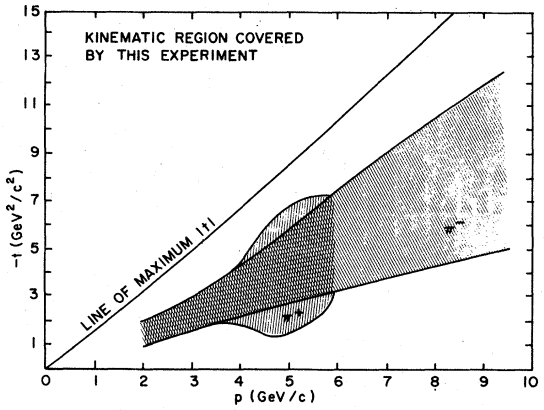

FIG. 1. The approximate kinematic region covered by the pion-proton data of this experiment.

differential cross section should have the following asymptotic form for large s and t:

$$\frac{d\sigma}{dt}=f(t/s)s^{-n},$$

where $n=n_a+n_b+n_c+n_d-2$, and n_i = number of fermion constituents in particle i. The rule is derived from dimensional arguments and a scaling hypothesis that the constituents are asymptotically free and have negligible mass. Thus at fixed t/s, $d\sigma/dt$ should fall with energy as a simple power of s. When s and t are large, fixing t/s is equivalent to fixing the c.m. scattering angle.

Sivers[5] has compiled the results of previous tests of the rule, as shown in Table I. The agreement quoted by Sivers appears to be good. In fact, though, the errors on the exponents are large and the agreement is far from conclusive. The pion-proton case is based on very few points, with large statistical errors.[6] The proton-proton case, while based on many more data points, is not consistent[7] with a pure s^{-n} power law. Our data supplement the existing proton-proton data and provide enough new pion-production data to make possible a stringent test of the rule.

2. *Constituent-interchange model*

In the constituent-interchange model (CIM) of Gunion, Brodsky, and Blankenbecler,[8] scattering proceeds not by quark-quark scattering, but by the interchange of quarks in the scattering process. Because the model provides a method of calculation, its predictions are more detailed but include the dimensional-counting rule.

The model makes specific predictions for the angular structure in pion-proton elastic scattering. With $z=\cos\theta_{\text{c.m.}}$,

$$\frac{d\sigma}{dt}(\pi^+p\to\pi^+p)=\frac{\sigma_0}{s^8}\frac{1+z}{(1-z)^4}\left(\frac{4\alpha}{(1+z)^2}+\beta\right)^2,$$

$$\frac{d\sigma}{dt}(\pi^-p\to\pi^-p)=\frac{\sigma_0}{s^8}\frac{1+z}{(1-z)^4}\left(\frac{4\beta}{(1+z)^2}+\alpha\right)^2,$$

where α and β are measures of the (st) and (ut) scattering amplitudes. The standard quark configuration corresponds to $\alpha=2$ and $\beta=1$. The angular functions are independent of energy. Gunion *et al.* claim agreement with this formula in the data of Owen *et al.*[6]

3. *Quark-rearrangement model*

Fishbane and Quigg[9] have proposed that such detailed predictions as we have just discussed are premature; operating in the same spirit as dimensional arguments, they propose tests of quark-parton ideas based on a quark-rearrangement scheme.

In the reaction $a+b\to c+d$, they picture the hadrons a and b dissociating into their constituent quarks. The constituents are then regarded "as marbles in an urn which may be drawn out in many ways to form the accessible states." The cross section is then proportional to the number of distinct ways the constituents (of a and b) can be combined to form c and d. Assuming the standard quark picture, this counting leads to simple predictions for baryon-baryon scattering. For example, $pp\to pp$ is proportional to $12B^2$, and $np\to np$ to $9B^2$, where the 12 and 9 comes from counting the ways the quark pool can be distributed, and B^2 is an association probability, assumed independent of the particular mechanism. Thus they predict

$$\frac{d\sigma/dt(pp\to pp)}{d\sigma/dt(pn\to pn)}=\frac{12}{9}$$

at large angles and energies. They claim experiments are consistent with this prediction. In meson-baryon scattering, the possibility of quark-antiquark annihilation and creation complicates the method, but they are able to arrive at a number of predictions. With the additional assumption that up and down quarks annihilate equally probably and have equal probability for forming pairs of any combination, Fishbane and Quigg predict that the ratio of the π^+p elastic-scattering cross section to that of π^-p is equal to 1.5.

B. Statistical models

A quite different explanation of wide-angle scattering is found in statistical models. In these

TABLE I. Previous fits to $d\sigma/dt$ (90° c.m.) from Ref. 5.

	$n=n_a+n_b+n_c+n_d-2$	Measured n	s range (GeV^2)
$\gamma N\to\pi N$	7	7.3±0.3	7.9–11.4
$K^+p\to K^+p$	8	7 ±1	4 –13
$\pi^-p\to\pi^-p$	8	8 ±1	4 –17
$\pi^+p\to\pi^+p$	8	7 ±1	4 –12
$pp\to pp$	10	9.7±0.5	6.3–37

models, a hadronic collision causes the particles to lose part of their energy to internal excitation of an intermediate state. The intermediate state comes into "thermodynamic" equilibrium and "boils off" hadrons in proportion to phase space.

In specific models, different assumptions are made as to what it is that is excited, but all the models require some sort of constituents which, when excited, appear as hadronic levels. In contrast to the parton model discussed in the previous section, these models do *not* assume that the constituents are essentially unbound. Frautschi[10] has argued that three popular theories (the "bag" model, the quark model, and the statistical bootstrap) are equivalent in the prediction that the density of states has the form $\rho(m) \propto e^{m/t_0}$, where $m = \sqrt{s}$ and that, therefore, statistical effects are to be expected.

Resonances occur in both $\pi^+ p$ and $\pi^- p$ states and are typically 100 to 200 MeV wide at low mass, while approximately 400 MeV wide at the highest observed mass. From the lowest $\Delta(1238)$, there are an increasing number of resonances up to masses of about 2 GeV but only a few between 2 and 3 GeV. About that, there are no well established resonances. The highest-mass resonances are exceedingly difficult to observe because the level separation is comparable to the width of the resonances.

However, it is argued by Ericson[11] and Frautschi that such a situation still leads to observable structure. Using statistical ideas, and making an analogy with nuclear physics, they predict "Ericson fluctuations" in hadronic collisions. In this picture, elastic scattering proceeds through a number n of overlapping resonances such that on average, $n = \rho(m)\Gamma$, where Γ is the width of a typical resonance. At a nearby energy where $\Delta m > \Gamma$, an independent set of resonances is excited which differs from the first set in number, phases, partial widths, and angular momenta. Thus as a function of energy, there will be fluctuations in the total cross section and stronger fluctuations in the angular distribution because of the changing mix of angular momenta. In general, there will also be a nonstatistical component in the cross section due to diffraction or other coherent processes. The amplitude can be written as the sum $A = A_C + A_F$, where A_C is the coherent part and A_F the fluctuating part of the amplitude. In a purely statistical reaction, $A_C = 0$ and

$$\frac{\delta\sigma}{\sigma} \approx 2\,\frac{\delta A_F}{|A_F|} \approx \frac{2}{\sqrt{n}}.$$

Even with a large coherent component present, the A_F term should produce fluctuations in the cross section

$$\frac{\delta\sigma}{\sigma} \approx 2\delta A_F/|A_C| .$$

The most sensitive search for these fluctuations can be made where $|A_C|$ is small, as is the case for elastic scattering well away from the forward and backward directions. In all cases, the fluctuations are characterized by an energy width $\Delta\sqrt{s} \approx \Gamma$ and an angular width $\Delta\theta_{\text{c.m.}} \approx L_{\max}^{-1}$. A case of Ericson fluctuations in nuclear physics is shown in Fig. 2, where random fluctuations can be seen superimposed on a diffractive background.[12]

A quantitative comparison with the theory can be made by calculating the correlation function

$$C = \langle(\sigma - \sigma_s)^2/\sigma_s^2\rangle ,$$

where the average is taken over a range of energy $\Delta\sqrt{s} \gg \Gamma$. Here σ_s is the smooth nonfluctuating part of the cross section and must be estimated from the data via a smooth fit.

Eilam *et al.*[13] have argued that if elastic scattering is due primarily to overlapping resonances, the density of states is directly observable at wide angles. They predict that the energy dependence at fixed large angles is

$$\frac{d\sigma}{d\Omega} \propto \frac{s\gamma(\sqrt{s})}{\rho(\sqrt{s})},$$

where γ is the average partial width. This leads to the result

$$\frac{d\sigma}{dt} \propto \exp\left(\frac{-\sqrt{s}}{T_0}\right).$$

The inverse exponential dependence comes essentially from the statistical competition of other (inelastic) processes. This model differs from Frautschi's in that nonstatistical components of the cross section are small at large angles.

Eilam *et al.* claim that this model fits the $\pi^{\pm} p$, $K^- p$, and $\bar{p}p$ elastic-scattering well for s greater than 4 GeV^2.

III. EXPERIMENTAL METHOD

A. The beam

The configuration of the magnets and counters in the beam line is shown in Fig. 3. The beam selected 0° negative secondaries or 3° positive secondaries produced by 12.5-GeV/c protons incident on a beryllium target. The acceptance of the beam was 0.5 msr. The beam line had an intermediate focus at the position of the momentum hodoscope shown in the figure. The momentum acceptance of the beam line was ±5% of the

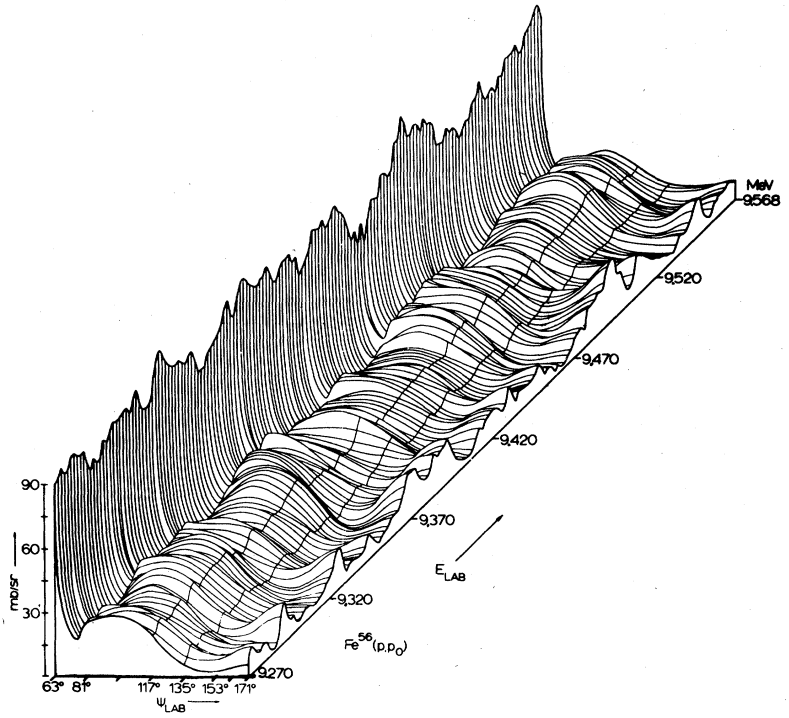

FIG. 2. Differential cross section for elastic p-^{56}Fe scattering: an example of Ericson fluctuations in nuclear physics. Figure is taken from Ref. 12.

central momentum. Because the beam was dispersed in the region of the momentum hodoscope, components of the beam with momenta differing from the central momentum passed through different elements of the array, thus signaling their momentum. In this way, the beam was divided into 19 momentum bins, each 0.5% wide. The beam was refocused to a 3-cm-by-2-cm spot at the target.

The central momentum of the beam was determined by a Monte Carlo simulation of the magnet system and by wire orbit studies. In addition, a separate experiment measuring proton-proton elastic scattering used the beam line as a spectrometer and verified the momentum determination.[14] A final check was provided by the kinematics of the elastic scattering in this experiment. The overall uncertainty of the absolute momentum calibration is estimated to be ±0.5%.

The positions of incoming beam particles were measured by scintillator hodoscopes upstream of the target. The hodoscopes were spaced 2 m apart and had a resolution of ±3 mm.

The Čerenkov counters in the beam, marked K and π in Fig. 4, were threshold-type counters filled with ethylene. Each contained two optically isolated sections to minimize accidental signals from knock-on electrons. The ethylene pressure for each beam momentum setting was set to optimize the signal for kaons and pions, respectively, while giving no signal for protons.

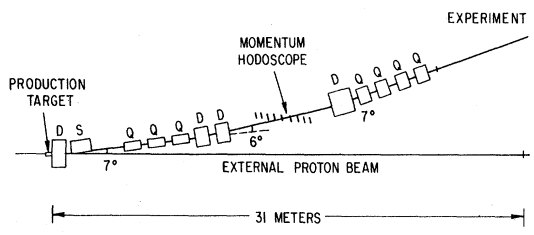

FIG. 3. Plan view of the beam line.

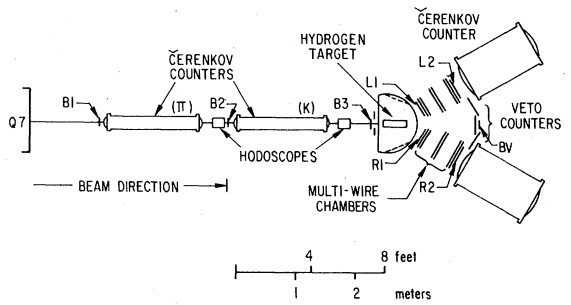

FIG. 4. Plan view of the detector.

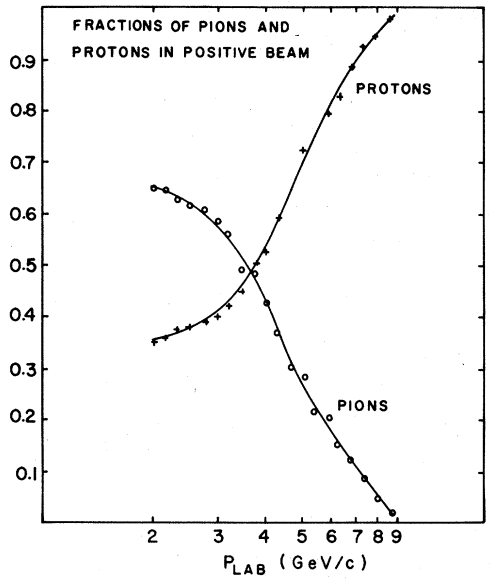

FIG. 5. Measured fraction of pions and protons in the positive beam, as a function of momentum.

The beam flux was measured by scalers counting the number of coincidences in the beam-defining counters $B1$, $B2$, and $B3$. With the polarities set to transmit positive particles, the beam was composed of mostly pions and protons. Figure 5 shows the pion and proton fraction of the beam as a function of momentum. With the opposite polarity, the beam consisted almost entirely of negative pions. In each case, there were a few kaons and leptons, generally less than 2%.

B. The detector

The detector was designed to measure the passage of particles undergoing wide-angle elastic scattering and to ignore all other scattering processes. A plan view of the apparatus is shown in Fig. 4.

In the center of the detector was the target—a 30-cm flask of liquid hydrogen.

The proportional wire chambers (PWC's) to the sides of the target measured the positions of scattered charged particles. The two rear chambers in each arm were of size 33 cm (horizontal) $\times$ 25 cm (vertical) and had wires spaced 2.5 mm apart. Each chamber had a horizontal and a vertical plane of wires. The Čerenkov counters in the arms were filled with Freon 12 and were used to distinguish between scattered pions and protons in the small fraction of events that were kinematically ambiguous.

The laboratory angles corresponding to wide center-of-mass angles varied with the beam momentum, so the arms were built to pivot around the hydrogen-target center point. The laboratory angles of the center of the arms were set between 30° and 48° from the beam direction. These angles were determined by optical measurements to an accuracy ±1 mr. Positions of the PWC wires relative to the arm centerlines were established by optical surveying, and verified by track reconstruction of the data taken with the arms placed in the beam. The effective angular resolution of the hodoscope PWC system was 4 mrad [full width at half maximum (FWHM)] in the laboratory scattering angle, corresponding to typically 9 mrad in the center-of-mass angle.

The trigger consisted of a coincidence of the scintillator counters $B1$, $B2$, $B3$, $L1$, $L2$, $R1$, and $R2$, indicating an entering beam particle and a particle in each arm of the detector. In addition, the small beam counter BV behind the target was required as a veto. To minimize triggers due to inelastic scattering, we also required that there not be any signals in the veto counters covering the other areas of the experiment.

All the veto counters, with the exception of BV, were made with lead-scintillator sandwiches, four radiation lengths thick, enabling us to veto inelastic π° production. To prevent accidental vetoing by knock-on electrons, the veto counters were faced with a 0.32-cm sheet of aluminum, sufficient to block most knock-ons. There were four counters downstream of the target and four surrounding the target area (two semicircular ones above and below, and two to the sides). The combination of trigger and veto counters covered most of the scattering area: In the center-of-mass system, about 3.5π sr were covered by counters, with only the backward direction uncovered.

Under typical running conditions, two million incident beam particles, in a spill of 0.6 seconds, caused 1000 $B1 \cdot B2 \cdot B3 \cdot L1 \cdot L2 \cdot R1 \cdot R2$ coincidences. The inclusion of the veto counters in the trigger reduced the number of triggers by factors of 10 to 100, resulting in typically 50 event triggers per 2×10^6 beam particles.

At intermediate energies, the fraction of protons in the beam was higher than the fraction of pions, and the cross section for pp is higher. In order to prevent domination of the data by proton-proton scattering in this situation, these triggers were prescaled. A proton-proton scatter trigger was defined as a scatter trigger with no signals in the beam Čerenkov counters.

In addition to the triggers caused by scattering, random "beam triggers" were taken with only an incident beam particle required in the logic. This gave a sample of the beam spectrum, position,

TABLE II. Summary of data sample.

(a) Negative runs

Momentum (GeV/c)	Flux (10^8)	Elastic $\pi^- p$ events[a] (10^3)	Subtraction[b]
1.963	5.24	40.8	0.02
2.120	5.13	38.4	0.01
2.303	8.00	51.0	0.01
2.488	9.05	38.8	0.01
2.688	31.6	84.7	0.01
2.885	61.2	93.4	0.01
3.130	97.5	81.3	0.01
3.393	122.7	58.6	0.02
3.668	175.6	31.8	0.04
3.963	238.9	27.7	0.06
4.283	469.0	23.6	0.08
4.658	662.3	10.1	0.11
5.030	513.9	5.1	0.17
5.433	413.9	3.7	0.15
5.867	513.4	4.0	0.16
6.337	675.5	3.8	0.17
6.844	849.4	4.5	0.15
7.392	1003	2.7	0.22
7.983	692.2	1.3	0.30
8.621	1763	1.6	0.30
9.311	472.8	0.31	0.37

(b) Positive runs

Momentum (GeV/c)	Flux (10^8)	Elastic $\pi^+ p$ events[a] (10^3)	$\pi^+ p$ background subtraction[b]	Elastic pp events[a] (10^3)	pp background subtraction[b]
1.970	7.31	40.0	0.02	31.6	0.01
2.129	9.55	45.9	0.01	31.0	0.01
2.310	11.99	46.5	0.03	24.8	0.01
2.496	15.6	55.3	0.01	24.8	0.01
2.698	19.2	46.1	0.01	24.7	0.01
2.906	17.8	30.0	0.01	12.0	0.01
3.135	23.0	18.4	0.01	4.5	0.01
3.393	87.5	31.8	0.02	25.6	0.01
3.668	105.2	15.6	0.03	24.8	0.01
3.963	125.9	10.2	0.04	12.9	0.01
4.283	260.0	8.09	0.07	10.2	0.01
4.658	355.2	29.3	0.04	13.1	0.02
5.030	1792	20.7	0.07	4.5	0.02
5.433	1360	9.1	0.10	17.3	0.02
5.867	237.2	0.56	0.17	3.3	0.04
6.337	56.9			4.1	0.05
6.844	70.3			2.8	0.07
7.392	143.3			2.8	0.09
7.983	234.0			2.1	0.17
8.621	238.3			1.4	0.22

[a] Events after background subtraction and kinematic cuts.
[b] Background/("raw" signal–background).

and composition, free of the bias caused by demanding a scatter trigger.

C. The data sample

Data were taken at momenta from 2 to 9.5 GeV/c. To cover this range, the momentum of the beam line was set, in the successive runs, in 8% increments. Because the beam had a ±5% momentum spread and was divided into 19 bins by the momentum hodoscope, each momentum setting overlapped the adjacent settings.

At incident momenta above 6.3 GeV/c, there

were not enough positive pions in the beam to make statistically meaningful measurements of $\pi^+p \to \pi^+p$, so our data taking was limited to $\pi^-p \to \pi^-p$ and $pp \to pp$ between 6.3 and 9.5 GeV/c.

The total flux of the experiment was 15×10^{11}, resulting in 28×10^6 triggers. Table II lists the data sample broken down into momentum setting and particle type.

D. Data analysis

1. Event identification

The first calculation was the reconstruction of tracks from particle "hits" in the PWC's and beam hodoscopes. We chose, from all the hits, one track in each arm and in the beam hodoscopes, according to the criterion of making the best vertex. In the arms, preference was given to tracks with three hits on a line. If there was only one hit instead of two or three, the track was reconstructed using the vertex determined by the other tracks, if this was possible. All subsequent analysis was done using the tracks chosen this way.

The thrust of the subsequent analysis was to recognize elastic events among all reconstructed events. The "spectrometer" of this experiment was magnetless (in order to make the acceptance large and smooth) so that only directions are available for kinematic constraints.

The first test of elasticity was made on the acoplanarity of these three tracks. Our definition of acoplanarity was the triple scalar product of the direction vectors of the tracks, so that the acoplanarity vanished for a perfectly elastic event with no measurement error. Figure 6(a), a typical acoplanarity histogram, shows a clear peak corresponding to elastic scatters (acoplanarity from −0.01 to +0.01) and a broad continuum of other events which caused a trigger.

A test was also applied to the scattering angles. This test uses the fact that for elastic collisions of known particles at a known momentum, the angles of the scatter and recoil particles are uniquely related. The quantity $\Delta\theta$, defined as shown in Fig. 7, is a measure of how closely the pair of measured angles matches this relationship. A typical histogram of $\Delta\theta$ for a positive beam is shown in Fig. 8. In this case, we calculated $\Delta\theta$ assuming all the incoming particles were pions. Peaks due to elastic scattering of pions and protons are clearly visible. In addition, for $\pi^\pm p$ scattering this method nearly always revealed which arm had the pion and which the proton. When the kinematics were ambiguous, the Čerenkov counters on the arms were used to identify the scattered particles.

The quantities, acoplanarity and $\Delta\theta$, are nearly independent because they are derived from horizontal and vertical measurements of the tracks, respectively. Applying the criterion that $\Delta\theta$ be approximately equal to zero to the events in the acoplanarity histogram of Fig. 6(a) results in Fig. 6(b), in which the background is much reduced.

We proceeded to compute cross sections by selecting and grouping elastic events. We required (1) good identification of the incoming particle, i.e., unambiguous signals in the beam Čerenkov counters, (2) unambiguous signals in the momentum hodoscope, and (3) an interaction vertex located in the hydrogen target.

The events chosen as elastic by these cuts were histogrammed according to their momentum and value of t. This histogram is then a raw distribution of elastic events. At this stage of the analysis, each momentum setting was divided into ten 1% momentum bins. (At the last stage of the

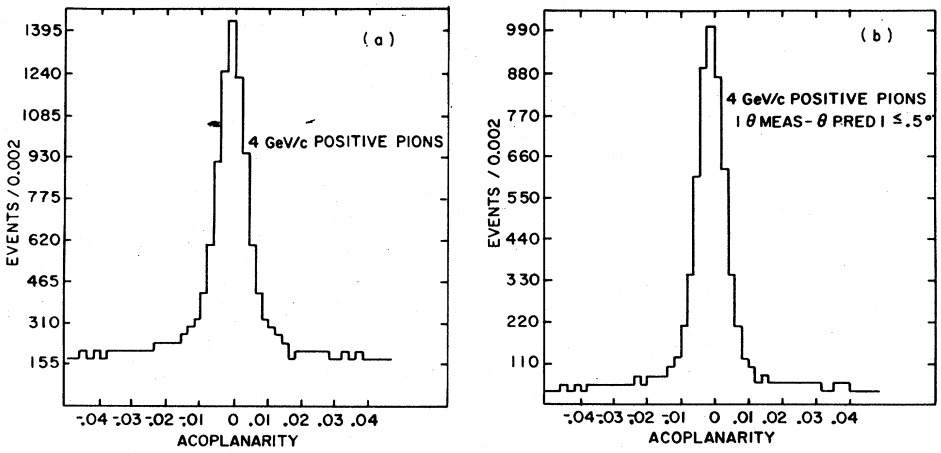

FIG. 6. (a) Example of coplanarity distribution with no cuts. (b) Same distribution with $\Delta\theta > 0.5°$.

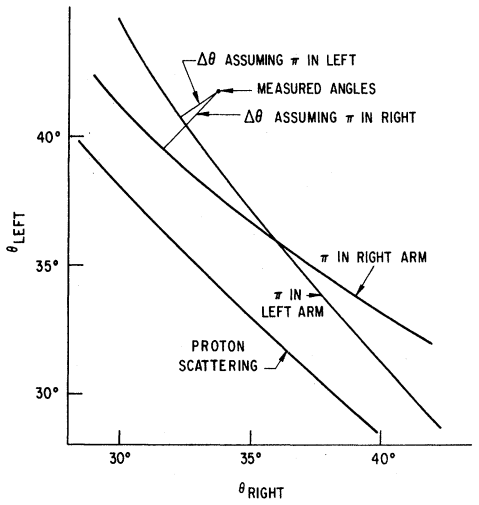

FIG. 7. Kinematics of πp and pp elastic scattering. The polar angle of the particle detected in the left arm is plotted against that in the right arm. The quantity $\Delta\theta$ is defined to be the closest distance, in two dimensions, from the measured point to the appropriate kinematic curve. The quantity discussed in the text is the smaller of the two distances to the πp curves.

analysis, the bin size was doubled, so the final cross sections are for 2% increments.)

To subtract the remaining nonelastic background, we divided the data into large t groups and estimated the background for each such group. This was done by fitting the acoplanarity distribution (with all cuts) to the sum of two Gaussian functions to represent the peak and a background polynomial. These functions were then used to fit the distributions for all t and momentum bins with the only adjustments being the normalization

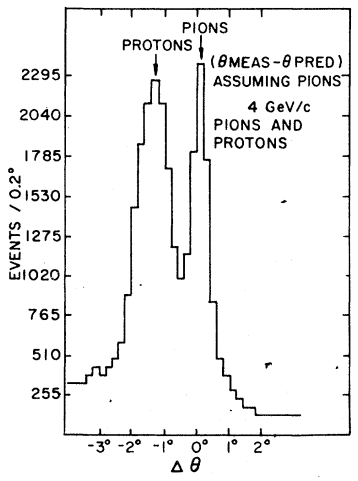

FIG. 8. Distribution of $\Delta\theta$ showing separation of elastically scattered pions and protons at 4 GeV/c.

of the signal and background parts. We subtracted from the raw distributions that number of events under the elastic peak which belonged to the polynomial background. We did *not* use the fit to the signal as the measure of the signal. The background subtraction after cuts varied a great deal with momentum, ranging from a few percent at 2 GeV/c to as much as 30% at 8.6 GeV/c. Figure 9 gives an example of a raw distribution with and without background subtraction.

The result of this procedure of selecting elastic scatters was to produce, from 28×10^6 triggers, 1.3×10^6 elastic events (4.1×10^5 π^+p, 2.8×10^5 pp, and 6.1×10^5 π^-p) with which we calculated differential cross sections.

2. *Acceptance*

The azimuthal acceptance was computed by a Monte Carlo simulation in which elastic scattering occurred in all directions (in the c.m. frame) and from all positions of the target which the beam was able to hit. The program counted, as a function of t and momentum, what fraction of the generated events passed into the apparatus. The trigger counters behind the arms were the limiting apertures. The maximum acceptance varied

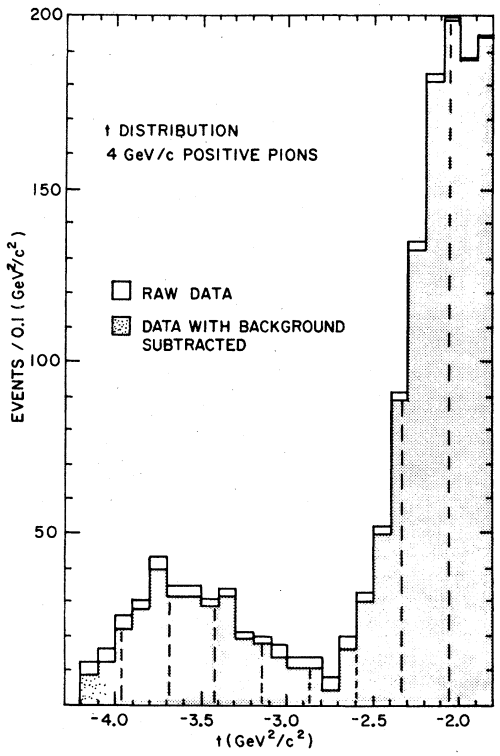

FIG. 9. Effect of background subtraction.

slowly as a function of momentum, from 17% at 2 GeV/c to 26% at 9 GeV/c.

It is of interest to point out here that two important advantages of the magnetless spectrometer used are that (1) the acceptance was large, allowing high data-taking rates and that (2) it was a smooth function of momentum and t. (A typical acceptance is shown in Fig. 10.) Thus, we were freed from the danger that we would introduce structure into the cross sections by a slight miscalculation of a complicated acceptance. We did not use data for which the acceptance was less than 20% of the maximum at that momentum.

3. Corrections to raw data

To convert the histograms in t to differential cross sections, we used the following formula:

$$\frac{d\sigma}{dt} = \frac{(\text{number of events in } \Delta t)(\text{corrections})}{(\text{acceptance})(\text{flux})(\Delta t)(\text{number of target protons per unit area})}.$$

The number of target protons per unit area was computed by the formula $N=\rho l A$, where ρ is the density (0.0715 g/cm^3), l is the length of the liquid (30 cm), and A is Avogadro's number. Uncontrollable fluctuations in the target pressure made the density and, therefore, this product uncertain by ±1.5%.

The flux was measured by the beam counters as discussed previously. The effective flux for each momentum bin was defined as the measured flux times the fraction of beam particles of the type being used (pions or protons). Beam trigger data were used to determine these fractions.

The correction factors to $d\sigma/dt$ were of two types: instrumental inefficiencies and inefficiencies of the analysis.

(1) Accidental vetoing. Scattered particles could be accidentally vetoed by random coincidences in the veto counters. During the running of the experiment, there was a delay circuit set up to give a measure of this effect. Beam rates were typically 2×10^6/sec, and the resolving time of the veto counters was about 20 nsec, so the accidental rates were ~4%, though there were sometimes higher losses when the instantaneous rates were very high.

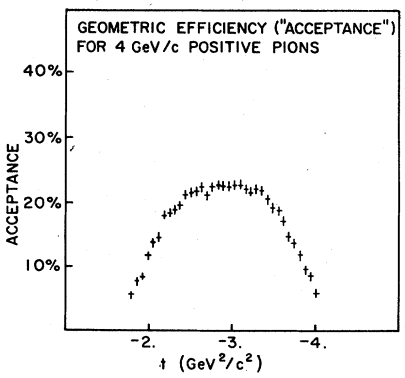

FIG. 10. Example of calculated acceptance.

(2) Empty-target scattering. Some data were taken with the target vessel emptied of hydrogen, but analysis of that data show that less than 1% of the elastic scattering was due to scatters off the target vessel. Hence, no correction was made for this effect.

(3) Chamber inefficiencies. Since there were three horizontal and three vertical chambers in each arm, we were able to use the redundancy to estimate the inefficiency of each. Reconstructed events were used to estimate the inefficiency of the hodoscopes. Those calculations were done for each momentum setting. The resulting corrections were typically ~7%.

(4) Lepton contamination. At low momenta, the electron and muon contamination of the beam was directly measured by the beam Čerenkov counters. The contamination was a few percent at the lowest momentum and decreased for increasing momentum. Since these leptons registered as pions but could not scatter at large angles with comparable probability, we reduced the effective pion flux accordingly.

(5) Absorption and decay. The beam was attenuated by absorption in the hydrogen as it passed through the target, so the effective flux was reduced. In passing through the remaining hydrogen, air, and trigger counters in the arms, scattered particles could be absorbed by nuclear processes. The total correction for these effects was 6%. The loss due to pion decay after scattering was less than 1% and was not corrected for.

(6) Reconstructed losses. In the track-reconstruction program, certain classes of complex events, such as events with too many hits or too many possible track combinations, were rejected as being inelastic to save computing time. We calculated a small sample of data of these types and found that they contributed a small number of elastic events, up to 3% in the worst case.

(7) Selection inefficiencies. In cuts using acoplanarity and $\Delta\theta$ to define elastic events, we excluded events in the tails of the Gaussian curve.

For each momentum, we estimated the loss due to these cuts by comparing the distributions obtained with wider cuts. These inefficiencies were typically 5% each.

(8) Momentum hodoscope losses. In order to determine the momentum, we required unambiguous hits in the momentum hodoscope. Typically, 20% (the amount varied with intensity and momentum) of the incident particles were ambiguous due to the simultaneous passage of two or more particles through the hodoscope and were therefore not usable. The flux used was reduced accordingly. This was done separately for each run.

We made many checks to verify the data and the corresponding calculations. We analyzed subsets of the data taken months apart, or under different conditions, to see if the final cross sections agreed. Independent analysis of some of the data was done by members of the collaboration at different laboratories. In some cases, different arm angle settings were used for runs at the same momentum. This last test was particularly useful for checking the acceptance calculations. Because the highest bins of each momentum setting corresponded to the lowest bins of the next setting, a comparison of the overlapping momentum bins provided an excellent test of the consistency of the data. In all cases of comparing independent data samples at a given momentum, the two differential cross sections were fit to each other as a function of t with only the relative normalization as a free parameter. For all such tests, satisfactory χ^2 values were found for the fits. The fitted relative normalizations revealed a random rms uncertainty in the normalizations of 3%.

In addition, we estimate the overall normalization uncertainty to be ±10%. The major contributions to this uncertainty are the flux corrections for accidental vetoing and momentum hodoscope losses.

The corrected cross sections are listed in Table III. The errors listed there are statistical only and do not include the systematic errors discussed above.

IV. RESULTS AND INTERPRETATIONS

A. Differential cross sections

In Figs. 11, 12, and 13, we have plotted examples of our differential cross sections $d\sigma/dt$ for π^+p, π^-p, and pp elastic scattering. Energies for these figures have been chosen to coincide with those of previous experiments[15-17] whose data are also shown. We see that our experiment covers a smaller angular range than the earlier ones, but we have comparable or greater statistical precision at each momentum and have data at many more momenta. Apart from normalization differences, the new data are consistent with the old.

Two differences between pp and πp scattering are noticed: pp cross sections are about an order of magnitude larger than the πp at the larger angles but about the same at the smaller angles, and the pp scattering shows relatively little angular structure. For both reasons, elastic proton-proton scattering has been comparatively well studied, and in this experiment the proton-proton data serve as a check on the experimental method. The important new results of this experiment are the pion-proton differential cross sections.

Elastic proton-proton scattering can be characterized rather simply.[18] The cross section decreases with increasing energy at a fixed angle (or t), and at a fixed energy, decreases with increasing angle. The energy dependence at a fixed angle becomes stronger, the larger the angle. The shape is approximately the same for all energies measured in this experiment. (A fixed-t dip appears in the differential cross section at much higher energies.[19])

To give an overall picture of πp scattering, we have shown differential cross sections of several momenta in Figs. 14 and 15. The lines are drawn to guide the eye. The dashed lines represent the forward cross sections measured by Eide *et al.*,[20] Rust *et al.*,[16] Coffin *et al.*,[15] and Aplin *et al.*[21] Several comments are in order:

(1) Both π^+p and π^-p cross sections have the same general shape and energy dependence.

(2) The forward cross section falls relatively slowly with energy while the large-angle cross section falls relatively quickly. This is similar to the proton-proton behavior mentioned above except that here the angular regions are distinct.

(3) There is a pronounced dip at an approximately constant t value of -2.8 GeV$^2/c^2$. This dip is a principal reason for displaying differential cross section as a function of t rather than $\cos\theta_{\text{c.m.}}$. In the latter, the dip would have different positions according to energy and could obscure any more subtle structure.

(4) The cross sections for $|t| > 2.8$ GeV$^2/c^2$ show a nonregular structure. Though characterized by a rapid decrease in energy, they also show minor peaks, dips, and changes of curvature.

It is fairly natural to regard the forward scattering as due to diffraction, but this idea is not without difficulties. For example, in low-energy scattering, the $t = -2.8$ GeV$^2/c^2$ dip occurs at very large angles, possibly even at 180°. This is contrary to the usual notions of diffraction as a forward-scattering process. However, a number

TABLE III. Elastic-scattering differential cross sections in units of $\mu b/(GeV/c)^2$.

	$\pi^- p \to \pi^- p$			
t [$(GeV/c)^2$] \ Momenta (GeV/c)	1.889	1.938	1.973	2.007
−0.675	517 ± 44	420 ± 40		
−0.725	413 ± 34	469 ± 36	359 ± 39	418 ± 38
−0.775	446 ± 34	442 ± 32	441 ± 37	419 ± 33
−0.825	540 ± 39	453 ± 33	416 ± 36	482 ± 34
−0.875	559 ± 36	591 ± 36	593 ± 44	511 ± 34
−0.925	671 ± 40	586 ± 36	588 ± 42	588 ± 36
−0.975	759 ± 41	703 ± 38	816 ± 49	696 ± 38
−1.025	780 ± 38	782 ± 37	703 ± 42	638 ± 35
−1.075	971 ± 39	812 ± 35	823 ± 42	742 ± 34
−1.125	1050 ± 39	900 ± 35	890 ± 40	888 ± 36
−1.175	985 ± 37	957 ± 34	933 ± 39	900 ± 33
−1.225	953 ± 37	959 ± 34	880 ± 36	950 ± 33
−1.275	865 ± 37	948 ± 34	924 ± 38	874 ± 30
−1.325	863 ± 39	943 ± 37	959 ± 41	920 ± 32
−1.375	796 ± 42	873 ± 38	848 ± 41	875 ± 33
−1.425	826 ± 47	816 ± 40	794 ± 43	852 ± 35
−1.475	653 ± 42	713 ± 41	751 ± 46	658 ± 33
−1.525	749 ± 47	614 ± 38	530 ± 40	650 ± 36
−1.575	712 ± 49	644 ± 42	708 ± 49	596 ± 36
−1.625	574 ± 47	635 ± 44	585 ± 46	592 ± 37
−1.675	605 ± 57	632 ± 49	566 ± 50	546 ± 38
−1.725			587 ± 57	538 ± 41
−1.775			506 ± 56	475 ± 42

	$\pi^- p \to \pi^- p$			
t [$(GeV/c)^2$] \ Momenta (GeV/c)	2.040	2.093	2.130	2.167
−0.725	342 ± 36			
−0.775	377 ± 26	471 ± 40	379 ± 45	
−0.825	474 ± 27	443 ± 34	409 ± 40	406 ± 36
−0.875	475 ± 26	435 ± 32	467 ± 38	461 ± 35
−0.925	573 ± 28	553 ± 36	506 ± 40	481 ± 33
−0.975	635 ± 30	546 ± 36	564 ± 42	534 ± 34
−1.025	718 ± 30	648 ± 38	634 ± 45	592 ± 36
−1.075	714 ± 28	671 ± 37	659 ± 44	680 ± 39
−1.125	760 ± 27	677 ± 34	685 ± 42	705 ± 37
−1.175	800 ± 26	752 ± 34	793 ± 43	745 ± 36
−1.225	905 ± 26	831 ± 34	845 ± 41	744 ± 34
−1.275	901 ± 26	910 ± 34	889 ± 40	730 ± 31
−1.325	829 ± 24	880 ± 33	911 ± 39	832 ± 32
−1.375	862 ± 25	815 ± 31	832 ± 37	809 ± 31
−1.425	807 ± 26	848 ± 34	812 ± 37	769 ± 30
−1.475	702 ± 26	770 ± 34	796 ± 38	778 ± 30
−1.525	697 ± 29	732 ± 36	748 ± 39	754 ± 31
−1.575	600 ± 28	675 ± 37	644 ± 39	656 ± 31
−1.625	602 ± 29	537 ± 35	527 ± 37	574 ± 31
−1.675	456 ± 26	506 ± 34	481 ± 38	533 ± 32
−1.725	465 ± 28	459 ± 35	471 ± 39	456 ± 31
−1.775	508 ± 31	435 ± 34	416 ± 37	357 ± 29
−1.825	389 ± 30	466 ± 38	405 ± 39	329 ± 28
−1.875	324 ± 39	386 ± 38	449 ± 47	266 ± 26
−1.925		371 ± 40	342 ± 42	285 ± 29
−1.975				265 ± 30

TABLE III. *(Continued.)*

t [(GeV/c)^2] \ Momenta (GeV/c)	$\pi^- p \to \pi^- p$ 2.217	2.274	2.314	2.354
−0.775	284 ± 29			
−0.825	354 ± 28			
−0.875	396 ± 23	358 ± 26		
−0.925	401 ± 22	383 ± 25	343 ± 28	342 ± 24
−0.975	448 ± 22	448 ± 26	393 ± 29	375 ± 23
−1.025	538 ± 24	514 ± 29	475 ± 32	397 ± 24
−1.075	505 ± 23	477 ± 27	424 ± 30	421 ± 24
−1.125	600 ± 24	591 ± 30	455 ± 30	494 ± 26
−1.175	590 ± 23	546 ± 27	529 ± 32	465 ± 25
−1.225	645 ± 22	561 ± 26	551 ± 30	487 ± 24
−1.275	699 ± 21	568 ± 25	470 ± 26	482 ± 23
−1.325	697 ± 20	592 ± 23	530 ± 26	477 ± 21
−1.375	736 ± 20	658 ± 24	556 ± 25	512 ± 21
−1.425	711 ± 20	652 ± 22	587 ± 25	524 ± 19
−1.475	681 ± 19	655 ± 22	544 ± 23	521 ± 19
−1.525	662 ± 19	670 ± 22	480 ± 21	494 ± 18
−1.575	604 ± 19	636 ± 22	536 ± 23	481 ± 17
−1.625	610 ± 21	583 ± 23	513 ± 23	504 ± 18
−1.675	516 ± 21	554 ± 24	474 ± 23	482 ± 18
−1.725	451 ± 20	526 ± 25	473 ± 25	449 ± 19
−1.775	429 ± 21	430 ± 24	378 ± 24	406 ± 19
−1.825	322 ± 19	328 ± 22	347 ± 24	378 ± 19
−1.875	314 ± 19	311 ± 22	307 ± 24	320 ± 19
−1.925	260 ± 18	319 ± 24	240 ± 22	272 ± 19
−1.975	258 ± 20	287 ± 23	264 ± 24	238 ± 18
−2.025	203 ± 31	206 ± 21	209 ± 22	217 ± 18
−2.075		207 ± 23	167 ± 22	174 ± 17
−2.125		223 ± 26	204 ± 26	130 ± 15
−2.175			149 ± 23	146 ± 17
−2.225				122 ± 18

t [(GeV/c)^2] \ Momenta (GeV/c)	$\pi^- p \to \pi^- p$ 2.395	2.456	2.500	2.543
−0.95	312 ± 13			
−1.05	352 ± 12	313 ± 15	292 ± 17	325 ± 16
−1.15	375 ± 12	353 ± 15	318 ± 18	293 ± 14
−1.25	403 ± 12	330 ± 14	365 ± 18	296 ± 13
−1.35	432 ± 11	344 ± 13	343 ± 16	294 ± 12
−1.45	433 ± 10	374 ± 12	347 ± 14	279 ± 10
−1.55	447 ± 10	388 ± 11	364 ± 13	285 ± 9
−1.65	407 ± 9	350 ± 10	335 ± 12	271 ± 9
−1.75	371 ± 9	362 ± 11	338 ± 12	257 ± 8
−1.85	294 ± 9	270 ± 10	267 ± 11	260 ± 9
−1.95	222 ± 9	210 ± 10	231 ± 12	197 ± 8
−2.05	165 ± 9	159 ± 10	190 ± 12	140 ± 8
−2.15	153 ± 9	136 ± 10	139 ± 12	98.6 ± 7.3
−2.25	111 ± 13	121 ± 11	103 ± 11	78.8 ± 7.2
−2.35			75.1 ± 10.8	66.5 ± 7.5

TABLE III. *(Continued.)*

t [(GeV/c)^2] \ Momenta (GeV/c)	$\pi^- p \to \pi^- p$ 2.587	2.654	2.701	2.748
−1.05	264 ±9	270 ±9		
−1.15	286 ±8	259 ±7	256 ±8	250 ±8
−1.25	289 ±8	283 ±8	273 ±8	266 ±7
−1.35	268 ±7	250 ±7	254 ±8	231 ±6
−1.45	274 ±6	250 ±6	235 ±7	225 ±6
−1.55	267 ±5	238 ±5	217 ±6	206 ±5
−1.65	256 ±5	231 ±5	221 ±6	193 ±5
−1.75	232 ±5	203 ±4	194 ±5	176 ±4
−1.85	215 ±5	195 ±4	165 ±4	152 ±4
−1.95	195 ±5	192 ±4	177 ±5	144 ±3
−2.05	142 ±4	155 ±4	147 ±5	130 ±3
−2.15	97.1±4.0	115 ±4	102 ±4	103 ±3
−2.25	75.6±3.9	79.7±3.9	77.1±4.2	78.1±3.2
−2.35	54.0±3.7	55.3±3.5	54.8±3.8	51.7±2.9
−2.45	36.6±3.4	39.7±3.3	44.3±3.8	33.3±2.5
−2.55		26.2±3.1	28.6±3.4	29.8±2.7
−2.65				17.3±2.3

t [(GeV/c)^2] \ Momenta (GeV/c)	$\pi^- p \to \pi^- p$ 2.777	2.848	2.899	2.949
−1.15	283 ±13			
−1.25	270 ± 6	238 ±7	221 ±8	
−1.35	242 ± 5	227 ±6	218 ±7	214 ±6
−1.45	217 ± 4	191 ±4	173 ±5	176 ±4
−1.55	199 ± 4	170 ±4	158 ±4	154 ±4
−1.65	185 ± 3	159 ±3	143 ±4	134 ±3
−1.75	168 ± 3	143 ±3	123 ±3	124 ±3
−1.85	146 ± 3	128 ±3	111 ±3	97.8±2.3
−1.95	126 ± 2	110 ±2	85.4±2.5	85.4±2.1
−2.05	115 ± 2	91.9±2.3	73.8±2.3	71.0±1.8
−2.15	93.6± 2.3	87.8±2.3	67.5±2.2	58.6±1.7
−2.25	75.4± 2.2	66.9±2.2	55.0±2.1	49.2±1.6
−2.35	49.4± 2.0	48.5±2.0	43.6±2.0	44.6±1.6
−2.45	36.4± 2.0	34.5±1.9	31.3±1.8	29.6±1.4
−2.55	22.6± 1.8	23.9±1.9	22.7±1.8	23.8±1.4
−2.65	18.9± 1.9	22.2±2.4	16.0±1.8	14.4±1.3
−2.75	22.3± 3.2	18.5±2.3	14.4±2.2	13.1±1.5
−2.85				14.8±1.8

t [(GeV/c)^2] \ Momenta (GeV/c)	$\pi^- p \to \pi^- p$ 3.013	3.090	3.145	3.200
−1.35	217 ±8			
−1.45	164 ±3			
−1.55	145 ±3	135 ±3	139 ±4	135 ±3
−1.65	124 ±2	121 ±2	121 ±3	115 ±2
−1.75	109 ±2	98.2±2.0	98.0±2.3	91.9 ±1.9
−1.85	86.7±1.6	80.2±1.7	76.5±1.9	73.8 ±1.6
−1.95	71.1±1.4	66.1±1.5	60.8±1.7	54.8 ±1.3
−2.05	58.8±1.3	51.4±1.4	49.4±1.5	41.3 ±1.1
−2.15	44.6±1.1	38.4±1.2	37.7±1.3	31.6 ±1.0
−2.25	39.0±1.1	31.9±1.1	27.8±1.1	23.7 ±0.8
−2.35	35.8±1.0	28.6±1.0	23.1±1.0	21.4 ±0.8
−2.45	25.8±0.9	23.5±0.9	20.3±1.0	16.2 ±0.7
−2.55	20.2±0.9	17.3±0.8	15.2±0.8	14.8 ±0.7
−2.65	14.4±0.8	14.5±0.8	12.2±0.8	9.96±0.57
−2.75	13.3±0.9	11.1±0.8	11.2±0.8	8.09±0.53
−2.85	13.3±1.1	13.3±1.0	11.9±1.0	6.91±0.53

TABLE III. *(Continued.)*

t [(GeV/c)^2] \ Momenta (GeV/c)	$\pi^-p \to \pi^-p$ 3.013	3.090	3.145	3.200
−2.95	12.8 ± 2.1		10.5 ± 1.1	9.02 ± 0.68
−3.05				9.48 ± 0.87

t [(GeV/c)^2] \ Momenta (GeV/c)	$\pi^-p \to \pi^-p$ 3.266	3.350	3.410	3.469
−1.55	115 ± 3			
−1.65	102 ± 2	95.3 ± 2.3		
−1.75	82.7 ± 1.5	77.0 ± 1.7	79.5 ± 2.1	75.7 ± 1.9
−1.85	65.1 ± 1.2	63.3 ± 1.5	60.8 ± 1.7	64.2 ± 1.5
−1.95	48.6 ± 1.0	47.9 ± 1.2	43.8 ± 1.3	46.5 ± 1.2
−2.05	36.0 ± 0.8	34.0 ± 1.0	33.2 ± 1.2	32.9 ± 1.0
−2.15	25.0 ± 0.7	25.4 ± 0.8	24.0 ± 0.9	22.2 ± 0.8
−2.25	21.0 ± 0.6	17.2 ± 0.7	17.4 ± 0.8	15.9 ± 0.7
−2.35	14.6 ± 0.5	13.1 ± 0.6	11.3 ± 0.6	10.9 ± 0.5
−2.45	12.8 ± 0.5	8.76 ± 0.49	8.38 ± 0.55	6.35 ± 0.40
−2.55	10.8 ± 0.5	8.25 ± 0.48	5.98 ± 0.47	4.50 ± 0.34
−2.65	8.41 ± 0.41	6.01 ± 0.42	5.69 ± 0.48	4.07 ± 0.33
−2.75	6.61 ± 0.37	5.13 ± 0.40	3.80 ± 0.39	2.81 ± 0.29
−2.85	6.13 ± 0.38	3.50 ± 0.36	3.82 ± 0.42	2.21 ± 0.27
−2.95	5.46 ± 0.40	3.08 ± 0.37	2.73 ± 0.39	2.17 ± 0.28
−3.05	7.69 ± 0.55	3.71 ± 0.46	3.47 ± 0.45	2.52 ± 0.31
−3.15	6.98 ± 0.86	6.59 ± 0.67	6.19 ± 0.67	3.27 ± 0.37
−3.25		8.43 ± 0.88	6.22 ± 0.77	3.95 ± 0.43
−3.35				6.71 ± 0.63

t [(GeV/c)^2] \ Momenta (GeV/c)	$\pi^-p \to \pi^-p$ 3.530	3.621	3.686	3.750
−1.75	70.9 ± 1.6			
−1.85	57.2 ± 1.2	53.3 ± 1.6	54.7 ± 2.0	
−1.95	41.5 ± 0.9	40.9 ± 1.2	38.0 ± 1.3	38.2 ± 1.2
−2.05	29.2 ± 0.7	30.1 ± 1.0	27.4 ± 1.0	28.6 ± 0.9
−2.15	20.0 ± 0.6	20.6 ± 0.8	20.2 ± 0.8	20.5 ± 0.7
−2.25	13.7 ± 0.5	12.4 ± 0.6	11.8 ± 0.6	12.1 ± 0.5
−2.35	8.74 ± 0.38	8.02 ± 0.46	7.06 ± 0.48	7.52 ± 0.42
−2.45	5.44 ± 0.30	5.24 ± 0.37	4.63 ± 0.38	4.14 ± 0.31
−2.55	3.60 ± 0.25	2.94 ± 0.28	2.43 ± 0.29	2.48 ± 0.24
−2.65	2.55 ± 0.21	1.65 ± 0.20	1.40 ± 0.22	1.15 ± 0.17
−2.75	2.05 ± 0.19	1.31 ± 0.19	1.25 ± 0.21	0.698 ± 0.132
−2.85	2.02 ± 0.20	1.75 ± 0.22	1.36 ± 0.22	0.598 ± 0.124
−2.95	1.75 ± 0.18	1.49 ± 0.21	1.41 ± 0.22	0.810 ± 0.143
−3.05	2.09 ± 0.21	1.29 ± 0.19	1.17 ± 0.21	0.762 ± 0.141
−3.15	2.03 ± 0.21	1.63 ± 0.23	1.28 ± 0.23	1.30 ± 0.18
−3.25	3.22 ± 0.28	2.15 ± 0.27	1.57 ± 0.24	1.60 ± 0.20
−3.35	4.59 ± 0.37	2.90 ± 0.33	1.70 ± 0.27	1.36 ± 0.19
−3.45	8.24 ± 0.59	4.51 ± 0.45	2.69 ± 0.36	2.66 ± 0.27
−3.55		6.29 ± 0.62	4.58 ± 0.53	3.00 ± 0.31
−3.65			5.61 ± 0.65	2.78 ± 0.34
−3.75				4.79 ± 0.52

t [(GeV/c)^2] \ Momenta (GeV/c)	$\pi^-p \to \pi^-p$ 3.814	3.913	3.982	4.051
−1.95	37.5 ± 1.6			
−2.05	25.3 ± 0.7	22.9 ± 0.8		
−2.15	17.3 ± 0.5	14.4 ± 0.6	14.9 ± 0.7	14.7 ± 0.7
−2.25	11.1 ± 0.4	10.9 ± 0.4	10.7 ± 0.5	9.22 ± 0.45
−2.35	6.76 ± 0.28	6.35 ± 0.32	5.96 ± 0.37	6.38 ± 0.34

TABLE III. *(Continued.)*

t [(GeV/c)^2] \ Momenta (GeV/c)	$\pi^- p \to \pi^- p$ 3.814	3.913	3.982	4.051
−2.45	4.25 ±0.22	3.77 ±0.24	3.26 ±0.25	3.71 ±0.24
−2.55	2.06 ±0.15	1.92 ±0.17	2.02 ±0.20	2.15 ±0.18
−2.65	1.01 ±0.11	0.820 ±0.111	1.06 ±0.15	1.15 ±0.13
−2.75	0.643 ±0.086	0.474 ±0.084	0.487 ±0.105	0.499 ±0.086
−2.85	0.602 ±0.084	0.417 ±0.081	0.257 ±0.077	0.380 ±0.073
−2.95	0.726 ±0.091	0.396 ±0.080	0.394 ±0.089	0.377 ±0.071
−3.05	0.776 ±0.095	0.904 ±0.110	0.466 ±0.096	0.501 ±0.079
−3.15	1.02 ±0.11	0.787 ±0.104	0.840 ±0.121	0.622 ±0.086
−3.25	1.07 ±0.11	0.971 ±0.118	0.874 ±0.124	0.816 ±0.097
−3.35	1.22 ±0.12	1.02 ±0.12	0.868 ±0.130	1.07 ±0.11
−3.45	1.28 ±0.13	1.22 ±0.14	0.880 ±0.135	0.681 ±0.096
−3.55	1.66 ±0.16	1.11 ±0.14	0.944 ±0.141	0.984 ±0.116
−3.65	2.81 ±0.21	1.49 ±0.18	0.846 ±0.144	0.900 ±0.118
−3.75	4.30 ±0.30	1.80 ±0.20	1.10 ±0.16	0.979 ±0.128
−3.85		3.25 ±0.32	2.02 ±0.25	1.12 ±0.14
−3.95			3.17 ±0.35	1.19 ±0.16
−4.05				2.41 ±0.26

t [(GeV/c)^2] \ Momenta (GeV/c)	$\pi^- p \to \pi^- p$ 4.122	4.229	4.304	4.379
−2.15	12.3 ±0.4			
−2.25	8.84 ±0.27	7.38 ±0.28	7.66 ±0.36	
−2.35	5.82 ±0.21	4.98 ±0.21	5.10 ±0.26	4.28 ±0.21
−2.45	3.54 ±0.15	3.13 ±0.16	3.00 ±0.19	2.80 ±0.16
−2.55	1.72 ±0.10	1.86 ±0.12	1.59 ±0.13	1.38 ±0.10
−2.65	0.765 ±0.069	0.834 ±0.078	0.911 ±0.096	0.763 ±0.076
−2.75	0.317 ±0.048	0.489 ±0.062	0.417 ±0.068	0.425 ±0.058
−2.85	0.302 ±0.046	0.252 ±0.047	0.173 ±0.048	0.359 ±0.052
−2.95	0.306 ±0.045	0.254 ±0.047	0.234 ±0.053	0.213 ±0.042
−3.05	0.471 ±0.053	0.417 ±0.055	0.471 ±0.066	0.301 ±0.047
−3.15	0.536 ±0.054	0.524 ±0.060	0.454 ±0.064	0.437 ±0.053
−3.25	0.638 ±0.057	0.609 ±0.063	0.603 ±0.072	0.656 ±0.062
−3.35	0.652 ±0.059	0.655 ±0.065	0.802 ±0.085	0.465 ±0.054
−3.45	0.897 ±0.071	0.737 ±0.071	0.886 ±0.089	0.709 ±0.064
−3.55	0.838 ±0.070	0.771 ±0.074	0.657 ±0.078	0.574 ±0.060
−3.65	0.785 ±0.070	0.764 ±0.074	0.989 ±0.096	0.620 ±0.063
−3.75	0.765 ±0.072	0.756 ±0.077	0.566 ±0.072	0.639 ±0.066
−3.85	0.712 ±0.072	0.641 ±0.075	0.643 ±0.080	0.578 ±0.063
−3.95	0.939 ±0.087	0.518 ±0.070	0.651 ±0.088	0.468 ±0.059
−4.05	1.25 ±0.11	0.688 ±0.084	0.488 ±0.079	0.580 ±0.068
−4.15	1.63 ±0.14	0.917 ±0.105	0.618 ±0.091	0.415 ±0.062
−4.25		1.41 ±0.15	0.894 ±0.124	0.358 ±0.063
−4.35			0.708 ±0.126	0.357 ±0.069
−4.45				0.818 ±0.113

t [(GeV/c)^2] \ Momenta (GeV/c)	$\pi^- p \to \pi^- p$ 4.483	4.599	4.681	4.762
−2.25	4.87 ±0.27			
−2.35	3.85 ±0.17	2.92 ±0.19	3.35 ±0.27	
−2.45	2.12 ±0.11	1.60 ±0.13	1.31 ±0.14	1.45 ±0.14
−2.55	1.24 ±0.08	0.991 ±0.092	1.03 ±0.12	0.796 ±0.092
−2.65	0.765 ±0.062	0.481 ±0.066	0.630 ±0.090	0.336 ±0.059
−2.75	0.398 ±0.047	0.288 ±0.051	0.339 ±0.062	0.362 ±0.057
−2.85	0.229 ±0.036	0.264 ±0.048	0.207 ±0.053	0.243 ±0.046
−2.95	0.159 ±0.030	0.151 ±0.039	0.178 ±0.047	0.143 ±0.037
−3.05	0.225 ±0.033	0.266 ±0.046	0.224 ±0.051	0.272 ±0.046
−3.15	0.387 ±0.040	0.288 ±0.046	0.269 ±0.054	0.273 ±0.044
−3.25	0.474 ±0.043	0.277 ±0.045	0.307 ±0.057	0.270 ±0.044

TABLE III. *(Continued.)*

t [(GeV/c)^2] \ Momenta (GeV/c)	$\pi^- p \to \pi^- p$ 4.483	4.599	4.681	4.762
−3.35	0.516 ± 0.044	0.431 ± 0.053	0.319 ± 0.053	0.333 ± 0.047
−3.45	0.571 ± 0.047	0.478 ± 0.056	0.354 ± 0.057	0.399 ± 0.051
−3.55	0.633 ± 0.048	0.431 ± 0.052	0.350 ± 0.052	0.334 ± 0.046
−3.65	0.659 ± 0.049	0.702 ± 0.065	0.536 ± 0.067	0.312 ± 0.044
−3.75	0.579 ± 0.048	0.592 ± 0.061	0.563 ± 0.068	0.414 ± 0.050
−3.85	0.592 ± 0.049	0.546 ± 0.059	0.573 ± 0.070	0.457 ± 0.053
−3.95	0.486 ± 0.046	0.555 ± 0.061	0.482 ± 0.064	0.489 ± 0.055
−4.05	0.340 ± 0.042	0.369 ± 0.052	0.505 ± 0.070	0.457 ± 0.055
−4.15	0.360 ± 0.044	0.365 ± 0.054	0.345 ± 0.061	0.430 ± 0.054
−4.25	0.339 ± 0.045	0.284 ± 0.050	0.287 ± 0.060	0.282 ± 0.047
−4.35	0.265 ± 0.045	0.157 ± 0.043	0.228 ± 0.054	0.277 ± 0.048
−4.45	0.447 ± 0.061	0.154 ± 0.046	0.289 ± 0.062	0.168 ± 0.041
−4.55	0.371 ± 0.063	0.379 ± 0.070	0.155 ± 0.049	0.181 ± 0.042
−4.65	0.731 ± 0.129	0.359 ± 0.075	0.202 ± 0.063	0.258 ± 0.050
−4.75		0.575 ± 0.106	0.278 ± 0.081	0.238 ± 0.053
−4.85			0.597 ± 0.127	0.292 ± 0.062
−4.95				0.429 ± 0.084

t [(GeV/c)^2] \ Momenta (GeV/c)	$\pi^- p \to \pi^- p$ 4.841	4.966	5.055	5.142
−2.35	1.90 ± 0.19			
−2.45	1.16 ± 0.10	0.891 ± 0.125		
−2.55	0.799 ± 0.076	0.469 ± 0.085	0.662 ± 0.130	
−2.65	0.317 ± 0.047	0.368 ± 0.067	0.368 ± 0.085	0.339 ± 0.077
−2.75	0.231 ± 0.039	0.238 ± 0.052	0.0856 ± 0.0465	0.112 ± 0.046
−2.85	0.195 ± 0.035	0.136 ± 0.040	0.0679 ± 0.0413	0.149 ± 0.045
−2.95	0.114 ± 0.028	0.170 ± 0.042	0.0650 ± 0.0425	0.180 ± 0.046
−3.05	0.204 ± 0.033	0.130 ± 0.037	0.212 ± 0.057	0.199 ± 0.046
−3.15	0.218 ± 0.033	0.265 ± 0.047	0.207 ± 0.054	0.209 ± 0.045
−3.25	0.229 ± 0.033	0.290 ± 0.047	0.224 ± 0.056	0.260 ± 0.049
−3.35	0.326 ± 0.037	0.367 ± 0.051	0.271 ± 0.057	0.275 ± 0.049
−3.45	0.301 ± 0.035	0.347 ± 0.049	0.379 ± 0.065	0.314 ± 0.051
−3.55	0.311 ± 0.036	0.282 ± 0.044	0.271 ± 0.055	0.333 ± 0.051
−3.65	0.313 ± 0.035	0.292 ± 0.045	0.274 ± 0.051	0.284 ± 0.046
−3.75	0.257 ± 0.032	0.274 ± 0.043	0.367 ± 0.062	0.252 ± 0.043
−3.85	0.380 ± 0.038	0.254 ± 0.041	0.192 ± 0.042	0.227 ± 0.041
−3.95	0.351 ± 0.037	0.219 ± 0.039	0.275 ± 0.052	0.266 ± 0.043
−4.05	0.385 ± 0.039	0.283 ± 0.044	0.351 ± 0.061	0.212 ± 0.039
−4.15	0.296 ± 0.036	0.219 ± 0.038	0.268 ± 0.051	0.175 ± 0.036
−4.25	0.241 ± 0.033	0.256 ± 0.043	0.271 ± 0.053	0.237 ± 0.042
−4.35	0.193 ± 0.031	0.240 ± 0.043	0.241 ± 0.053	0.189 ± 0.038
−4.45	0.300 ± 0.038	0.318 ± 0.049	0.236 ± 0.054	0.223 ± 0.042
−4.55	0.166 ± 0.031	0.168 ± 0.039	0.185 ± 0.049	0.138 ± 0.035
−4.65	0.206 ± 0.035	0.123 ± 0.036	0.146 ± 0.042	0.325 ± 0.051
−4.75	0.233 ± 0.039	0.178 ± 0.042	0.231 ± 0.056	0.134 ± 0.037
−4.85	0.159 ± 0.036	0.217 ± 0.047	0.258 ± 0.058	0.181 ± 0.042
−4.95	0.313 ± 0.051	0.148 ± 0.043	0.225 ± 0.060	0.217 ± 0.047
−5.05	0.388 ± 0.064	0.150 ± 0.048	0.215 ± 0.063	0.214 ± 0.047
−5.15	0.349 ± 0.068	0.337 ± 0.075	0.224 ± 0.068	0.190 ± 0.047
−5.25		0.342 ± 0.083	0.272 ± 0.085	0.331 ± 0.063
−5.35			0.315 ± 0.098	0.238 ± 0.062
−5.45			0.444 ± 0.133	0.313 ± 0.079
−5.55				0.342 ± 0.096

TABLE III. *(Continued.)*

t [(GeV/c)^2] \ Momenta (GeV/c)	$\pi^- p \to \pi^- p$ 5.229	5.364	5.460	5.554
−2.65	0.304 ± 0.063			
−2.75	0.197 ± 0.045	0.138 ± 0.052	0.108 ± 0.063	
−2.85	0.174 ± 0.039	0.0594 ± 0.0335	0.112 ± 0.052	0.0776 ± 0.0436
−2.95	0.209 ± 0.039	0.118 ± 0.040	0.205 ± 0.062	0.104 ± 0.043
−3.05	0.1000 ± 0.0290	0.142 ± 0.040	0.142 ± 0.053	0.160 ± 0.047
−3.15	0.226 ± 0.037	0.214 ± 0.046	0.240 ± 0.060	0.292 ± 0.055
−3.25	0.232 ± 0.037	0.300 ± 0.051	0.280 ± 0.063	0.272 ± 0.051
−3.35	0.268 ± 0.038	0.294 ± 0.050	0.351 ± 0.067	0.272 ± 0.049
−3.45	0.290 ± 0.039	0.275 ± 0.048	0.254 ± 0.053	0.254 ± 0.045
−3.55	0.184 ± 0.031	0.196 ± 0.040	0.296 ± 0.056	0.306 ± 0.049
−3.65	0.278 ± 0.036	0.298 ± 0.047	0.285 ± 0.053	0.287 ± 0.046
−3.75	0.178 ± 0.030	0.309 ± 0.048	0.205 ± 0.046	0.174 ± 0.036
−3.85	0.184 ± 0.029	0.224 ± 0.041	0.343 ± 0.059	0.308 ± 0.046
−3.95	0.204 ± 0.031	0.159 ± 0.034	0.224 ± 0.047	0.201 ± 0.038
−4.05	0.185 ± 0.029	0.172 ± 0.036	0.239 ± 0.047	0.194 ± 0.037
−4.15	0.143 ± 0.026	0.239 ± 0.040	0.164 ± 0.042	0.149 ± 0.032
−4.25	0.173 ± 0.028	0.150 ± 0.033	0.167 ± 0.039	0.150 ± 0.032
−4.35	0.162 ± 0.028	0.144 ± 0.032	0.165 ± 0.040	0.167 ± 0.033
−4.45	0.164 ± 0.028	0.199 ± 0.038	0.133 ± 0.038	0.161 ± 0.033
−4.55	0.180 ± 0.030	0.148 ± 0.034	0.155 ± 0.037	0.104 ± 0.028
−4.65	0.221 ± 0.034	0.136 ± 0.032	0.192 ± 0.046	0.145 ± 0.032
−4.75	0.158 ± 0.029	0.191 ± 0.039	0.166 ± 0.040	0.116 ± 0.030
−4.85	0.170 ± 0.031	0.166 ± 0.037	0.136 ± 0.038	0.111 ± 0.030
−4.95	0.176 ± 0.032	0.123 ± 0.033	0.0988 ± 0.0369	0.154 ± 0.034
−5.05	0.224 ± 0.036	0.172 ± 0.038	0.108 ± 0.040	0.105 ± 0.029
−5.15	0.205 ± 0.035	0.171 ± 0.040	0.121 ± 0.042	0.0875 ± 0.0281
−5.25	0.193 ± 0.036	0.196 ± 0.043	0.135 ± 0.043	0.166 ± 0.038
−5.35	0.210 ± 0.040	0.291 ± 0.052	0.142 ± 0.042	0.189 ± 0.040
−5.45	0.191 ± 0.044	0.168 ± 0.044	0.292 ± 0.066	0.162 ± 0.038
−5.55	0.205 ± 0.051	0.103 ± 0.039	0.211 ± 0.059	0.230 ± 0.045
−5.65	0.257 ± 0.071	0.249 ± 0.062	0.192 ± 0.061	0.196 ± 0.044
−5.75		0.0696 ± 0.0441	0.141 ± 0.052	0.209 ± 0.049
−5.85			0.146 ± 0.061	0.192 ± 0.051
−5.95				0.201 ± 0.056
−6.05				0.198 ± 0.063

t [(GeV/c)^2] \ Momenta (GeV/c)	$\pi^- p \to \pi^- p$ 5.647	5.792	5.896	5.998
−2.75	0.0779 ± 0.0487			
−2.85	0.0914 ± 0.0471	0.131 ± 0.051		
−2.95	0.0412 ± 0.0285	0.163 ± 0.050	0.166 ± 0.070	
−3.05	0.237 ± 0.043	0.186 ± 0.050	0.226 ± 0.073	0.224 ± 0.061
−3.15	0.220 ± 0.040	0.208 ± 0.046	0.267 ± 0.067	0.189 ± 0.051
−3.25	0.228 ± 0.037	0.352 ± 0.056	0.238 ± 0.059	0.172 ± 0.044
−3.35	0.204 ± 0.034	0.239 ± 0.044	0.407 ± 0.072	0.298 ± 0.052
−3.45	0.210 ± 0.033	0.321 ± 0.049	0.141 ± 0.040	0.357 ± 0.055
−3.55	0.339 ± 0.039	0.297 ± 0.045	0.311 ± 0.056	0.293 ± 0.049
−3.65	0.358 ± 0.040	0.250 ± 0.042	0.361 ± 0.059	0.241 ± 0.043
−3.75	0.228 ± 0.032	0.289 ± 0.044	0.222 ± 0.046	0.286 ± 0.045
−3.85	0.207 ± 0.030	0.279 ± 0.043	0.286 ± 0.054	0.274 ± 0.043
−3.95	0.176 ± 0.028	0.284 ± 0.042	0.229 ± 0.047	0.253 ± 0.041
−4.05	0.245 ± 0.031	0.175 ± 0.033	0.221 ± 0.045	0.240 ± 0.039
−4.15	0.167 ± 0.026	0.214 ± 0.037	0.148 ± 0.036	0.181 ± 0.034
−4.25	0.151 ± 0.025	0.176 ± 0.033	0.204 ± 0.044	0.175 ± 0.033
−4.35	0.114 ± 0.022	0.125 ± 0.028	0.112 ± 0.029	0.149 ± 0.031
−4.45	0.0869 ± 0.0194	0.112 ± 0.026	0.121 ± 0.033	0.0751 ± 0.0225
−4.55	0.0816 ± 0.0188	0.137 ± 0.029	0.132 ± 0.033	0.0895 ± 0.0238
−4.65	0.0414 ± 0.0152	0.104 ± 0.025	0.122 ± 0.030	0.150 ± 0.029

TABLE III. *(Continued.)*

t [(GeV/c)^2] \ Momenta (GeV/c)	$\pi^- p \to \pi^- p$ 5.647	5.792	5.896	5.998
−4.75	0.110 ±0.022	0.0851 ± 0.0230	0.119 ±0.030	0.161 ±0.031
−4.85	0.120 ±0.023	0.121 ±0.028	0.0981 ± 0.0310	0.0724 ± 0.0220
−4.95	0.160 ±0.026	0.147 ±0.031	0.115 ±0.031	0.0995 ± 0.0253
−5.05	0.116 ±0.023	0.103 ±0.026	0.107 ±0.034	0.122 ±0.028
−5.15	0.114 ±0.023	0.110 ±0.029	0.110 ±0.032	0.0394 ± 0.0179
−5.25	0.146 ±0.026	0.150 ±0.032	0.0888 ± 0.0295	0.0974 ± 0.0261
−5.35	0.121 ±0.025	0.0826 ± 0.0246	0.0795 ± 0.0267	0.0613 ± 0.0219
−5.45	0.156 ±0.029	0.0826 ± 0.0250	0.148 ±0.039	0.105 ±0.027
−5.55	0.139 ±0.028	0.108 ±0.031	0.166 ±0.044	0.123 ±0.030
−5.65	0.149 ±0.029	0.116 ±0.031	0.0971 ± 0.0359	0.109 ±0.029
−5.75	0.179 ±0.033	0.124 ±0.033	0.0899 ± 0.0308	0.115 ±0.030
−5.85	0.157 ±0.034	0.204 ±0.041	0.101 ±0.036	0.223 ±0.041
−5.95	0.152 ±0.036	0.121 ±0.039	0.230 ±0.054	0.147 ±0.035
−6.05	0.143 ±0.037	0.112 ±0.038	0.147 ±0.051	0.110 ±0.032
−6.15	0.0407 ± 0.0280	0.229 ±0.054	0.112 ±0.042	0.178 ±0.040
−6.25	0.231 ±0.079	0.167 ±0.053	0.0482 ± 0.0304	0.0899 ± 0.0320
−6.35		0.119 ±0.052	0.121 ±0.051	0.107 ±0.037
−6.45			0.100 ±0.059	0.0885 ± 0.0380
−6.55			0.167 ±0.075	0.146 ±0.050
−6.65				0.0884 ± 0.0477

t [(GeV/c)^2] \ Momenta (GeV/c)	$\pi^- p \to \pi^- p$ 6.099	6.257	6.368	6.478
−3.3	0.168 ±0.029	0.199 ±0.031	0.153 ±0.035	
−3.5	0.198 ±0.028	0.197 ±0.027	0.184 ±0.033	0.205 ±0.031
−3.7	0.247 ±0.028	0.155 ±0.022	0.197 ±0.029	0.173 ±0.026
−3.9	0.126 ±0.020	0.140 ±0.019	0.174 ±0.027	0.218 ±0.026
−4.1	0.124 ±0.019	0.153 ±0.019	0.131 ±0.021	0.161 ±0.021
−4.3	0.151 ±0.018	0.119 ±0.017	0.132 ±0.021	0.0919 ± 0.0159
−4.5	0.147 ±0.017	0.106 ±0.015	0.100 ±0.017	0.0864 ± 0.0148
−4.7	0.131 ±0.015	0.0856 ± 0.0138	0.115 ±0.019	0.0906 ± 0.0146
−4.9	0.116 ±0.014	0.0955 ± 0.0140	0.0982 ± 0.0170	0.0835 ± 0.0139
−5.1	0.0968 ± 0.0128	0.0910 ± 0.0137	0.0770 ± 0.0142	0.0810 ± 0.0134
−5.3	0.0966 ± 0.0131	0.0942 ± 0.0139	0.0638 ± 0.0140	0.0722 ± 0.0127
−5.5	0.116 ±0.014	0.0741 ± 0.0129	0.0684 ± 0.0146	0.0778 ± 0.0131
−5.7	0.0953 ± 0.0130	0.0852 ± 0.0143	0.0648 ± 0.0147	0.0743 ± 0.0133
−5.9	0.0963 ± 0.0138	0.0738 ± 0.0139	0.0967 ± 0.0178	0.0650 ± 0.0130
−6.1	0.0943 ± 0.0141	0.0925 ± 0.0156	0.0709 ± 0.0167	0.0562 ± 0.0130
−6.3	0.0903 ± 0.0145	0.0610 ± 0.0139	0.0615 ± 0.0167	0.0713 ± 0.0147
−6.5	0.0919 ± 0.0158	0.101 ±0.019	0.0707 ± 0.0190	0.0562 ± 0.0141
−6.7	0.107 ±0.018	0.0480 ± 0.0159	0.0583 ± 0.0202	0.0671 ± 0.0159
−6.9	0.166 ±0.030	0.0646 ± 0.0227	0.0971 ± 0.0275	0.0724 ± 0.0177
−7.1	0.152 ±0.030			0.0751 ± 0.0212
−7.3	0.134 ±0.030			
−7.5	0.118 ±0.033			
−7.7	0.0768 ± 0.0340			

t [(GeV/c)^2] \ Momenta (GeV/c)	$\pi^- p \to \pi^- p$ 6.587	6.757	6.878	6.997
−3.5	0.186 ±0.022	0.126 ±0.023		
−3.7	0.148 ±0.017	0.141 ±0.020	0.122 ±0.024	0.165 ±0.026
−3.9	0.172 ±0.017	0.135 ±0.018	0.144 ±0.024	0.147 ±0.022
−4.1	0.143 ±0.014	0.139 ±0.017	0.145 ±0.021	0.134 ±0.019
−4.3	0.110 ±0.012	0.0849 ± 0.0125	0.136 ±0.019	0.110 ±0.016

TABLE III. *(Continued.)*

t [(GeV/c)^2]	$\pi^- p \to \pi^- p$ Momenta (GeV/c) 6.587	6.757	6.878	6.997
−4.5	0.0980 ± 0.0108	0.0824 ± 0.0120	0.131 ± 0.018	0.0967 ± 0.0140
−4.7	0.0846 ± 0.0097	0.0883 ± 0.0114	0.104 ± 0.015	0.0703 ± 0.0115
−4.9	0.0773 ± 0.0090	0.0925 ± 0.0112	0.0945 ± 0.0147	0.0651 ± 0.0106
−5.1	0.0883 ± 0.0094	0.0695 ± 0.0096	0.0578 ± 0.0114	0.0737 ± 0.0109
−5.3	0.0792 ± 0.0089	0.0681 ± 0.0093	0.0772 ± 0.0120	0.0529 ± 0.0091
−5.5	0.0591 ± 0.0079	0.0824 ± 0.0103	0.0713 ± 0.0114	0.0696 ± 0.0100
−5.7	0.0760 ± 0.0089	0.0626 ± 0.0092	0.0494 ± 0.0101	0.0729 ± 0.0102
−5.9	0.0564 ± 0.0081	0.0806 ± 0.0107	0.0511 ± 0.0104	0.0601 ± 0.0093
−6.1	0.0577 ± 0.0085	0.0397 ± 0.0081	0.0643 ± 0.0120	0.0544 ± 0.0091
−6.3	0.0599 ± 0.0090	0.0510 ± 0.0091	0.0636 ± 0.0121	0.0562 ± 0.0093
−6.5	0.0571 ± 0.0091	0.0424 ± 0.0091	0.0431 ± 0.0096	0.0533 ± 0.0095
−6.7	0.0563 ± 0.0096	0.0586 ± 0.0108	0.0378 ± 0.0102	0.0529 ± 0.0099
−6.9	0.0736 ± 0.0112	0.0344 ± 0.0092	0.0253 ± 0.0099	0.0422 ± 0.0095
−7.1	0.0348 ± 0.0094	0.0683 ± 0.0129	0.0498 ± 0.0116	0.0336 ± 0.0095
−7.3	0.0470 ± 0.0126	0.0699 ± 0.0145	0.0246 ± 0.0118	0.0390 ± 0.0105
−7.5		0.0430 ± 0.0151	0.0239 ± 0.0130	0.0351 ± 0.0112
−7.7			0.0505 ± 0.0209	0.0351 ± 0.0127

t [(GeV/c)^2]	$\pi^- p \to \pi^- p$ Momenta (GeV/c) 7.115	7.298	7.428	7.557
−3.7	0.100 ± 0.029			
−3.9	0.156 ± 0.024	0.0827 ± 0.0310	0.129 ± 0.045	
−4.1	0.0992 ± 0.0151	0.101 ± 0.021	0.126 ± 0.029	0.0719 ± 0.0215
−4.3	0.128 ± 0.015	0.119 ± 0.020	0.112 ± 0.023	0.113 ± 0.022
−4.5	0.102 ± 0.013	0.0626 ± 0.0139	0.0855 ± 0.0190	0.0807 ± 0.0177
−4.7	0.0725 ± 0.0100	0.0560 ± 0.0120	0.0780 ± 0.0165	0.0495 ± 0.0132
−4.9	0.0669 ± 0.0090	0.0941 ± 0.0138	0.0952 ± 0.0166	0.0644 ± 0.0138
−5.1	0.0779 ± 0.0092	0.0520 ± 0.0101	0.0427 ± 0.0112	0.0453 ± 0.0111
−5.3	0.0661 ± 0.0082	0.0493 ± 0.0093	0.0600 ± 0.0119	0.0478 ± 0.0104
−5.5	0.0698 ± 0.0079	0.0423 ± 0.0081	0.0660 ± 0.0116	0.0327 ± 0.0084
−5.7	0.0498 ± 0.0068	0.0477 ± 0.0083	0.0477 ± 0.0098	0.0495 ± 0.0095
−5.9	0.0545 ± 0.0069	0.0565 ± 0.0087	0.0391 ± 0.0088	0.0208 ± 0.0066
−6.1	0.0514 ± 0.0067	0.0412 ± 0.0073	0.0313 ± 0.0078	0.0381 ± 0.0079
−6.3	0.0431 ± 0.0062	0.0449 ± 0.0075	0.0461 ± 0.0090	0.0378 ± 0.0078
−6.5	0.0353 ± 0.0057	0.0431 ± 0.0074	0.0261 ± 0.0071	0.0170 ± 0.0058
−6.7	0.0281 ± 0.0054	0.0384 ± 0.0074	0.0222 ± 0.0069	0.0396 ± 0.0082
−6.9	0.0266 ± 0.0054	0.0190 ± 0.0059	0.0496 ± 0.0097	0.0310 ± 0.0076
−7.1	0.0340 ± 0.0061	0.0219 ± 0.0063	0.0262 ± 0.0077	0.0141 ± 0.0060
−7.3	0.0203 ± 0.0054	0.0200 ± 0.0063	0.0292 ± 0.0082	0.0285 ± 0.0079
−7.5	0.0162 ± 0.0053	0.0154 ± 0.0061	0.0308 ± 0.0089	0.0273 ± 0.0083
−7.7	0.0344 ± 0.0072	0.0176 ± 0.0066	0.0163 ± 0.0072	0.0277 ± 0.0086
−7.9	0.0312 ± 0.0072	0.0179 ± 0.0069	0.0106 ± 0.0068	0.0179 ± 0.0080
−8.1	0.0150 ± 0.0063	0.0288 ± 0.0084	0.0319 ± 0.0104	0.0247 ± 0.0096
−8.3		$(0.870 \pm 0.615) \times 10^{-2}$	0.0137 ± 0.0081	0.0133 ± 0.0083
−8.5	0.0109 ± 0.0066	0.0133 ± 0.0074	0.0113 ± 0.0083	0.0273 ± 0.0116
−8.7				0.0194 ± 0.0111

TABLE III. *(Continued.)*

t [(GeV/c)^2] \ Momenta (GeV/c)	$\pi^- p \to \pi^- p$ 7.684	7.882	8.022	8.161
−4.1	0.0875 ± 0.0301			
−4.3	0.0511 ± 0.0213			
−4.5	0.0984 ± 0.0176	0.0759 ± 0.0228	0.0740 ± 0.0263	0.0820 ± 0.0277
−4.7	0.0353 ± 0.0106	0.0594 ± 0.0181	0.117 ± 0.029	0.0555 ± 0.0207
−4.9	0.0556 ± 0.0116	0.0475 ± 0.0147	0.0592 ± 0.0187	0.0764 ± 0.0208
−5.1	0.0514 ± 0.0098	0.0644 ± 0.0145	0.0842 ± 0.0196	0.0441 ± 0.0148
−5.3	0.0445 ± 0.0087	0.0755 ± 0.0143	0.0538 ± 0.0143	0.0313 ± 0.0114
−5.5	0.0605 ± 0.0093	0.0544 ± 0.0116	0.0644 ± 0.0146	0.0267 ± 0.0102
−5.7	0.0318 ± 0.0067	0.0112 ± 0.0061	0.0382 ± 0.0108	0.0112 ± 0.0069
−5.9	0.0481 ± 0.0076	0.0218 ± 0.0071	0.0230 ± 0.0085	0.0324 ± 0.0094
−6.1	0.0363 ± 0.0063	0.0197 ± 0.0064	0.0312 ± 0.0090	0.0332 ± 0.0089
−6.3	0.0202 ± 0.0050	0.0319 ± 0.0075	0.0230 ± 0.0078	0.0277 ± 0.0079
−6.5	0.0151 ± 0.0045	0.0289 ± 0.0070	0.0212 ± 0.0073	0.0242 ± 0.0072
−6.7	0.0280 ± 0.0055	0.0131 ± 0.0052	$(0.939 \pm 0.543)\times 10^{-2}$	0.0165 ± 0.0061
−6.9	0.0126 ± 0.0042	0.0284 ± 0.0068	0.0236 ± 0.0074	0.0209 ± 0.0066
−7.1	0.0188 ± 0.0048	0.0176 ± 0.0057	0.0179 ± 0.0067	0.0306 ± 0.0078
−7.3	0.0169 ± 0.0048	0.0164 ± 0.0056	0.0199 ± 0.0071	0.0329 ± 0.0082
−7.5	$(0.997 \pm 0.425)\times 10^{-2}$	0.0194 ± 0.0061	$(0.531 \pm 0.504)\times 10^{-2}$	0.0143 ± 0.0061
−7.7	0.0190 ± 0.0054	0.0176 ± 0.0061	0.0197 ± 0.0074	0.0116 ± 0.0058
−7.9	0.0178 ± 0.0054	0.0276 ± 0.0074	$(0.879 \pm 0.592)\times 10^{-2}$	0.0145 ± 0.0065
−8.1	$(0.667 \pm 0.415)\times 10^{-2}$	0.0103 ± 0.0057	0.0125 ± 0.0070	0.0140 ± 0.0069
−8.3	0.0125 ± 0.0059	$(0.767 \pm 0.561)\times 10^{-2}$	0.0213 ± 0.0086	0.0271 ± 0.0091
−8.5	0.0123 ± 0.0056		0.0161 ± 0.0083	
−8.7	$(0.781 \pm 0.513)\times 10^{-2}$		$(0.687 \pm 0.676)\times 10^{-2}$	
−8.9	0.0121 ± 0.0063		0.0275 ± 0.0113	0.0244 ± 0.0106
−9.1	$(0.939 \pm 0.650)\times 10^{-2}$	0.0170 ± 0.0087	$(0.905 \pm 0.814)\times 10^{-2}$	
−9.5		0.0110 ± 0.0088	0.0137 ± 0.0109	

t [(GeV/c)^2] \ Momenta (GeV/c)	$\pi^- p \to \pi^- p$ 8.298	8.512	8.663	8.813
−4.5	0.0345 ± 0.0105	0.0624 ± 0.0147		
−4.7	0.0482 ± 0.0103	0.0572 ± 0.0130		
−4.9	0.0477 ± 0.0098	0.0544 ± 0.0117	0.0293 ± 0.0113	0.0166 ± 0.0095
−5.1	0.0377 ± 0.0078	0.0310 ± 0.0081	0.0311 ± 0.0101	0.0325 ± 0.0109
−5.3	0.0493 ± 0.0083	0.0349 ± 0.0079	0.0460 ± 0.0102	0.0432 ± 0.0099
−5.5	0.0392 ± 0.0068	0.0195 ± 0.0056	0.0251 ± 0.0083	0.0238 ± 0.0069
−5.7	0.0353 ± 0.0061	0.0185 ± 0.0051	0.0238 ± 0.0066	0.0212 ± 0.0071
−5.9	0.0353 ± 0.0056	0.0234 ± 0.0053	0.0255 ± 0.0063	0.0191 ± 0.0053
−6.1	0.0218 ± 0.0043	0.0165 ± 0.0042	0.0184 ± 0.0051	0.0106 ± 0.0040
−6.3	0.0273 ± 0.0044	0.0137 ± 0.0036	0.0229 ± 0.0054	$(0.873 \pm 0.370)\times 10^{-2}$
−6.5	0.0183 ± 0.0036	0.0161 ± 0.0037	0.0163 ± 0.0044	0.0118 ± 0.0038
−6.7	0.0158 ± 0.0032	0.0121 ± 0.0032	0.0101 ± 0.0040	0.0108 ± 0.0035
−6.9	0.0111 ± 0.0027	0.0120 ± 0.0030	0.0149 ± 0.0039	0.0124 ± 0.0035
−7.1	0.0138 ± 0.0029	$(0.501 \pm 0.230)\times 10^{-2}$	$(0.830 \pm 0.300)\times 10^{-2}$	$(0.760 \pm 0.273)\times 10^{-2}$
−7.3	0.0134 ± 0.0031	0.0181 ± 0.0034	$(0.538 \pm 0.292)\times 10^{-2}$	$(0.947 \pm 0.290)\times 10^{-2}$
−7.5	0.0165 ± 0.0032	0.0108 ± 0.0031	0.0142 ± 0.0035	$(0.546 \pm 0.284)\times 10^{-2}$
−7.7	0.0102 ± 0.0027	0.0157 ± 0.0032	0.0108 ± 0.0038	0.0131 ± 0.0033
−7.9	0.0136 ± 0.0030	0.0152 ± 0.0032	$(0.777 \pm 0.340)\times 10^{-2}$	$(0.712 \pm 0.318)\times 10^{-2}$
−8.1	0.0109 ± 0.0029	$(0.754 \pm 0.257)\times 10^{-2}$	$(0.789 \pm 0.352)\times 10^{-2}$	0.0101 ± 0.0031
−8.3	$(0.762 \pm 0.277)\times 10^{-2}$	$(0.666 \pm 0.251)\times 10^{-2}$	0.0120 ± 0.0036	0.0118 ± 0.0034
−8.5	0.0138 ± 0.0034	0.0136 ± 0.0038	0.0107 ± 0.0036	$(0.625 \pm 0.550)\times 10^{-2}$
−8.7	$(0.725 \pm 0.293)\times 10^{-2}$	$(0.532 \pm 0.266)\times 10^{-2}$	0.0124 ± 0.0039	$(0.992 \pm 0.425)\times 10^{-2}$
−8.9	0.0104 ± 0.0032	0.0116 ± 0.0035	$(0.862 \pm 0.425)\times 10^{-2}$	0.0125 ± 0.0040
−9.1	$(0.362 \pm 0.254)\times 10^{-2}$	0.0104 ± 0.0035	0.0116 ± 0.0042	$(0.777 \pm 0.425)\times 10^{-2}$
−9.3	$0.656 \pm 0.315)\times 10^{-2}$	0.0128 ± 0.0042	$(0.534 \pm 0.413)\times 10^{-2}$	0.0212 ± 0.0062
−9.5	$(0.679 \pm 0.347)\times 10^{-2}$	0.0139 ± 0.0046		$(0.700 \pm 0.453)\times 10^{-2}$
−9.7	$(0.684 \pm 0.342)\times 10^{-2}$	0.0115 ± 0.0045	0.0125 ± 0.0111	$(0.984 \pm 0.526)\times 10^{-2}$

TABLE III. *(Continued.)*

t [(GeV/c)^2]	$\pi^- p \to \pi^- p$ Momenta (GeV/c) 8.962	9.193	9.357	9.519
−4.9	0.0175 ± 0.0092			
−5.1	0.0139 ± 0.0073	0.0414 ± 0.0198		
−5.3	0.0231 ± 0.0078	0.0309 ± 0.0172		
−5.5	0.0186 ± 0.0085	0.0114 ± 0.0101		
−5.7	0.0137 ± 0.0058	0.0522 ± 0.0175	0.0301 ± 0.0193	
−5.9	0.0143 ± 0.0049	0.0215 ± 0.0111		
−6.1	0.0205 ± 0.0052	0.0275 ± 0.0116		0.0294 ± 0.0176
−6.3	0.0117 ± 0.0041	0.0243 ± 0.0104	0.0180 ± 0.0120	0.0172 ± 0.0130
−6.5	0.0107 ± 0.0040	0.0182 ± 0.0087		
−6.7	0.0108 ± 0.0035	0.0102 ± 0.0066	0.0139 ± 0.0096	0.0255 ± 0.0135
−6.9	(0.853 ± 0.301)×10^{-2}	(0.925 ± 0.616)×10^{-2}		
−7.1	(0.800 ± 0.306)×10^{-2}	(0.593 ± 0.511)×10^{-2}		
−7.3	(0.989 ± 0.409)×10^{-2}	0.0130 ± 0.0065		0.0102 ± 0.0082
−7.5	(0.826 ± 0.307)×10^{-2}	(0.775 ± 0.517)×10^{-2}		
−7.7	0.0146 ± 0.0051		(0.981 ± 0.687)×10^{-2}	
−7.9	(0.886 ± 0.288)×10^{-2}		0.0130 ± 0.0075	
−8.1	(0.284 ± 0.230)×10^{-2}	(0.504 ± 0.416)×10^{-2}		
−8.3	(0.874 ± 0.290)×10^{-2}	0.0112 ± 0.0055		(0.902 ± 0.694)×10^{-2}
−8.5	(0.506 ± 0.321)×10^{-2}			0.0132 ± 0.0081
−8.7	(0.836 ± 0.310)×10^{-2}	(0.517 ± 0.417)×10^{-2}		
−8.9	(0.612 ± 0.310)×10^{-2}			
−9.1	(0.733 ± 0.337)×10^{-2}		0.0110 ± 0.0074	
−9.3	(0.994 ± 0.383)×10^{-2}			
−9.5	(0.903 ± 0.370)×10^{-2}		0.0171 ± 0.0093	
−9.7				
−9.9	(0.616 ± 0.350)×10^{-2}			
−10.1	0.0119 ± 0.0059			
−10.3		(0.906 ± 0.689)×10^{-2}		
−10.5				
−10.7				0.0135 ± 0.0130
−10.9	(0.992 ± 0.704)×10^{-2}			

t [(GeV/c)^2]	$\pi^+ p \to \pi^+ p$ Momenta (GeV/c) 1.896	1.945	1.980	2.014
−0.725	610 ± 44	824 ± 52	744 ± 59	
−0.775	753 ± 48	777 ± 47	719 ± 53	666 ± 45
−0.825	886 ± 53	895 ± 51	751 ± 51	697 ± 44
−0.875	881 ± 50	870 ± 49	811 ± 55	810 ± 47
−0.925	886 ± 50	984 ± 52	838 ± 54	766 ± 44
−0.975	869 ± 46	951 ± 48	809 ± 53	878 ± 47
−1.025	919 ± 44	1030 ± 46	984 ± 54	817 ± 43
−1.075	986 ± 41	958 ± 42	1070 ± 52	855 ± 40
−1.125	1060 ± 41	1030 ± 40	941 ± 45	886 ± 39
−1.175	1000 ± 39	1090 ± 39	995 ± 44	997 ± 38
−1.225	1130 ± 43	1020 ± 38	918 ± 40	969 ± 35
−1.275	1120 ± 44	1200 ± 42	1090 ± 45	883 ± 33
−1.325	1000 ± 45	1130 ± 44	1090 ± 46	1090 ± 38
−1.375	990 ± 50	1050 ± 46	994 ± 49	1090 ± 40
−1.425	882 ± 48	881 ± 45	902 ± 50	963 ± 40
−1.475	771 ± 47	796 ± 46	881 ± 54	828 ± 40
−1.525	974 ± 57	723 ± 45	718 ± 50	836 ± 45
−1.575	846 ± 56	899 ± 54	899 ± 60	647 ± 41
−1.625	962 ± 67	985 ± 59	814 ± 58	684 ± 44
−1.675	1110 ± 78	1100 ± 69	719 ± 58	636 ± 43
−1.725			825 ± 71	741 ± 50
−1.775			847 ± 75	744 ± 55

TABLE III. *(Continued.)*

t [(GeV/c)^2] \ Momenta (GeV/c)	$\pi^+p \to \pi^+p$ 2.049	2.102	2.139	2.176
−0.775	594 ± 32	663 ± 43		
−0.825	654 ± 31	540 ± 35	523 ± 43	621 ± 41
−0.875	662 ± 31	611 ± 36	594 ± 42	538 ± 35
−0.925	790 ± 34	673 ± 38	720 ± 46	623 ± 36
−0.975	742 ± 31	685 ± 37	634 ± 42	637 ± 35
−1.025	776 ± 31	709 ± 38	709 ± 44	621 ± 34
−1.075	848 ± 32	784 ± 38	756 ± 44	702 ± 36
−1.125	847 ± 29	699 ± 34	685 ± 39	688 ± 34
−1.175	859 ± 27	813 ± 34	765 ± 39	677 ± 32
−1.225	940 ± 27	855 ± 33	773 ± 37	686 ± 30
−1.275	815 ± 24	807 ± 31	768 ± 35	765 ± 29
−1.325	884 ± 25	742 ± 28	731 ± 33	684 ± 27
−1.375	915 ± 26	810 ± 30	666 ± 31	608 ± 25
−1.425	869 ± 27	883 ± 32	722 ± 32	603 ± 24
−1.475	768 ± 27	799 ± 32	811 ± 36	768 ± 28
−1.525	697 ± 28	618 ± 31	714 ± 37	625 ± 26
−1.575	600 ± 28	654 ± 33	558 ± 33	548 ± 26
−1.625	633 ± 30	522 ± 31	489 ± 34	498 ± 26
−1.675	583 ± 29	522 ± 33	483 ± 36	491 ± 28
−1.725	588 ± 31	585 ± 36	484 ± 37	420 ± 27
−1.775	624 ± 34	570 ± 37	483 ± 38	423 ± 29
−1.825	771 ± 41	553 ± 39	458 ± 39	368 ± 27
−1.875	569 ± 47	631 ± 46	401 ± 39	369 ± 28
−1.925		566 ± 45	615 ± 54	383 ± 31
−1.975				343 ± 32

t [(GeV/c)^2] \ Momenta (GeV/c)	$\pi^+p \to \pi^+p$ 2.223	2.281	2.321	2.362
−0.875	482 ± 25			
−0.925	498 ± 24	468 ± 30		
−0.975	514 ± 23	489 ± 29	462 ± 32	432 ± 27
−1.025	535 ± 23	557 ± 30	475 ± 31	410 ± 25
−1.075	599 ± 25	501 ± 28	501 ± 31	429 ± 24
−1.125	547 ± 22	527 ± 28	569 ± 34	476 ± 25
−1.175	549 ± 21	465 ± 24	583 ± 32	472 ± 25
−1.225	581 ± 20	546 ± 24	521 ± 28	431 ± 22
−1.275	605 ± 19	572 ± 24	577 ± 28	496 ± 22
−1.325	597 ± 18	565 ± 22	583 ± 27	506 ± 21
−1.375	536 ± 16	558 ± 21	572 ± 25	500 ± 20
−1.425	540 ± 16	524 ± 20	535 ± 23	460 ± 18
−1.475	539 ± 16	459 ± 18	479 ± 22	473 ± 18
−1.525	582 ± 17	541 ± 20	431 ± 21	371 ± 16
−1.575	468 ± 16	535 ± 21	560 ± 23	372 ± 15
−1.625	449 ± 17	478 ± 20	429 ± 21	424 ± 16
−1.675	402 ± 17	454 ± 21	455 ± 22	415 ± 17
−1.725	355 ± 17	326 ± 19	368 ± 21	350 ± 16
−1.775	328 ± 18	358 ± 21	293 ± 20	295 ± 15
−1.825	271 ± 17	255 ± 19	286 ± 22	253 ± 15
−1.875	247 ± 17	228 ± 19	235 ± 21	207 ± 15
−1.925	274 ± 18	214 ± 19	195 ± 21	204 ± 15
−1.975	281 ± 19	252 ± 22	179 ± 21	186 ± 16
−2.025	293 ± 23	245 ± 23	185 ± 22	148 ± 15
−2.075		232 ± 26	204 ± 25	144 ± 15
−2.125			222 ± 29	155 ± 17
−2.175				148 ± 18

TABLE III. *(Continued.)*

t [(GeV/c)^2] \ Momenta (GeV/c)	$\pi^+p \to \pi^+p$ 2.402	2.464	2.508	2.552
−1.05	467 ± 14			
−1.15	506 ± 14	506 ± 17	551 ± 22	448 ± 16
−1.25	502 ± 13	484 ± 16	518 ± 20	480 ± 16
−1.35	529 ± 12	495 ± 14	483 ± 17	437 ± 14
−1.45	477 ± 10	471 ± 12	475 ± 15	444 ± 12
−1.55	435 ± 9	452 ± 11	433 ± 13	435 ± 11
−1.65	412 ± 9	379 ± 10	352 ± 11	359 ± 9
−1.75	342 ± 8	394 ± 11	347 ± 11	294 ± 8
−1.85	273 ± 8	305 ± 10	271 ± 10	270 ± 8
−1.95	188 ± 8	223 ± 10	218 ± 11	208 ± 8
−2.05	147 ± 8	142 ± 9	155 ± 10	144 ± 7
−2.15	136 ± 8	117 ± 9	124 ± 10	82.8 ± 6.4
−2.25	181 ± 23	156 ± 12	98.5 ± 9.7	75.6 ± 6.8
−2.35			121 ± 13	88.6 ± 8.2

t [(GeV/c)^2] \ Momenta (GeV/c)	$\pi^+p \to \pi^+p$ 2.597	2.664	2.711	2.758
−1.25	438 ± 12	427 ± 15	392 ± 17	367 ± 14
−1.35	401 ± 10	360 ± 13	371 ± 15	333 ± 12
−1.45	406 ± 10	358 ± 12	351 ± 14	355 ± 12
−1.55	368 ± 8	352 ± 10	310 ± 12	308 ± 10
−1.65	341 ± 7	333 ± 9	315 ± 11	266 ± 9
−1.75	279 ± 6	271 ± 8	264 ± 9	240 ± 8
−1.85	262 ± 6	236 ± 7	209 ± 8	190 ± 6
−1.95	205 ± 6	217 ± 7	217 ± 8	168 ± 6
−2.05	135 ± 5	154 ± 7	163 ± 8	148 ± 6
−2.15	95.4 ± 5.0	112 ± 6	105 ± 7	102 ± 5
−2.25	63.4 ± 4.5	57.7 ± 5.2	64.5 ± 6.1	61.6 ± 4.4
−2.35	53.3 ± 4.6	44.2 ± 5.0	33.7 ± 5.3	45.6 ± 4.4
−2.45	62.1 ± 7.5	40.6 ± 5.4	21.9 ± 4.2	23.4 ± 3.5
−2.55		72.7 ± 7.9	45.6 ± 6.6	22.7 ± 3.7
−2.65				49.4 ± 5.9

t [(GeV/c)^2] \ Momenta (GeV/c)	$\pi^+p \to \pi^+p$ 2.797	2.869	2.920	2.971
−1.35	292 ± 14			
−1.45	283 ± 8	249 ± 10		
−1.55	279 ± 7	236 ± 8	232 ± 10	235 ± 9
−1.65	245 ± 6	218 ± 8	213 ± 9	200 ± 7
−1.75	218 ± 6	198 ± 7	176 ± 8	174 ± 7
−1.85	180 ± 5	157 ± 6	147 ± 7	151 ± 6
−1.95	147 ± 5	121 ± 6	119 ± 6	120 ± 5
−2.05	122 ± 4	110 ± 5	85.0 ± 5.2	86.4 ± 4.4
−2.15	96.9 ± 3.9	83.6 ± 4.6	91.3 ± 5.4	72.6 ± 4.1
−2.25	68.6 ± 3.4	68.1 ± 4.3	67.0 ± 4.8	59.5 ± 3.7
−2.35	36.9 ± 2.8	37.9 ± 3.4	45.8 ± 4.0	48.2 ± 3.4
−2.45	26.8 ± 2.8	20.6 ± 2.9	19.2 ± 2.6	28.9 ± 2.7
−2.55	24.3 ± 3.2	17.5 ± 3.2	21.1 ± 3.4	18.9 ± 2.4
−2.65	22.6 ± 4.5		15.1 ± 3.6	17.5 ± 2.7
−2.75	56.6 ± 7.7			10.4 ± 2.5

t [(GeV/c)^2] \ Momenta (GeV/c)	$\pi^+p \to \pi^+p$ 3.017	3.095	3.150	3.205
−1.55	166 ± 6			
−1.65	168 ± 5	131 ± 6	144 ± 8	117 ± 6
−1.75	150 ± 5	132 ± 5	133 ± 7	109 ± 5

TABLE III. *(Continued.)*

t [(GeV/c)^2] \ Momenta (GeV/c)	$\pi^+p \to \pi^+p$ 3.017	3.095	3.150	3.205
−1.85	125 ±4	98.6 ±4.5	104 ±6	78.0 ±3.9
−1.95	96.8±3.5	84.4 ±4.1	75.7 ±4.6	78.3 ±3.9
−2.05	78.3±3.2	67.1 ±3.6	64.5 ±4.2	58.2 ±3.2
−2.15	61.6±2.8	53.0 ±3.2	46.4 ±3.5	48.2 ±2.9
−2.25	57.0±2.7	43.7 ±2.9	43.5 ±3.5	33.1 ±2.4
−2.35	37.7±2.2	42.9 ±2.9	37.4 ±3.2	28.4 ±2.3
−2.45	24.6±1.8	27.3 ±2.4	28.7 ±2.9	24.3 ±2.1
−2.55	16.1±1.6	18.1 ±2.0	17.4 ±2.1	15.1 ±1.7
−2.65	12.4±1.5	11.9 ±1.7	10.1 ±1.8	10.3 ±1.4
−2.75	12.7±1.8	6.92±1.54	8.02±1.66	7.58±1.30
−2.85	10.1±3.1	11.9 ±2.3	9.21±2.05	7.36±1.36
−2.95			7.47±2.19	9.26±1.71
−3.05				12.7 ±2.5

t [(GeV/c)^2] \ Momenta (GeV/c)	$\pi^+p \to \pi^+p$ 3.266	3.350	3.410	3.469
−1.65	147 ±6	111 ±4		
−1.75	112 ±3	97.1 ±2.8	94.4 ±3.9	77.5 ±3.0
−1.85	95.8 ±3.0	82.6 ±2.4	74.6 ±3.1	68.0 ±2.4
−1.95	78.8 ±2.6	65.6 ±2.0	58.7 ±2.5	54.1 ±1.9
−2.05	66.3 ±2.3	50.6 ±1.7	46.7 ±2.2	42.2 ±1.6
−2.15	54.4 ±2.1	40.5 ±1.5	31.1 ±1.7	29.1 ±1.3
−2.25	36.8 ±1.7	28.0 ±1.2	26.8 ±1.6	21.3 ±1.1
−2.35	24.6 ±1.4	19.6 ±1.0	17.4 ±1.2	15.6 ±0.9
−2.45	23.8 ±1.4	15.7 ±0.9	13.6 ±1.1	10.3 ±0.7
−2.55	16.3 ±1.2	13.9 ±0.9	9.72±0.98	7.53±0.63
−2.65	12.4 ±1.0	9.13±0.71	8.87±0.92	6.60±0.60
−2.75	10.5 ±1.0	6.86±0.64	6.88±0.81	6.17±0.58
−2.85	8.96±0.93	6.71±0.63	7.08±0.84	5.70±0.56
−2.95	11.2 ±1.1	6.90±0.67	5.11±0.72	5.85±0.57
−3.05	13.0 ±1.4	9.46±0.87	6.78±0.82	5.73±0.59
−3.15	19.8 ±2.5	13.1 ±1.2	8.49±1.08	7.34±0.70
−3.25			10.5 ±1.5	10.9 ±1.0
−3.35				13.4 ±1.3

t [(GeV/c)^2] \ Momenta (GeV/c)	$\pi^+p \to \pi^+p$ 3.530	3.621	3.686	3.750
−1.85	56.8 ±1.9	64.1 ±2.6	44.0 ±2.6	
−1.95	45.0 ±1.5	49.6 ±2.0	36.5 ±2.0	35.1 ±1.7
−2.05	32.1 ±1.2	30.3 ±1.5	23.6 ±1.4	26.4 ±1.3
−2.15	24.2 ±1.0	23.1 ±1.2	19.8 ±1.2	17.5 ±1.0
−2.25	18.1 ±0.8	17.3 ±1.0	12.0 ±1.0	11.7 ±0.8
−2.35	13.2 ±0.7	11.5 ±0.8	8.28±0.81	8.23±0.65
−2.45	8.53±0.57	8.24±0.72	5.02±0.63	4.96±0.51
−2.55	5.43±0.45	4.88±0.55	3.27±0.47	2.70±0.37
−2.65	4.40±0.40	3.37±0.46	1.86±0.38	1.57±0.29
−2.75	3.28±0.36	2.63±0.41	1.73±0.38	1.43±0.27
−2.85	3.18±0.36	3.05±0.44	1.33±0.34	1.06±0.24
−2.95	3.75±0.39	2.08±0.39	1.57±0.37	1.25±0.26
−3.05	4.20±0.41	3.85±0.51	1.85±0.37	1.23±0.26
−3.15	5.35±0.49	3.17±0.48	1.57±0.34	1.85±0.32
−3.25	6.43±0.57	5.50±0.64	4.02±0.59	2.68±0.39
−3.35	8.08±0.73	7.28±0.78	2.60±0.45	4.04±0.48
−3.45	6.95±1.11	7.88±0.90	4.59±0.68	4.09±0.50
−3.55		9.43±1.15	6.47±0.89	5.63±0.62
−3.65			5.82±0.99	7.35±0.79
−3.75				6.16±0.83

TABLE III. *(Continued.)*

t [(GeV/c)^2] \ Momenta (GeV/c)	$\pi^+p \to \pi^+p$ 3.814	3.913	3.982	4.051
−1.85	45.9 ±2.7			
−1.95	29.9 ±1.4	33.8 ±1.9	30.1 ±2.0	
−2.05	22.8 ±1.0	23.6 ±1.3	22.2 ±1.4	20.4 ±1.3
−2.15	17.1 ±0.8	18.5 ±1.1	14.4 ±1.1	16.5 ±1.1
−2.25	10.7 ±0.6	11.4 ±0.8	7.98 ±0.70	10.9 ±0.8
−2.35	5.97 ±0.47	7.95 ±0.66	6.39 ±0.64	5.59 ±0.53
−2.45	3.73 ±0.36	3.71 ±0.43	3.36 ±0.45	4.47 ±0.47
−2.55	2.16 ±0.28	2.00 ±0.32	1.69 ±0.32	1.98 ±0.31
−2.65	1.49 ±0.23	1.13 ±0.25	1.31 ±0.28	0.924 ±0.221
−2.75	1.13 ±0.21	0.597 ±0.191	0.870 ±0.234	0.361 ±0.151
−2.85	0.910 ±0.184	0.977 ±0.225	0.370 ±0.168	0.464 ±0.166
−2.95	1.10 ±0.21	0.950 ±0.219	0.654 ±0.195	0.539 ±0.170
−3.05	1.37 ±0.22	1.26 ±0.25	0.662 ±0.186	0.592 ±0.177
−3.15	1.47 ±0.24	1.22 ±0.25	1.11 ±0.25	0.766 ±0.197
−3.25	1.53 ±0.24	1.21 ±0.25	1.01 ±0.26	0.863 ±0.209
−3.35	2.57 ±0.31	2.17 ±0.33	1.38 ±0.28	1.54 ±0.27
−3.45	3.15 ±0.35	2.24 ±0.36	1.72 ±0.32	1.44 ±0.26
−3.55	4.07 ±0.44	2.96 ±0.43	2.06 ±0.37	1.79 ±0.30
−3.65	3.62 ±0.43	3.32 ±0.50	1.65 ±0.33	2.54 ±0.36
−3.75	4.86 ±0.57	3.64 ±0.54	2.39 ±0.44	2.23 ±0.36
−3.85	3.26 ±0.71	4.29 ±0.69	2.70 ±0.50	2.93 ±0.44
−3.95		4.98 ±0.81	3.06 ±0.63	2.05 ±0.40
−4.05			4.52 ±0.82	3.81 ±0.61
−4.15				3.04 ±0.59

t [(GeV/c)^2] \ Momenta (GeV/c)	$\pi^+p \to \pi^+p$ 4.122	4.229	4.304	4.379
−2.05	21.4 ±1.0	17.3 ±1.1		
−2.15	14.4 ±0.7	13.6 ±0.8	10.3 ±0.8	12.1 ±0.9
−2.25	9.99 ±0.55	8.44 ±0.57	5.66 ±0.52	7.75 ±0.65
−2.35	5.77 ±0.39	6.37 ±0.45	4.74 ±0.44	5.81 ±0.50
−2.45	3.47 ±0.29	3.31 ±0.32	2.30 ±0.29	3.33 ±0.34
−2.55	1.65 ±0.20	1.53 ±0.21	1.26 ±0.21	1.76 ±0.24
−2.65	1.05 ±0.16	1.05 ±0.18	0.674 ±0.154	0.863 ±0.178
−2.75	0.613 ±0.131	0.681 ±0.149	0.508 ±0.141	0.447 ±0.139
−2.85	0.233 ±0.090	0.250 ±0.102	0.497 ±0.135	0.300 ±0.119
−2.95	0.639 ±0.125	0.551 ±0.133	0.373 ±0.117	0.218 ±0.098
−3.05	0.773 ±0.131	0.758 ±0.142	0.615 ±0.142	0.572 ±0.137
−3.15	1.19 ±0.16	1.06 ±0.17	0.781 ±0.156	0.718 ±0.146
−3.25	0.967 ±0.149	1.35 ±0.19	1.10 ±0.19	1.01 ±0.17
−3.35	1.17 ±0.16	1.27 ±0.18	0.688 ±0.146	0.861 ±0.162
−3.45	1.52 ±0.19	1.25 ±0.18	1.01 ±0.18	0.921 ±0.164
−3.55	1.78 ±0.21	1.54 ±0.20	1.08 ±0.19	0.922 ±0.159
−3.65	1.72 ±0.21	1.40 ±0.20	1.08 ±0.19	1.08 ±0.18
−3.75	2.25 ±0.25	1.35 ±0.20	1.10 ±0.19	0.887 ±0.164
−3.85	2.03 ±0.25	1.57 ±0.23	0.919 ±0.185	0.899 ±0.173
−3.95	2.04 ±0.26	1.07 ±0.20	0.802 ±0.186	1.07 ±0.19
−4.05	2.25 ±0.29	1.50 ±0.25	0.817 ±0.196	0.629 ±0.160
−4.15	2.16 ±0.33	2.02 ±0.31	1.03 ±0.24	0.762 ±0.177
−4.25	3.34 ±0.62	1.90 ±0.34	1.50 ±0.30	0.812 ±0.194
−4.35		1.20 ±0.31	1.21 ±0.29	1.28 ±0.25
−4.45				1.35 ±0.28
−4.55				1.43 ±0.31

TABLE III. *(Continued.)*

t [(GeV/c)^2] \ Momenta (GeV/c)	4.483	4.599	4.681	4.762
−1.15	61.3 ±3.2	65.0 ±6.7		
−1.25	61.5 ±2.4	66.8 ±3.2		
−1.35	64.0 ±2.2	59.6 ±2.3	57.5 ±3.1	24.2 ±7.8
−1.45	54.0 ±1.8	55.2 ±2.0	55.5 ±2.6	46.1 ±2.2
−1.55	41.3 ±1.4	42.9 ±1.6	50.3 ±2.2	42.6 ±1.9
−1.65	39.6 ±1.4	34.8 ±1.3	35.1 ±1.7	33.4 ±1.5
−1.75	32.4 ±1.3	32.8 ±1.3	29.3 ±1.4	24.0 ±1.2
−1.85	23.3 ±1.0	24.6 ±1.0	23.5 ±1.3	18.8 ±1.0
−1.95	16.4 ±0.8	15.7 ±0.8	17.1 ±1.0	15.6 ±0.8
−2.05	11.8 ±0.7	11.9 ±0.7	13.9 ±0.9	12.4 ±0.7
−2.15	9.34 ±0.52	8.21 ±0.46	7.80 ±0.69	7.44 ±0.56
−2.25	6.33 ±0.36	6.05 ±0.37	5.13 ±0.41	5.09 ±0.37
−2.35	4.45 ±0.29	4.48 ±0.32	3.56 ±0.34	3.10 ±0.27
−2.45	2.34 ±0.20	2.37 ±0.23	2.28 ±0.27	1.98 ±0.22
−2.55	1.44 ±0.16	1.83 ±0.21	0.952±0.180	1.30 ±0.18
−2.65	0.999±0.139	0.989±0.169	0.605±0.160	0.820±0.148
−2.75	0.557±0.106	0.436±0.118	0.817±0.185	0.738±0.143
−2.85	0.533±0.108	0.412±0.127	0.294±0.120	0.323±0.108
−2.95	0.469±0.100	0.330±0.101	0.382±0.167	0.386±0.109
−3.05	0.535±0.104	0.673±0.131	0.525±0.145	0.288±0.096
−3.15	0.762±0.115	0.447±0.107	0.623±0.159	0.381±0.103
−3.25	0.767±0.115	0.571±0.118	0.549±0.133	0.367±0.100
−3.35	0.675±0.110	0.861±0.142	0.642±0.136	0.615±0.148
−3.45	0.756±0.113	0.917±0.147	0.592±0.143	0.546±0.115
−3.55	0.960±0.124	0.732±0.128	0.725±0.142	0.581±0.115
−3.65	0.647±0.107	0.828±0.139	0.665±0.130	0.525±0.110
−3.75	0.881±0.132	0.966±0.176	0.945±0.158	0.608±0.116
−3.85	1.06 ±0.14	0.707±0.145	1.05 ±0.18	0.420±0.101
−3.95	0.700±0.117	0.654±0.139	0.519±0.115	0.569±0.115
−4.05	0.696±0.119	0.604±0.125	0.549±0.134	0.618±0.123
−4.15	0.699±0.115	0.615±0.142	0.431±0.126	0.432±0.116
−4.25	0.493±0.098	0.670±0.141	0.475±0.151	0.450±0.119
−4.35	0.374±0.091	0.530±0.123	0.546±0.152	0.454±0.126
−4.45	0.676±0.122	0.511±0.114	0.569±0.154	0.535±0.126
−4.55	0.646±0.121	0.737±0.175	0.660±0.217	0.367±0.140
−4.65	0.447±0.117	0.508±0.161	0.381±0.156	0.439±0.122
−4.75	0.446±0.154	0.380±0.114	0.353±0.123	0.399±0.107
−4.85	0.654±0.183	0.845±0.161	0.362±0.150	0.313±0.108
−4.95	0.843±0.210	0.643±0.179	0.613±0.167	0.606±0.173
−5.05	0.409±0.165	0.503±0.159	0.457±0.177	0.286±0.126
−5.15	0.920±0.228	0.493±0.166	0.788±0.241	0.486±0.156
−5.25	1.20 ±0.26	0.692±0.192	0.525±0.176	0.514±0.159
−5.35	1.38 ±0.27	1.39 ±0.26	0.793±0.250	0.560±0.166
−5.45	1.64 ±0.31	1.28 ±0.26	0.916±0.266	0.885±0.208
−5.55	3.04 ±0.46	1.72 ±0.31	1.01 ±0.28	0.663±0.189
−5.65	1.77 ±0.42	2.74 ±0.43	1.28 ±0.32	1.06 ±0.24
−5.75		1.89 ±0.44	1.40 ±0.39	1.38 ±0.28
−5.85			2.04 ±0.52	1.46 ±0.31

$\pi^+p \to \pi^+p$

t [(GeV/c)^2] \ Momenta (GeV/c)	4.841	4.966	5.055	5.142
−1.45	57.3 ±2.6	49.3 ±2.6	33.4 ±2.9	
−1.55	37.7 ±1.4	40.1 ±1.9	35.4 ±2.4	28.5 ±2.2
−1.65	32.4 ±1.2	29.8 ±1.5	33.5 ±2.1	30.0 ±1.8
−1.75	24.8 ±1.0	24.8 ±1.2	23.6 ±1.5	22.2 ±1.4
−1.85	18.5 ±0.8	17.3 ±1.0	19.6 ±1.3	14.6 ±1.0
−1.95	13.6 ±0.6	12.0 ±0.8	13.8 ±1.1	10.4 ±0.8
−2.05	8.87 ±0.50	9.53 ±0.67	9.81 ±0.84	7.49 ±0.63

TABLE III. *(Coninued.)*

t [(GeV/c)^2] \ Momenta (GeV/c)	$\pi^+p \to \pi^+p$ 4.841	4.966	5.055	5.142
−2.15	7.14 ±0.43	6.22 ±0.51	6.54 ±0.66	4.95 ±0.48
−2.25	4.19 ±0.33	4.63 ±0.45	4.44 ±0.52	4.01 ±0.42
−2.35	2.81 ±0.19	2.78 ±0.29	3.04 ±0.40	2.50 ±0.33
−2.45	1.91 ±0.15	1.50 ±0.15	1.34 ±0.20	0.987±0.166
−2.55	1.13 ±0.11	0.925±0.116	0.652±0.122	0.873±0.115
−2.65	0.571±0.086	0.487±0.086	0.397±0.093	0.539±0.085
−2.75	0.286±0.070	0.264±0.063	0.282±0.079	0.326±0.075
−2.85	0.262±0.063	0.214±0.055	0.338±0.092	0.206±0.054
−2.95	0.302±0.071	0.235±0.055	0.262±0.094	0.302±0.069
−3.05	0.331±0.061	0.305±0.059	0.318±0.073	0.248±0.066
−3.15	0.400±0.064	0.283±0.055	0.428±0.078	0.302±0.055
−3.25	0.589±0.080	0.422±0.065	0.392±0.075	0.278±0.052
−3.35	0.531±0.070	0.444±0.065	0.350±0.069	0.424±0.060
−3.45	0.681±0.076	0.529±0.071	0.566±0.083	0.342±0.054
−3.55	0.752±0.078	0.577±0.071	0.447±0.076	0.432±0.059
−3.65	0.854±0.082	0.636±0.075	0.495±0.076	0.387±0.056
−3.75	0.593±0.069	0.548±0.067	0.501±0.078	0.610±0.068
−3.85	0.589±0.070	0.599±0.070	0.515±0.078	0.374±0.054
−3.95	0.537±0.067	0.466±0.063	0.477±0.076	0.313±0.049
−4.05	0.387±0.058	0.547±0.068	0.398±0.068	0.481±0.059
−4.15	0.525±0.067	0.500±0.067	0.540±0.080	0.354±0.052
−4.25	0.481±0.067	0.440±0.063	0.385±0.072	0.338±0.052
−4.35	0.369±0.062	0.504±0.069	0.220±0.053	0.330±0.051
−4.45	0.407±0.066	0.286±0.053	0.328±0.067	0.253±0.046
−4.55	0.465±0.069	0.301±0.057	0.347±0.067	0.318±0.052
−4.65	0.227±0.057	0.409±0.068	0.302±0.067	0.232±0.047
−4.75	0.288±0.064	0.265±0.056	0.283±0.064	0.367±0.057
−4.85	0.322±0.069	0.258±0.060	0.326±0.070	0.234±0.048
−4.95	0.469±0.080	0.331±0.069	0.247±0.071	0.159±0.053
−5.05	0.525±0.090	0.338±0.067	0.286±0.082	0.340±0.060
−5.15	0.514±0.096	0.368±0.075	0.206±0.108	0.298±0.061
−5.25	0.329±0.106	0.508±0.094	0.453±0.153	0.273±0.062
−5.35	0.798±0.154	0.644±0.140	0.423±0.113	0.343±0.069
−5.45	0.824±0.159	0.675±0.188	0.569±0.191	0.428±0.083
−5.55	0.965±0.173	1.48 ±0.26	0.491±0.199	0.730±0.119
−5.65	1.29 ±0.20	2.10 ±0.31	0.358±0.185	0.370±0.127
−5.75	1.01 ±0.18	2.10 ±0.32	1.20 ±0.30	0.714±0.184
−5.85	1.41 ±0.22	2.16 ±0.32	2.25 ±0.40	1.22 ±0.24
−5.95	1.71 ±0.33	1.32 ±0.27	2.03 ±0.39	1.01 ±0.22
−6.05		1.47 ±0.29	0.831±0.272	1.80 ±0.30
−6.15		1.74 ±0.34	0.785±0.272	1.23 ±0.25
−6.25			0.915±0.302	1.06 ±0.24
−6.35				1.07 ±0.26
−6.45				1.06 ±0.28

t [(GeV/c)^2] \ Momenta (GeV/c)	$\pi^+p \to \pi^+p$ 5.229	5.364	5.460	5.554
−1.75	16.9 ±1.0			
−1.85	12.9 ±0.7	11.8 ±0.9		
−1.95	9.30 ±0.59	9.45 ±0.75	8.21 ±0.89	8.06 ±0.85
−2.05	7.02 ±0.49	6.95 ±0.60	6.16 ±0.73	6.03 ±0.66
−2.15	4.45 ±0.36	5.47 ±0.50	3.92 ±0.51	4.80 ±0.54
−2.25	3.28 ±0.30	2.92 ±0.35	3.17 ±0.45	2.30 ±0.34
−2.35	2.01 ±0.23	1.78 ±0.26	1.97 ±0.34	2.04 ±0.31
−2.45	1.05 ±0.17	0.923 ±0.188	1.44 ±0.30	0.963±0.206
−2.55	0.737±0.132	0.726 ±0.172	0.378±0.138	0.430±0.140
−2.65	0.543±0.095	0.446 ±0.092	0.244±0.119	0.311±0.117
−2.75	0.286±0.066	0.322 ±0.072	0.416±0.127	0.190±0.066

TABLE III. *(Continued.)*

t [(GeV/c)^2] \ Momenta (GeV/c)	$\pi^+p \to \pi^+p$ 5.229	5.364	5.460	5.554
−2.85	0.165 ± 0.048	0.179 ± 0.073	0.145 ± 0.074	0.139 ± 0.068
−2.95	0.321 ± 0.060	0.145 ± 0.072	0.245 ± 0.086	0.135 ± 0.060
−3.05	0.295 ± 0.050	0.274 ± 0.065	0.246 ± 0.076	0.151 ± 0.047
−3.15	0.345 ± 0.055	0.241 ± 0.055	0.217 ± 0.068	0.227 ± 0.063
−3.25	0.346 ± 0.055	0.339 ± 0.061	0.295 ± 0.076	0.410 ± 0.068
−3.35	0.391 ± 0.051	0.417 ± 0.066	0.218 ± 0.058	0.152 ± 0.049
−3.45	0.408 ± 0.054	0.386 ± 0.063	0.278 ± 0.069	0.342 ± 0.063
−3.55	0.401 ± 0.052	0.428 ± 0.066	0.383 ± 0.075	0.307 ± 0.059
−3.65	0.379 ± 0.048	0.374 ± 0.062	0.341 ± 0.071	0.290 ± 0.055
−3.75	0.362 ± 0.047	0.473 ± 0.071	0.451 ± 0.081	0.379 ± 0.065
−3.85	0.425 ± 0.051	0.330 ± 0.057	0.340 ± 0.069	0.166 ± 0.044
−3.95	0.375 ± 0.047	0.298 ± 0.052	0.363 ± 0.070	0.261 ± 0.052
−4.05	0.392 ± 0.048	0.331 ± 0.057	0.148 ± 0.044	0.253 ± 0.050
−4.15	0.316 ± 0.044	0.317 ± 0.056	0.253 ± 0.059	0.313 ± 0.055
−4.25	0.282 ± 0.042	0.258 ± 0.051	0.250 ± 0.058	0.166 ± 0.041
−4.35	0.336 ± 0.045	0.155 ± 0.041	0.265 ± 0.059	0.236 ± 0.049
−4.45	0.403 ± 0.049	0.276 ± 0.054	0.251 ± 0.057	0.234 ± 0.047
−4.55	0.299 ± 0.045	0.225 ± 0.047	0.216 ± 0.058	0.196 ± 0.045
−4.65	0.327 ± 0.046	0.251 ± 0.053	0.156 ± 0.051	0.236 ± 0.047
−4.75	0.261 ± 0.044	0.226 ± 0.051	0.131 ± 0.043	0.191 ± 0.045
−4.85	0.292 ± 0.045	0.249 ± 0.052	0.295 ± 0.066	0.196 ± 0.046
−4.95	0.269 ± 0.046	0.236 ± 0.052	0.366 ± 0.073	0.165 ± 0.043
−5.05	0.286 ± 0.048	0.215 ± 0.047	0.285 ± 0.065	0.281 ± 0.054
−5.15	0.429 ± 0.064	0.301 ± 0.060	0.281 ± 0.069	0.233 ± 0.052
−5.25	0.369 ± 0.055	0.349 ± 0.061	0.458 ± 0.085	0.369 ± 0.062
−5.35	0.350 ± 0.057	0.352 ± 0.062	0.198 ± 0.058	0.295 ± 0.056
−5.45	0.304 ± 0.058	0.419 ± 0.080	0.259 ± 0.072	0.214 ± 0.049
−5.55	0.445 ± 0.074	0.162 ± 0.052	0.340 ± 0.073	0.191 ± 0.053
−5.65	0.330 ± 0.083	0.347 ± 0.073	0.357 ± 0.085	0.328 ± 0.070
−5.75	0.407 ± 0.097	0.372 ± 0.083	0.341 ± 0.089	0.249 ± 0.056
−5.85	0.116 ± 0.079	0.0871 ± 0.0560	0.362 ± 0.126	0.313 ± 0.065
−5.95	0.366 ± 0.109	0.365 ± 0.128	0.183 ± 0.099	0.239 ± 0.063
−6.05	0.689 ± 0.144	0.375 ± 0.126	0.362 ± 0.153	0.279 ± 0.109
−6.15	0.427 ± 0.124	0.430 ± 0.136	0.415 ± 0.162	0.216 ± 0.098
−6.25	0.661 ± 0.154	0.361 ± 0.129	0.309 ± 0.157	0.453 ± 0.137
−6.35	0.746 ± 0.167	0.608 ± 0.182	0.414 ± 0.174	0.245 ± 0.108
−6.45	0.536 ± 0.157	0.474 ± 0.171	0.414 ± 0.171	0.619 ± 0.164
−6.55	0.752 ± 0.206	0.594 ± 0.198	0.414 ± 0.195	0.496 ± 0.152
−6.65		0.773 ± 0.253	0.227 ± 0.145	0.509 ± 0.160
−6.75			0.689 ± 0.305	0.172 ± 0.107
−6.85				0.620 ± 0.209

t [(GeV/c)^2] \ Momenta (GeV/c)	$\pi^+p \to \pi^+p$ 5.647	5.792	5.896	5.998
−1.9	6.48 ± 1.10			
−2.1	4.87 ± 0.54			
−2.3	2.21 ± 0.31			
−2.5	0.669 ± 0.162			
−2.7	0.315 ± 0.108			
−2.9	0.166 ± 0.064			
−3.1	0.248 ± 0.058	0.508 ± 0.225	0.522 ± 0.259	0.349 ± 0.197
−3.3	0.298 ± 0.051	0.441 ± 0.166	0.767 ± 0.243	0.537 ± 0.180
−3.5	0.335 ± 0.050	0.430 ± 0.142	0.285 ± 0.141	0.305 ± 0.126
−3.7	0.288 ± 0.044	0.579 ± 0.149	0.431 ± 0.152	0.325 ± 0.117
−3.9	0.337 ± 0.047	0.250 ± 0.098	0.308 ± 0.125	0.269 ± 0.101
−4.1	0.293 ± 0.042	0.212 ± 0.086	0.494 ± 0.149	0.417 ± 0.118
−4.3	0.168 ± 0.040	0.365 ± 0.108	0.441 ± 0.141	0.137 ± 0.069
−4.5	0.234 ± 0.036	0.205 ± 0.081	0.230 ± 0.101	0.0504 ± 0.0481

TABLE III. *(Continued.)*

t [(GeV/c)^2] \ Momenta (GeV/c)	$\pi^+p \to \pi^+p$ 5.647	5.792	5.896	5.998
−4.7	0.177 ±0.032	0.0614±0.0487	0.119 ±0.075	0.101 ±0.060
−4.9	0.269 ±0.041	0.195 ±0.078	0.109 ±0.073	
−5.1	0.152 ±0.031	0.282 ±0.093	0.0657±0.0649	0.0840±0.0541
−5.3	0.211 ±0.038	0.315 ±0.100	0.292 ±0.114	0.0887±0.0552
−5.5	0.287 ±0.045	0.194 ±0.084	0.198 ±0.098	0.145 ±0.070
−5.7	0.229 ±0.043	0.280 ±0.101	0.257 ±0.109	0.116 ±0.067
−5.9	0.237 ±0.046	0.142 ±0.080	0.268 ±0.114	0.244 ±0.094
−6.1	0.0915±0.0497	0.225 ±0.096	0.229 ±0.108	0.247 ±0.096
−6.3	0.218 ±0.069	0.152 ±0.088	0.205 ±0.110	0.166 ±0.086
−6.5			0.0921±0.0865	
−6.7	0.206 ±0.075		0.254 ±0.156	0.138 ±0.110
−6.9	0.231 ±0.110			0.145 ±0.145
−7.1	0.542 ±0.252			

t [(GeV/c)^2] \ Momenta (GeV/c)	$pp \to pp$ 1.896	1.945	1.980	2.014
−0.475	6900±1020			
−0.525	7070± 511	5680±417	4840±546	4160±822
−0.575	4740± 273	5720±261	5610±291	4400±354
−0.625	4510± 233	4970±194	4720±195	4280±223
−0.675	3650± 196	4500±166	4280±159	4170±187
−0.725	3070± 168	3230±130	3640±132	3340±145
−0.775	3100± 168	3120±126	3080±118	2860±124
−0.825	2500± 148	2650±111	2740±106	2750±116
−0.875	2460± 141	2430±105	2350± 93	2260±101
−0.925	2210± 126	2190± 95	2430± 94	2140± 96
−0.975	2100± 114	2270± 92	2080± 81	2200± 92
−1.025	2190± 115	2250± 86	2120± 77	2070± 85
−1.075	1930± 108	2010± 80	2110± 74	2020± 78
−1.125			1990± 73	1970± 76
−1.175				1960± 77

t [(GeV/c)^2] \ Momenta (GeV/c)	$pp \to pp$ 2.049	2.102	2.139	2.176
−0.525	3890±829	2380±1020		
−0.575	3680±297	2880± 330	1020±309	
−0.625	3710±192	4040± 232	2290±185	1340±207
−0.675	3720±154	3070± 147	2960±152	2500±172
−0.725	2850±117	2990± 128	2460±114	2460±130
−0.775	2190± 91	2540± 109	2550±108	1990±106
−0.825	2380± 91	2230± 94	2110± 88	1950± 92
−0.875	2200± 85	2100± 89	2340± 91	1780± 82
−0.925	1850± 75	1840± 80	1940± 78	1920± 83
−0.975	1740± 70	1780± 78	1830± 73	1610± 72
−1.025	1700± 65	1570± 71	1670± 67	1420± 67
−1.075	1620± 61	1630± 67	1530± 61	1460± 64
−1.125	1710± 61	1540± 63	1440± 56	1390± 59
−1.175	1650± 60	1530± 62	1480± 56	1310± 54
−1.225		1530± 62	1390± 54	1390± 56
−1.275			1380± 54	1320± 54
−1.325				1040± 48

TABLE III. *(Continued.)*

t [(GeV/c)^2] \ Momenta (GeV/c)	$pp \to pp$ 2.223	2.281	2.321	2.362
−0.625	3010 ± 715			
−0.675	1760 ± 232			
−0.725	2150 ± 169			
−0.775	1640 ± 121			
−0.825	1710 ± 90	2290 ± 133	2090 ± 126	
−0.875	1560 ± 77	2060 ± 106	1860 ± 98	1830 ± 119
−0.925	1620 ± 77	1690 ± 90	1610 ± 83	1460 ± 88
−0.975	1530 ± 71	1560 ± 83	1530 ± 78	1460 ± 80
−1.025	1910 ± 87	1360 ± 73	1390 ± 69	1260 ± 72
−1.075	1430 ± 67	1470 ± 76	1360 ± 67	1210 ± 66
−1.125	1620 ± 70	1250 ± 63	1210 ± 58	1220 ± 65
−1.175	1350 ± 58	1220 ± 58	1190 ± 54	991 ± 52
−1.225	1220 ± 50	1190 ± 54	1160 ± 49	1070 ± 52
−1.275	1290 ± 52	1250 ± 53	1100 ± 48	991 ± 47
−1.325	1260 ± 51	1130 ± 51	1190 ± 48	1040 ± 47
−1.375		1170 ± 52	1120 ± 46	991 ± 45
−1.425			1170 ± 47	1060 ± 47
−1.475				940 ± 44

t [(GeV/c)^2] \ Momenta (GeV/c)	$pp \to pp$ 2.402	2.464	2.508	2.552
−0.675	2290 ± 607			
−0.725	3550 ± 477	1800 ± 314		
−0.775	2250 ± 239	2690 ± 236	1050 ± 185	
−0.825	2110 ± 181	1910 ± 142	1860 ± 165	1170 ± 158
−0.875	1510 ± 121	1630 ± 105	1520 ± 103	1440 ± 122
−0.925	1480 ± 81	1430 ± 87	1510 ± 89	1620 ± 103
−0.975	1260 ± 69	1320 ± 77	1450 ± 79	1250 ± 80
−1.025	1220 ± 64	1290 ± 74	1230 ± 66	1050 ± 67
−1.075	1130 ± 60	1180 ± 70	1260 ± 68	1040 ± 63
−1.125	1120 ± 56	1190 ± 67	1220 ± 65	998 ± 61
−1.175	1030 ± 50	1090 ± 62	1080 ± 57	972 ± 58
−1.225	1040 ± 48	889 ± 53	1050 ± 55	794 ± 49
−1.275	962 ± 43	960 ± 52	869 ± 46	694 ± 45
−1.325	925 ± 41	938 ± 48	936 ± 46	842 ± 46
−1.375	1030 ± 41	973 ± 46	898 ± 41	767 ± 41
−1.425	967 ± 39	926 ± 43	923 ± 41	802 ± 40
−1.475	931 ± 38	898 ± 41	871 ± 38	763 ± 37
−1.525	716 ± 45	952 ± 42	851 ± 36	759 ± 36
−1.575			852 ± 36	753 ± 35
−1.625				806 ± 36

t [(GeV/c)^2] \ Momenta (GeV/c)	$pp \to pp$ 2.597	2.664	2.711	2.758
−0.775	1440 ± 357			
−0.825	1500 ± 174	1120 ± 176		
−0.875	1440 ± 114	1290 ± 130	697 ± 111	
−0.925	1310 ± 89	1170 ± 99	1290 ± 116	1200 ± 144
−0.975	1310 ± 76	1320 ± 84	1050 ± 74	1330 ± 113
−1.025	1150 ± 65	1220 ± 73	1100 ± 67	966 ± 74
−1.075	1040 ± 57	1010 ± 63	1060 ± 62	1040 ± 70
−1.125	930 ± 52	911 ± 57	912 ± 53	935 ± 61
−1.175	1010 ± 52	994 ± 57	970 ± 53	864 ± 55
−1.225	844 ± 46	822 ± 50	839 ± 48	894 ± 54
−1.275	849 ± 44	805 ± 48	738 ± 43	751 ± 47
−1.325	807 ± 42	828 ± 48	734 ± 42	726 ± 44
−1.375	833 ± 40	808 ± 45	721 ± 40	712 ± 43

TABLE III. *(Continued.)*

t [(GeV/c)^2] \ Momenta (GeV/c)	$pp \to pp$ 2.597	2.664	2.711	2.758
−1.425	757 ± 36	789 ± 42	618 ± 34	626 ± 38
−1.475	807 ± 36	736 ± 38	736 ± 37	621 ± 35
−1.525	743 ± 33	697 ± 36	689 ± 33	698 ± 36
−1.575	781 ± 33	656 ± 33	761 ± 34	637 ± 33
−1.625	822 ± 33	785 ± 37	675 ± 31	586 ± 31
−1.675	736 ± 31	726 ± 34	698 ± 31	625 ± 31
−1.725		603 ± 31	618 ± 28	629 ± 30
−1.775			594 ± 28	561 ± 28
−1.825				531 ± 27

t [(GeV/c)^2] \ Momenta (GeV/c)	$pp \to pp$ 2.797	2.869	2.920	2.971
−0.925	1170 ± 268			
−0.975	763 ± 117			
−1.025	1140 ± 116			
−1.075	1130 ± 96			
−1.125	795 ± 64			
−1.175	765 ± 57	615 ± 126	182 ± 115	433 ± 195
−1.225	838 ± 53	493 ± 86	560 ± 129	257 ± 92
−1.275	721 ± 44	570 ± 72	590 ± 93	570 ± 100
−1.325	585 ± 37	504 ± 59	723 ± 91	458 ± 68
−1.375	711 ± 39	499 ± 52	707 ± 76	614 ± 67
−1.425	591 ± 34	608 ± 53	597 ± 62	434 ± 48
−1.475	536 ± 30	505 ± 46	442 ± 49	499 ± 47
−1.525	563 ± 30	519 ± 44	550 ± 53	495 ± 43
−1.575	516 ± 27	524 ± 43	469 ± 47	419 ± 38
−1.625	580 ± 29	521 ± 42	518 ± 48	473 ± 39
−1.675	534 ± 27	544 ± 42	408 ± 41	381 ± 34
−1.725	563 ± 27	443 ± 38	484 ± 45	442 ± 36
−1.775	530 ± 26	476 ± 39	505 ± 46	352 ± 32
−1.825	536 ± 26	518 ± 41	397 ± 39	430 ± 34
−1.875	412 ± 22	550 ± 42	480 ± 44	400 ± 33
−1.925		429 ± 36	428 ± 40	377 ± 32
−1.975			315 ± 34	339 ± 30
−2.025				314 ± 29

t [(GeV/c)^2] \ Momenta (GeV/c)	$pp \to pp$ 3.017	3.095	3.150	3.205
−1.225	486 ± 161	245 ± 235		
−1.275	358 ± 80	700 ± 209		
−1.325	496 ± 69	281 ± 87		366 ± 165
−1.375	609 ± 65	473 ± 90	347 ± 98	357 ± 116
−1.425	426 ± 45	350 ± 64	219 ± 63	305 ± 82
−1.475	396 ± 39	340 ± 57	303 ± 62	371 ± 70
−1.525	406 ± 37	376 ± 54	303 ± 58	439 ± 66
−1.575	416 ± 35	302 ± 46	405 ± 62	311 ± 50
−1.625	399 ± 33	364 ± 47	332 ± 51	398 ± 53
−1.675	374 ± 30	376 ± 46	373 ± 51	320 ± 45
−1.725	433 ± 32	327 ± 41	437 ± 54	339 ± 44
−1.775	375 ± 29	292 ± 38	298 ± 45	326 ± 42
−1.825	330 ± 27	376 ± 43	278 ± 40	221 ± 33
−1.875	394 ± 29	386 ± 43	359 ± 45	272 ± 36
−1.925	344 ± 27	277 ± 35	318 ± 40	233 ± 32
−1.975	393 ± 29	366 ± 41	247 ± 36	283 ± 35
−2.025	344 ± 27	291 ± 36	321 ± 40	212 ± 30
−2.075	271 ± 24	309 ± 37	227 ± 35	291 ± 35
−2.125		243 ± 33	299 ± 40	332 ± 37

TABLE III. *(Continued.)*

t [(GeV/c)^2] \ Momenta (GeV/c)	$pp \to pp$ 3.017	3.095	3.150	3.205
−2.175			220 ± 33	327 ± 36
−2.225				233 ± 30

t [(GeV/c)^2] \ Momenta (GeV/c)	$pp \to pp$ 3.266	3.350	3.410	3.469
−1.275	232 ± 85			
−1.325	164 ± 47	79.1 ± 40.9		
−1.375	393 ± 53	188 ± 41	96.3 ± 61.0	
−1.425	314 ± 34	239 ± 34	137 ± 45	
−1.475	317 ± 27	303 ± 29	133 ± 29	170 ± 37
−1.525	322 ± 24	243 ± 21	264 ± 34	171 ± 26
−1.575	296 ± 19	228 ± 17	273 ± 26	230 ± 24
−1.625	311 ± 18	254 ± 16	234 ± 22	206 ± 17
−1.675	287 ± 17	252 ± 15	228 ± 19	224 ± 16
−1.725	270 ± 16	254 ± 14	215 ± 18	217 ± 14
−1.775	288 ± 15	234 ± 13	215 ± 16	202 ± 13
−1.825	249 ± 14	231 ± 12	194 ± 14	197 ± 12
−1.875	233 ± 13	214 ± 12	190 ± 14	188 ± 11
−1.925	259 ± 13	213 ± 11	240 ± 15	169 ± 10
−1.975	254 ± 13	202 ± 10	195 ± 13	179 ± 10
−2.025	259 ± 13	203 ± 10	181 ± 12	166 ± 9
−2.075	239 ± 12	203 ± 10	186 ± 12	146 ± 8
−2.125	232 ± 12	186 ± 9	166 ± 11	163 ± 9
−2.175	225 ± 12	201 ± 10	175 ± 11	155 ± 8
−2.225	220 ± 11	191 ± 9	159 ± 10	147 ± 8
−2.275	198 ± 11	188 ± 9	172 ± 11	152 ± 8
−2.325		184 ± 9	146 ± 10	138 ± 7
−2.375			150 ± 10	135 ± 7
−2.425				142 ± 7

t [(GeV/c)^2] \ Momenta (GeV/c)	$pp \to pp$ 3.350	3.621	3.686	3.750
−1.375	351 ± 139			
−1.425	249 ± 63			
−1.475	314 ± 50	250 ± 58		
−1.525	181 ± 23	218 ± 34		
−1.575	202 ± 18	167 ± 22	78.4 ± 25.2	84.2 ± 42.4
−1.625	176 ± 13	148 ± 16	160 ± 26	100.0 ± 19.7
−1.675	194 ± 12	159 ± 13	173 ± 21	153 ± 19
−1.725	195 ± 11	163 ± 12	167 ± 16	143 ± 15
−1.775	162 ± 9	149 ± 10	120 ± 12	138 ± 11
−1.825	171 ± 9	161 ± 10	133 ± 12	151 ± 11
−1.875	187 ± 9	138 ± 8	156 ± 12	160 ± 10
−1.925	167 ± 8	155 ± 9	138 ± 10	122 ± 8
−1.975	169 ± 8	158 ± 9	127 ± 9	125 ± 8
−2.025	135 ± 7	140 ± 8	141 ± 10	118 ± 7
−2.075	144 ± 7	122 ± 7	126 ± 9	115 ± 7
−2.125	137 ± 6	133 ± 7	120 ± 9	112 ± 7
−2.175	116 ± 6	115 ± 6	113 ± 8	116 ± 7
−2.225	120 ± 6	109 ± 6	107 ± 8	95.3 ± 5.8
−2.275	132 ± 6	95.8 ± 5.9	105 ± 8	93.1 ± 5.7
−2.325	120 ± 6	103 ± 6	98.1 ± 7.3	103 ± 6
−2.375	126 ± 6	99.8 ± 5.8	89.4 ± 6.7	82.3 ± 5.1
−2.425	119 ± 6	95.9 ± 5.7	103 ± 7	83.5 ± 5.1
−2.475	115 ± 5	103 ± 6	87.4 ± 6.5	85.3 ± 5.1
−2.525	113 ± 5	108 ± 6	75.6 ± 6.1	78.8 ± 4.9
−2.575		102 ± 6	81.0 ± 6.5	77.6 ± 4.8
−2.625		88.4 ± 5.3	85.0 ± 6.6	69.5 ± 4.5
−2.675			91.9 ± 6.6	84.1 ± 5.0
−2.725				84.8 ± 5.0

TABLE III. (*Continued.*)

t [(GeV/c)^2] \ Momenta (GeV/c)	$pp \to pp$ 3.843	3.942	4.013	4.082
−1.35	170 ±109			
−1.45	131 ± 34	21.7± 20.6		
−1.55	152 ± 25	69.8± 18.6	33.2± 25.1	
−1.65	142 ± 14	94.1± 13.8	52.7± 16.5	
−1.75	158 ± 10	114 ± 12	90.4± 14.8	79.2± 12.6
−1.85	133 ± 7	119 ± 9	105 ± 11	82.9± 8.8
−1.95	122 ± 5	107 ± 7	107 ± 9	91.7± 7.3
−2.05	126 ± 5	108 ± 7	94.7± 7.6	90.5± 6.2
−2.15	100 ± 4	94.7± 5.6	85.8± 6.6	83.6± 5.2
−2.25	100 ± 4	91.7± 5.2	77.6± 6.0	82.0± 4.8
−2.35	82.3± 3.5	77.3± 4.6	73.7± 5.7	63.7± 4.1
−2.45	83.7± 3.5	65.8± 4.2	66.5± 5.2	67.5± 4.0
−2.55	71.9± 3.1	61.1± 3.9	62.8± 5.1	55.3± 3.6
−2.65	73.3± 3.1	65.9± 4.0	59.9± 4.7	53.6± 3.5
−2.75	71.2± 3.1	62.3± 3.9	49.8± 4.3	45.2± 3.2
−2.85	51.0± 4.8	63.6± 3.9	47.2± 4.1	43.3± 3.0
−2.95				41.6± 3.0

t [(GeV/c)^2] \ Momenta (GeV/c)	$pp \to pp$ 4.151	4.258	4.334	4.409
−1.65	44.5± 12.9			
−1.75	70.4± 10.2	64.3± 15.0		
−1.85	88.4± 8.2	48.2± 8.3	33.9± 12.1	
−1.95	83.3± 6.0	77.3± 8.1	67.5± 11.8	58.8± 10.5
−2.05	77.3± 4.9	71.6± 5.9	47.8± 6.5	54.7± 6.7
−2.15	69.9± 4.0	67.4± 4.9	50.3± 5.8	58.4± 5.3
−2.25	64.2± 3.4	58.3± 4.2	53.8± 5.5	44.7± 4.0
−2.35	57.0± 3.1	48.7± 3.5	59.5± 5.2	52.0± 3.9
−2.45	56.7± 2.9	44.9± 3.2	44.8± 4.2	44.5± 3.3
−2.55	47.3± 2.6	45.4± 3.1	45.7± 4.1	43.9± 3.2
−2.65	48.3± 2.6	34.7± 2.7	36.4± 3.6	42.9± 3.1
−2.75	47.3± 2.5	44.3± 3.0	32.1± 3.3	37.6± 2.8
−2.85	46.4± 2.5	40.3± 2.9	43.2± 3.8	34.0± 2.6
−2.95	46.8± 2.5	40.3± 2.8	30.3± 3.1	33.3± 2.6
−3.05	38.0± 2.2	36.0± 2.7	34.0± 3.3	27.3± 2.3
−3.15		34.0± 2.5	33.6± 3.3	35.1± 2.6
−3.25				33.4± 2.5

t [(GeV/c)^2] \ Momenta (GeV/c)	$pp \to pp$ 4.483	4.599	4.681	4.762
−1.65	66.0± 19.1			
−1.75	80.3± 14.0	27.6± 10.2		
−1.85	53.6± 7.6	52.8± 9.0		
−1.95	50.9± 5.5	37.5± 5.2	17.4± 5.3	
−2.05	48.8± 4.4	42.5± 4.5	27.9± 5.0	25.4± 4.3
−2.15	46.7± 3.4	36.5± 3.5	39.9± 5.1	27.9± 3.5
−2.25	41.4± 2.7	32.5± 2.7	42.4± 4.1	28.6± 2.9
−2.35	38.7± 2.4	34.5± 2.5	27.7± 2.9	26.7± 2.3
−2.45	37.0± 2.2	31.4± 2.2	28.0± 2.7	25.1± 2.0
−2.55	35.5± 2.0	30.6± 2.0	29.1± 2.5	23.3± 1.8
−2.65	29.2± 1.7	25.0± 1.7	26.7± 2.3	23.6± 1.7
−2.75	31.8± 1.8	25.3± 1.7	27.9± 2.3	18.9± 1.4
−2.85	28.6± 1.6	26.5± 1.7	24.2± 2.0	20.8± 1.4
−2.95	25.5± 1.5	22.8± 1.6	23.5± 2.0	19.7± 1.4
−3.05	24.4± 1.5	23.5± 1.6	21.5± 1.9	17.8± 1.3
−3.15	28.3± 1.6	19.0± 1.4	19.8± 1.8	19.2± 1.3
−3.25	23.5± 1.4	21.7± 1.5	16.9± 1.7	16.7± 1.2

TABLE III. (*Continued.*)

t [(GeV/c)^2] \ Momenta (GeV/c)	$pp \to pp$ 4.483	4.599	4.681	4.762
−3.35	22.5± 1.4	20.3± 1.5	21.0±1.9	16.8±1.2
−3.45		21.0± 1.4	18.6±1.7	16.9±1.2
−3.55			17.3±1.6	16.8±1.2

t [(GeV/c)^2] \ Momenta (GeV/c)	$pp \to pp$ 4.841	4.966	5.055	5.142
−2.05	16.3±4.4	19.9± 7.0	11.2 ±8.3	
−2.15	31.5±4.0	21.8±5.1	15.3 ±7.6	12.9 ±6.5
−2.25	23.8±3.0	35.9±5.5	6.51±3.76	14.6 ±5.1
−2.35	26.3±2.4	20.4±3.5	19.5 ±4.7	19.5 ±4.6
−2.45	22.1±1.9	21.2±3.0	24.0 ±4.3	19.0 ±3.4
−2.55	22.2±1.8	20.1±2.6	16.2 ±3.1	12.7 ±2.4
−2.65	22.3±1.6	19.8±2.4	18.1 ±3.0	17.6 ±2.5
−2.75	20.7±1.5	20.6±2.2	15.5 ±2.5	16.0 ±2.2
−2.85	18.6±1.4	19.0±2.1	17.4 ±2.6	15.7 ±2.0
−2.95	16.6±1.3	16.3±1.9	14.1 ±2.3	12.7 ±1.7
−3.05	18.9±1.3	13.6±1.7	14.8 ±2.2	13.0 ±1.7
−3.15	15.0±1.2	14.8±1.7	13.3 ±2.1	15.4 ±1.8
−3.25	16.9±1.2	17.0±1.8	16.9 ±2.4	14.6 ±1.8
−3.35	14.9±1.1	11.6±1.5	13.0 ±2.1	10.9 ±1.5
−3.45	15.7±1.2	10.5±1.4	17.0 ±2.3	12.9 ±1.6
−3.55	15.1±1.1	11.5±1.5	11.6 ±1.9	8.63±1.31
−3.65	14.5±1.1	14.9±1.7	13.9 ±2.1	12.3 ±1.5
−3.75		13.7±1.6	11.4 ±1.8	12.5 ±1.5
−3.85			7.25±1.44	10.3 ±1.4
−3.95				8.90±1.28

t [(GeV/c)^2] \ Momenta (GeV/c)	$pp \to pp$ 5.229	5.364	5.460	5.554
−2.15	14.0 ±8.0			
−2.25	12.9 ±2.8			
−2.35	15.3 ±2.2	5.81±1.94		
−2.45	15.3 ±1.6	12.6 ±1.8	4.57 ±1.65	4.39±1.84
−2.55	14.8 ±1.2	11.8 ±1.3	6.68 ±1.29	8.35±1.52
−2.65	11.9 ±0.9	10.8 ±1.0	9.28 ±1.14	11.1 ±1.3
−2.75	13.1 ±0.9	9.82±0.81	10.3 ±1.0	9.48±0.93
−2.85	12.2 ±0.8	10.8 ±0.8	11.2 ±0.9	9.19±0.79
−2.95	12.5 ±0.8	10.0 ±0.7	9.74 ±0.83	7.92±0.69
−3.05	12.7 ±0.8	10.2 ±0.7	8.54 ±0.72	8.97±0.68
−3.15	11.2 ±0.7	11.3 ±0.7	7.62 ±0.64	8.76±0.62
−3.25	9.84±0.61	9.55±0.60	8.72 ±0.68	6.81±0.53
−3.35	10.1 ±0.6	8.88±0.56	7.91 ±0.62	7.07±0.52
−3.45	10.0 ±0.6	6.65±0.48	6.56 ±0.54	7.61±0.51
−3.55	9.68±0.57	9.15±0.56	8.44 ±0.62	7.83±0.51
−3.65	9.53±0.57	9.04±0.54	7.80 ±0.57	6.46±0.45
−3.75	9.60±0.57	7.76±0.49	6.76 ±0.52	7.07±0.46
−3.85	8.33±0.53	8.37±0.51	7.28 ±0.54	6.22±0.42
−3.95	9.30±0.54	7.72±0.49	6.84 ±0.51	6.04±0.41
−4.05	7.44±0.49	7.89±0.49	7.13 ±0.54	6.96±0.44
−4.15		8.49±0.51	7.17 ±0.53	6.70±0.43
−4.25			6.60 ±0.49	6.17±0.41
−4.35				5.88±0.40

TABLE III. (*Continued.*)

t [(GeV/c)^2] \ Momenta (GeV/c)	$pp \to pp$ 5.647	5.792	5.896	5.998
−2.25	4.40 ± 3.16			
−2.35	7.83 ± 3.51			
−2.45	16.6 ± 4.5			
−2.55	9.47 ± 1.64	7.16 ± 2.55		
−2.65	8.15 ± 1.19	7.81 ± 2.18	5.00 ± 2.26	5.74 ± 2.65
−2.75	8.28 ± 0.97	6.76 ± 1.76	5.24 ± 2.15	8.60 ± 2.32
−2.85	7.00 ± 0.76	8.92 ± 1.62	7.60 ± 1.81	3.51 ± 1.30
−2.95	9.28 ± 0.76	6.64 ± 1.24	8.51 ± 1.82	7.00 ± 1.50
−3.05	6.77 ± 0.61	9.05 ± 1.32	5.53 ± 1.25	5.30 ± 1.14
−3.15	6.67 ± 0.56	10.1 ± 1.4	5.06 ± 1.06	4.54 ± 0.95
−3.25	5.76 ± 0.50	6.72 ± 1.04	4.53 ± 1.02	6.17 ± 1.02
−3.35	6.28 ± 0.50	6.47 ± 1.00	6.65 ± 1.29	5.07 ± 0.89
−3.45	6.31 ± 0.48	6.61 ± 0.98	6.01 ± 1.11	4.38 ± 0.79
−3.55	5.28 ± 0.43	7.14 ± 0.98	4.32 ± 0.90	3.18 ± 0.66
−3.65	5.32 ± 0.42	4.88 ± 0.80	4.92 ± 0.91	3.95 ± 0.70
−3.75	5.01 ± 0.40	4.51 ± 0.75	4.73 ± 0.88	3.49 ± 0.64
−3.85	4.91 ± 0.38	3.62 ± 0.67	4.53 ± 0.90	3.76 ± 0.65
−3.95	5.01 ± 0.38	4.77 ± 0.74	4.13 ± 0.79	3.01 ± 0.57
−4.05	4.78 ± 0.37	4.31 ± 0.70	5.89 ± 0.93	3.95 ± 0.63
−4.15	5.27 ± 0.38	4.55 ± 0.70	3.37 ± 0.71	3.59 ± 0.61
−4.25	5.77 ± 0.39	4.29 ± 0.68	3.66 ± 0.76	2.96 ± 0.54
−4.35	5.41 ± 0.38	5.20 ± 0.74	2.98 ± 0.61	2.99 ± 0.53
−4.45	4.71 ± 0.36	5.24 ± 0.73	3.38 ± 0.67	3.08 ± 0.53
−4.55		3.44 ± 0.59	6.15 ± 0.97	3.84 ± 0.59
−4.65			3.20 ± 0.65	2.71 ± 0.50
−4.75				3.20 ± 0.54

t [(GeV/c)^2] \ Momenta (GeV/c)	$pp \to pp$ 6.099	6.257	6.368	6.478
−2.55	2.91 ± 1.39			
−2.65	5.45 ± 1.55	1.10 ± 1.01		
−2.75	3.97 ± 1.05	5.33 ± 1.68		
−2.85	5.63 ± 1.31	1.96 ± 0.89	5.23 ± 2.27	
−2.95	4.20 ± 0.79	3.16 ± 1.02	5.23 ± 1.71	4.70 ± 1.76
−3.05	4.70 ± 0.71	4.78 ± 0.93	5.34 ± 1.41	2.10 ± 0.80
−3.15	4.25 ± 0.65	2.93 ± 0.66	4.15 ± 0.99	3.57 ± 0.90
−3.25	5.01 ± 0.66	5.71 ± 0.88	4.36 ± 0.96	4.40 ± 0.88
−3.35	4.76 ± 0.60	5.00 ± 0.78	4.58 ± 0.92	2.99 ± 0.66
−3.45	4.50 ± 0.55	4.67 ± 0.70	4.55 ± 0.78	3.70 ± 0.68
−3.55	4.85 ± 0.56	5.46 ± 0.73	2.82 ± 0.60	3.71 ± 0.63
−3.65	3.96 ± 0.48	4.15 ± 0.61	3.05 ± 0.63	3.50 ± 0.57
−3.75	3.37 ± 0.43	3.65 ± 0.54	5.15 ± 0.80	2.93 ± 0.50
−3.85	3.75 ± 0.44	2.86 ± 0.46	3.07 ± 0.55	2.83 ± 0.48
−3.95	3.94 ± 0.44	3.70 ± 0.52	2.33 ± 0.48	3.40 ± 0.50
−4.05	3.44 ± 0.40	2.84 ± 0.44	3.73 ± 0.57	2.05 ± 0.37
−4.15	3.64 ± 0.39	2.57 ± 0.41	2.63 ± 0.49	3.01 ± 0.44
−4.25	3.86 ± 0.41	2.96 ± 0.42	2.37 ± 0.46	2.61 ± 0.40
−4.35	3.43 ± 0.38	2.20 ± 0.37	1.31 ± 0.34	2.26 ± 0.37
−4.45	3.42 ± 0.38	2.67 ± 0.40	2.00 ± 0.37	1.91 ± 0.33
−4.55	2.91 ± 0.35	2.83 ± 0.40	1.70 ± 0.38	1.69 ± 0.31
−4.65	2.61 ± 0.33	2.46 ± 0.38	1.96 ± 0.38	1.76 ± 0.31
−4.75	2.98 ± 0.35	1.85 ± 0.32	2.64 ± 0.44	1.94 ± 0.32
−4.85	2.78 ± 0.33	2.87 ± 0.41	1.91 ± 0.40	1.92 ± 0.32
−4.95		2.13 ± 0.34	2.51 ± 0.43	1.38 ± 0.27
−5.05			2.10 ± 0.40	1.71 ± 0.29
−5.15				1.97 ± 0.31

TABLE III. (*Continued.*)

t [(GeV/c)^2] \ Momenta (GeV/c)	$pp \to pp$ 6.587	6.757	6.878	6.997
−2.85	4.10 ± 3.29			
−2.95	8.46 ± 3.15			
−3.05	3.88 ± 0.94	1.96 ± 0.95	1.77 ± 1.43	
−3.15	4.04 ± 0.79	3.83 ± 1.10	3.99 ± 1.74	2.65 ± 1.57
−3.25	3.50 ± 0.64	2.43 ± 0.76	2.51 ± 1.02	3.70 ± 1.24
−3.35	4.30 ± 0.64	3.23 ± 0.75	1.74 ± 0.68	1.62 ± 0.70
−3.45	3.65 ± 0.57	3.25 ± 0.73	2.12 ± 0.68	2.43 ± 0.71
−3.55	4.34 ± 0.57	4.53 ± 0.79	3.05 ± 0.76	1.20 ± 0.45
−3.65	2.44 ± 0.38	2.18 ± 0.51	2.99 ± 0.73	2.08 ± 0.53
−3.75	2.82 ± 0.37	2.84 ± 0.51	1.51 ± 0.44	2.29 ± 0.51
−3.85	2.63 ± 0.34	2.11 ± 0.42	2.47 ± 0.52	2.18 ± 0.46
−3.95	2.02 ± 0.30	2.14 ± 0.39	1.41 ± 0.40	2.14 ± 0.42
−4.05	2.04 ± 0.29	2.16 ± 0.39	2.18 ± 0.46	1.78 ± 0.37
−4.15	1.68 ± 0.25	1.73 ± 0.34	1.70 ± 0.42	1.22 ± 0.29
−4.25	1.73 ± 0.24	1.90 ± 0.33	1.39 ± 0.35	1.32 ± 0.30
−4.35	1.64 ± 0.23	1.05 ± 0.25	1.43 ± 0.34	1.69 ± 0.32
−4.45	1.86 ± 0.25	1.85 ± 0.32	1.25 ± 0.30	1.01 ± 0.24
−4.55	1.51 ± 0.22	1.30 ± 0.26	1.47 ± 0.34	1.38 ± 0.27
−4.65	1.96 ± 0.25	1.65 ± 0.29	1.17 ± 0.26	1.18 ± 0.24
−4.75	1.61 ± 0.22	1.79 ± 0.30	1.03 ± 0.24	1.37 ± 0.25
−4.85	1.45 ± 0.21	1.70 ± 0.29	1.34 ± 0.29	0.592 ± 0.170
−4.95	1.56 ± 0.21	1.11 ± 0.24	1.09 ± 0.24	1.05 ± 0.21
−5.05	1.70 ± 0.22	1.37 ± 0.25	0.698 ± 0.204	1.02 ± 0.21
−5.15	1.09 ± 0.17	1.01 ± 0.21	1.15 ± 0.26	1.07 ± 0.21
−5.25	1.39 ± 0.20	0.972 ± 0.212	0.992 ± 0.239	0.957 ± 0.197
−5.35		0.906 ± 0.203	0.549 ± 0.179	0.867 ± 0.188
−5.45		0.662 ± 0.171	0.799 ± 0.212	1.08 ± 0.20
−5.55			1.21 ± 0.27	0.943 ± 0.184
−5.65				0.768 ± 0.168

t [(GeV/c)^2] \ Momenta (GeV/c)	$pp \to pp$ 7.115	7.298	7.428	7.557
−3.05	2.47 ± 1.01			
−3.15	4.23 ± 1.37	1.18 ± 0.79		
−3.25	1.96 ± 0.77	0.860 ± 0.711		
−3.35	2.85 ± 0.68	1.52 ± 0.65	1.15 ± 0.97	
−3.45	3.91 ± 0.74	1.88 ± 0.66	0.985 ± 0.906	
−3.55	2.34 ± 0.44	1.52 ± 0.49	2.74 ± 0.89	
−3.65	1.13 ± 0.27	1.22 ± 0.36	0.906 ± 0.464	1.25 ± 0.52
−3.75	1.07 ± 0.24	1.24 ± 0.32	0.759 ± 0.353	1.80 ± 0.55
−3.85	1.47 ± 0.26	2.07 ± 0.40	1.39 ± 0.41	0.561 ± 0.268
−3.95	1.42 ± 0.24	1.73 ± 0.34	1.50 ± 0.42	0.838 ± 0.281
−4.05	1.24 ± 0.21	1.39 ± 0.28	0.896 ± 0.326	0.837 ± 0.273
−4.15	1.74 ± 0.23	1.08 ± 0.23	1.62 ± 0.37	1.21 ± 0.29
−4.25	0.989 ± 0.173	0.806 ± 0.194	1.21 ± 0.30	0.915 ± 0.226
−4.35	1.55 ± 0.22	1.18 ± 0.23	0.884 ± 0.225	1.01 ± 0.22
−4.45	1.11 ± 0.17	0.903 ± 0.196	0.764 ± 0.209	0.929 ± 0.203
−4.55	1.06 ± 0.16	0.753 ± 0.164	0.901 ± 0.207	0.539 ± 0.150
−4.65	0.928 ± 0.145	0.991 ± 0.180	0.428 ± 0.142	0.636 ± 0.156
−4.75	0.766 ± 0.127	0.773 ± 0.154	0.762 ± 0.172	0.570 ± 0.140
−4.85	0.748 ± 0.123	0.518 ± 0.128	0.533 ± 0.142	0.418 ± 0.115
−4.95	0.850 ± 0.130	0.655 ± 0.138	0.731 ± 0.170	0.499 ± 0.122
−5.05	0.861 ± 0.130	1.17 ± 0.18	0.608 ± 0.155	0.542 ± 0.127
−5.15	0.865 ± 0.124	0.677 ± 0.137	0.414 ± 0.117	0.371 ± 0.103
−5.25	0.679 ± 0.111	0.522 ± 0.117	0.363 ± 0.117	0.486 ± 0.114
−5.35	0.818 ± 0.121	0.478 ± 0.111	0.404 ± 0.126	0.698 ± 0.130

TABLE III. (*Continued.*)

$t[(\mathrm{GeV}/c)^2]$ \ Momenta (GeV/c)	$pp \to pp$ 7.115	7.298	7.428	7.557
−5.45	0.686 ± 0.109	0.646 ± 0.124	0.643 ± 0.147	0.512 ± 0.110
−5.55	0.553 ± 0.098	0.344 ± 0.092	0.555 ± 0.132	0.390 ± 0.096
−5.65	0.805 ± 0.115	0.473 ± 0.104	0.594 ± 0.133	0.400 ± 0.094
−5.75	0.821 ± 0.116	0.522 ± 0.117	0.364 ± 0.110	0.320 ± 0.086
−5.85		0.596 ± 0.115	0.474 ± 0.120	0.446 ± 0.097
−5.95			0.463 ± 0.112	0.443 ± 0.095
−6.05			0.392 ± 0.109	0.476 ± 0.096
−6.15				0.341 ± 0.082

t $[(\mathrm{GeV}/c)^2]$ \ Momenta (GeV/c)	$pp \to pp$ 7.684	7.882	8.022	8.161
−3.35	0.810 ± 0.473			
−3.45				
−3.55	1.15 ± 0.58			
−3.65	1.25 ± 0.50			
−3.75	1.29 ± 0.33	1.73 ± 0.62		
−3.85	1.28 ± 0.27	0.364 ± 0.211		
−3.95	0.790 ± 0.183	0.369 ± 0.165	0.713 ± 0.358	
−4.05	0.673 ± 0.166	0.658 ± 0.218		
−4.15	0.603 ± 0.151	0.732 ± 0.220		0.327 ± 0.185
−4.25	0.437 ± 0.116	0.895 ± 0.223	0.565 ± 0.238	0.325 ± 0.184
−4.35	0.505 ± 0.116	0.261 ± 0.118	0.360 ± 0.189	0.421 ± 0.198
−4.45	0.734 ± 0.131	0.502 ± 0.145	0.392 ± 0.175	0.796 ± 0.224
−4.55	0.668 ± 0.117	0.478 ± 0.140	0.850 ± 0.224	0.348 ± 0.129
−4.65	0.477 ± 0.097	0.434 ± 0.124	0.622 ± 0.195	0.254 ± 0.106
−4.75	0.419 ± 0.092	0.348 ± 0.106	0.363 ± 0.138	0.538 ± 0.144
−4.85	0.457 ± 0.086	0.395 ± 0.108	0.291 ± 0.111	0.393 ± 0.121
−4.95	0.338 ± 0.075	0.268 ± 0.084	0.373 ± 0.121	0.272 ± 0.095
−5.05	0.461 ± 0.083	0.273 ± 0.083	0.299 ± 0.103	0.257 ± 0.087
−5.15	0.417 ± 0.075	0.229 ± 0.074	0.430 ± 0.117	0.187 ± 0.074
−5.25	0.257 ± 0.058	0.263 ± 0.075	0.204 ± 0.082	0.316 ± 0.086
−5.35	0.296 ± 0.062	0.169 ± 0.060	0.0958 ± 0.0583	0.165 ± 0.064
−5.45	0.324 ± 0.061	0.313 ± 0.076	0.483 ± 0.115	0.295 ± 0.078
−5.55	0.306 ± 0.058	0.410 ± 0.083	0.163 ± 0.064	0.238 ± 0.069
−5.65	0.325 ± 0.060	0.274 ± 0.067	0.316 ± 0.087	0.260 ± 0.068
−5.75	0.354 ± 0.061	0.266 ± 0.067	0.283 ± 0.082	0.286 ± 0.067
−5.85	0.233 ± 0.052	0.281 ± 0.069	0.305 ± 0.084	0.329 ± 0.071
−5.95	0.322 ± 0.058	0.273 ± 0.065	0.312 ± 0.085	0.214 ± 0.058
−6.05	0.283 ± 0.053	0.332 ± 0.070	0.410 ± 0.092	0.284 ± 0.064
−6.15	0.267 ± 0.051	0.375 ± 0.071	0.215 ± 0.068	0.325 ± 0.066
−6.25	0.347 ± 0.057	0.353 ± 0.071	0.111 ± 0.053	0.254 ± 0.059
−6.35		0.248 ± 0.060	0.195 ± 0.062	0.203 ± 0.052
−6.45		0.340 ± 0.067	0.333 ± 0.076	0.138 ± 0.043
−6.55			0.260 ± 0.064	0.222 ± 0.052
−6.65				0.202 ± 0.049
−6.75				0.158 ± 0.044

t $[(\mathrm{GeV}/c)^2]$ \ Momenta (GeV/c)	$pp \to pp$ 8.298	8.512	8.663	8.813
−4.25	0.332 ± 0.241			
−4.35	1.44 ± 0.49			
−4.45	0.348 ± 0.222			
−4.55	0.153 ± 0.130			
−4.65	0.294 ± 0.129			
−4.75	0.0850 ± 0.0755			
−4.85	0.154 ± 0.094			
−4.95	0.0978 ± 0.0594			

TABLE III. (*Continued.*)

t [(GeV/c)^2]	Momenta (GeV/c)	$pp \to pp$ 8.298	8.512	8.663	8.813
−5.05		0.229 ±0.076	0.399 ±0.169		
−5.15		0.161 ±0.064	0.403 ±0.149		0.196 ±0.163
−5.25		0.163 ±0.066	0.191 ±0.106	0.184 ±0.116	0.218 ±0.108
−5.35		0.274 ±0.073	0.307 ±0.119	0.250 ±0.122	0.0696±0.0690
−5.45		0.199 ±0.064	0.256 ±0.102	0.292 ±0.120	0.257 ±0.102
−5.55		0.290 ±0.069	0.191 ±0.085	0.252 ±0.105	0.128 ±0.071
−5.65		0.277 ±0.066	0.367 ±0.108	0.163 ±0.085	
−5.75		0.181 ±0.053	0.256 ±0.089	0.145 ±0.078	
−5.85		0.312 ±0.063	0.249 ±0.083		0.0641±0.0521
−5.95		0.176 ±0.047	0.247 ±0.080	0.209 ±0.080	0.197 ±0.071
−6.05		0.215 ±0.050	0.183 ±0.068	0.211 ±0.077	0.100 ±0.053
−6.15		0.156 ±0.043	0.113 ±0.054	0.235 ±0.077	0.175 ±0.062
−6.25		0.216 ±0.048	0.192 ±0.065	0.200 ±0.071	0.0950±0.0481
−6.35		0.148 ±0.041	0.131 ±0.055	0.220 ±0.071	0.131 ±0.052
−6.45		0.179 ±0.042	0.341 ±0.077	0.220 ±0.069	0.0926±0.0449
−6.55		0.143 ±0.037	0.126 ±0.051	0.146 ±0.059	0.126 ±0.049
−6.65		0.151 ±0.038	0.200 ±0.059	0.0702±0.0457	0.178 ±0.054
−6.75		0.266 ±0.047	0.0998±0.0454	0.137 ±0.054	0.128 ±0.046
−6.85		0.233 ±0.060	0.181 ±0.053	0.117 ±0.049	0.126 ±0.045
−6.95			0.169 ±0.050	0.161 ±0.054	0.0920±0.0385
−7.05			0.137 ±0.045	0.152 ±0.051	0.0913±0.0369
−7.15				0.184 ±0.053	0.151 ±0.043
−7.25					0.170 ±0.044
−7.35					0.162 ±0.043

of authors have argued that diffractive effects are seen at all angles.[7,22]

We might consider the scattering beyond this dip to be due to all "other" processes; that is, the scattering is not explained by diffractive (or peripheral) processes. The same distinction is not so easily made in pp scattering due to the absence of dips at these energies, but we might expect that at large angles we avoid the diffraction part. In Secs. IV B and IV C we will compare our data with the predictions of constituent and statistical models.

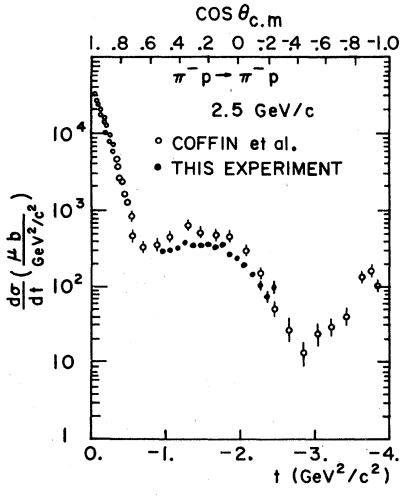

FIG. 11. Differential cross section for $\pi^- p \to \pi^- p$ at 2.5 GeV/c.

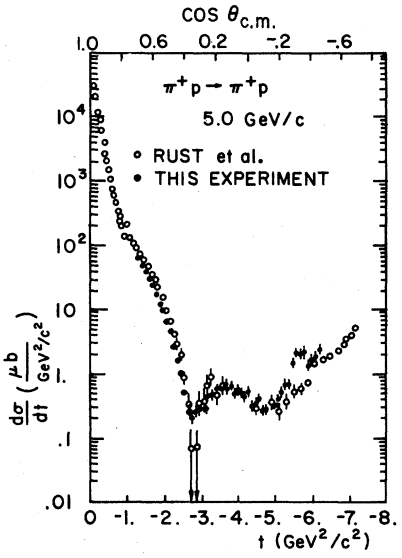

FIG. 12. Differential cross section for $\pi^+ p \to \pi^+ p$ at 5.0 GeV/c.

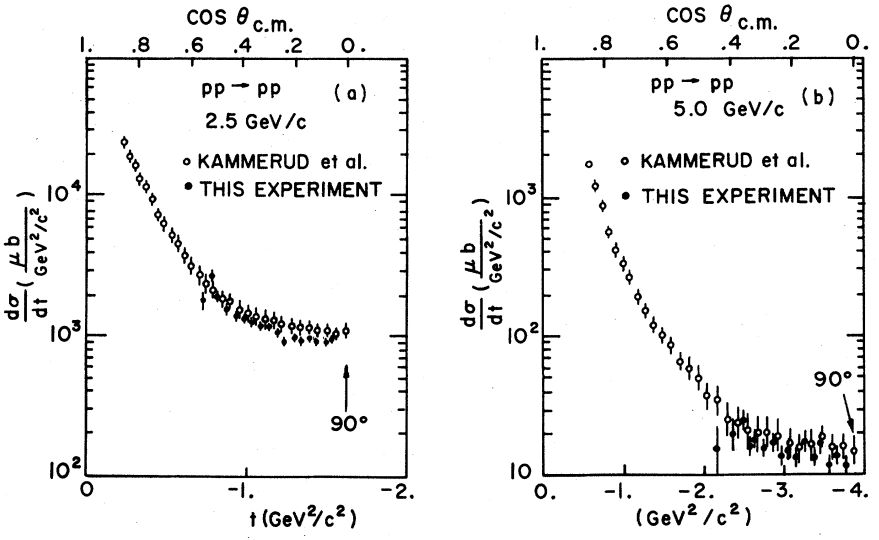

FIG. 13. Differential cross section for $pp \to pp$ at (a) 2.5 GeV/c and (b) 5.0 GeV/c.

B. Comparison of constituent models with data

1. Dimensional-counting rule

The previous proton-proton data do not follow the predicted s^{-10} rule at all energies: Plotted against t, the logarithm of the 90° cross section falls into sections of straight lines with several abrupt changes of slope.[16,23] Plotted against s, these changes appear as an s-shaped curve. Of course, the data should follow the dimensional-counting rule only asymptotically, but there is wide disagreement about the behavior of the existing data.[7,22,24]

In Fig. 16, we present our proton-proton data at two angles on a $\log(d\sigma/dt)$ vs $\log(s)$ plot. An s^{-10} line is drawn to match the data at the high-energy end. This line does not follow the data at low energies. We have fitted the data above $s = 12$

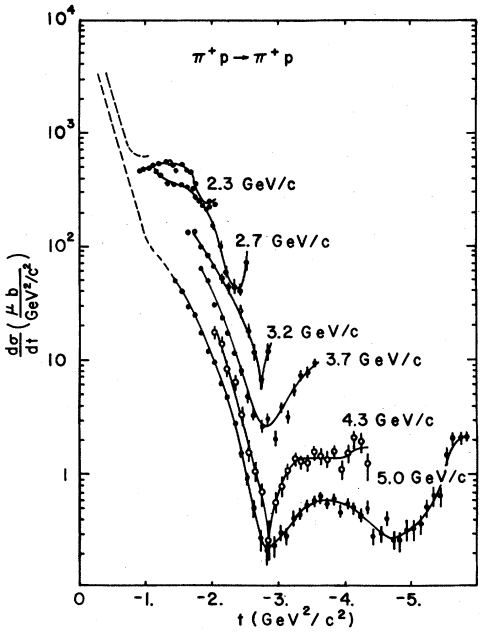

FIG. 14. Differential cross sections for positive-pion–proton scattering at several momenta. Dashed lines represent the forward cross sections measured by Refs. 15 and 20.

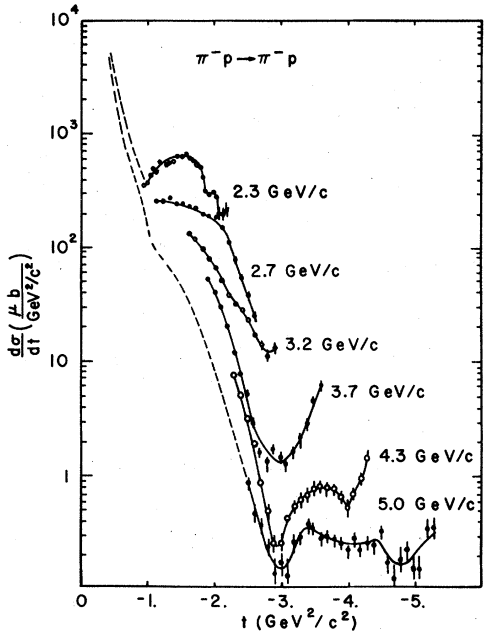

FIG. 15. Differential cross sections for negative-pion–proton scattering at several momenta. Dashed lines represent the forward cross sections measured by Refs. 16 and 21.

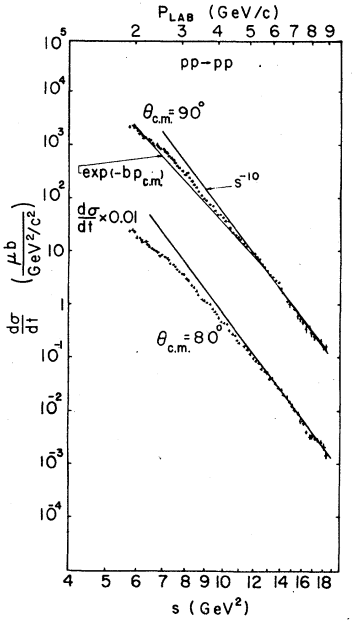

FIG. 16. Proton-proton differential cross sections at constant c.m. angles, plotted as functions of energy. The lines are described in the text.

GeV² to the form $\ln(d\sigma/dt)=a-n\ln(s)$, obtaining for the 90° data, $n=10.07\pm0.11$ with a χ^2 of 30 for 24 degrees of freedom. The dimensional-counting rule is in excellent agreement with our result. Fits at nearby angles are similar but the value of n decreases: At 75°, $n=9.21\pm0.13$. Thus the exact agreement at 90° may be accidental. Results of fits for a number of angles are given in Table IV.

Our data suggest that the asymptotic region begins at about $s=12$ GeV². This conclusion can also be reached by looking at the previous data in this energy range. Our agreement with previous experiments (Kammerud *et al.*[17] and Akerlof *et al.*[23]) is very good. However, for 90° cross sections at higher energy there is uncertainty about whether or not there is evidence for a constant power (Barger[24]), or if there are oscillations around a constant power (Schrempp and Schrempp,[22] Hendry[7]). Some authors[8] claim that the data develop

TABLE IV. Values of n in fits of $pp\to pp$ data to form $\ln(d\sigma/dt)=a-n\ln(s)$.

$\theta_{c.m.}$	n $(12\leq s\leq 19$ GeV²)	χ^2/DF
90°	10.07±0.11	30/24
85°	10.05±0.11	41/24
80°	9.74±0.11	68/24
75°	9.21±0.13	116/24

an s^{-12} dependence at about $s=25$ GeV². Our own examination of the previous 90° data indicates a poor fit for $n=10$ in the range $12<s<60$ GeV², with the highest few points deviating seriously.

It must be pointed out, though, that above $s=12$ GeV², the parametrizations[25]

(a) $d\sigma/dt=a\exp(-bp_{c.m.})$,

(b) $d\sigma/dt=a\exp(-b\sqrt{s})$,

(c) $d\sigma/d\Omega=a/s\exp(-bp_t)$,

fit the present data as well as s^{-10}. The forms (a) and (b) follow the data fairly well to lower energy also. A plot of $d\sigma/dt=a\exp(-bp_{c.m.})$ is included in Fig. 16. These forms do not fit the higher-energy data of Akerlof *et al.*[23] and Allaby *et al.*[26]

The evidence first cited for agreement with the dimensional-counting rule in pion-proton scattering is very weak. For π^-p, it is based on three points[6] with errors of ~30%. There are no previous data for π^+p above $s=10$ GeV².

In Fig. 17, we have plotted our new data for angles of 80°, 90°, and 100° (averaged over ±0.05 in $\cos\theta_{c.m.}$) and have included in these plots all the previous data with momentum greater than 3 GeV/c.[27] It is clear that a straight s^{-8} line is not tenable over the entire range of data. Both positive and negative pion data show a large dip, which is caused by the diffractive dip at $t=-2.8$ GeV²/c^2. The dip has a different position for the different angles because it is constant in t. Clearly, one cannot hope to make the dimensional-counting rule apply in the region of the dip, so the s^{-8} lines are drawn to approximate the highest-energy cross sections. Even at these energies, there are clear deviations from the predicted power law. We have fitted the data to $\ln(d\sigma/dt)=a-n\ln(s)$ for several angles at energies above $s=10$ GeV². The results are listed in Table V. It is clear that the data are not well described by a single power of s, although it is possible that the cross sections oscillate about the s^{-8} line. To make this region clearer, Fig. 18 plots $s^8(d\sigma/dt)$ vs s. The energy dependence is seen to become steeper with increasing energy, without necessarily stopping at s^{-8}. The lines drawn in Figs. 17 and 18 do appear to describe an "average" energy dependence of the cross section. The fit to negative-pion data at 90° does approach s^{-8} as the lower energy limit is raised. (The positive pion data do not go to high enough energy to allow a similar observation.) This suggests that the data may be approaching the dimensional-counting-rule prediction asymptotically, but it seems equally likely that the slope changes again at higher energy. Finally, we note that the value

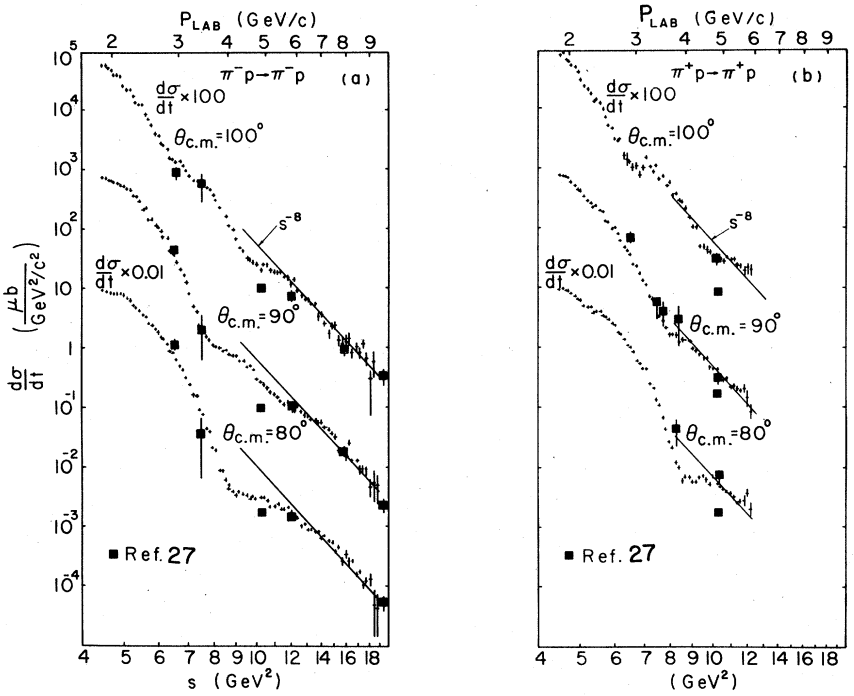

FIG. 17. Differential cross sections at constant c.m. angles for (a) $\pi^- p$ and (b) $\pi^+ p$ scattering. Data from Ref. 27 are also plotted. The lines are described in the text.

TABLE V. Values of n in fits of (a) $\pi^- p \to \pi^- p$ and (b) $\pi^+ p \to \pi^+ p$. Data to form $\ln(d\sigma/dt) = a - n \ln(s)$.

$\pi^- p$

$\theta_{c.m.}$	n $(10 \leq s \leq 19\ \text{GeV}^2)$	χ^2/DF	n $(12 \leq s \leq 19\ \text{GeV}^2)$	χ^2/DF	n $(14 \leq s \leq 19\ \text{GeV}^2)$[a]	χ^2/DF
105°	7.76±0.26	38/30	8.81±0.45	22/20	6.52±0.89	15/11
100°	6.88±0.16	68/32	7.62±0.29	34/22	6.79±0.49	23/14
95°	6.10±0.14	67/32	7.29±0.25	26/22	6.96±0.29	26/15
90°	5.69±0.12	82/33	6.67±0.22	45/23	8.32±0.33	23/15
85°	5.41±0.11	134/32	6.67±0.20	46/22	8.22±0.29	19/15
80°	5.36±0.10	95/33	6.05±0.19	49/23	7.34±0.29	36/15
75°	4.72±0.11	252/35	5.91±0.18	71/23	6.63±0.29	36/18

$\pi^+ p$

$\theta_{c.m.}$	n $(10 \leq s \leq 13\ \text{GeV}^2)$[a]	χ^2/DF
105°	12.01±0.83	27/9
100°	4.82±0.67	5/9
95°	3.29±0.54	12/9
90°	6.42±0.51	11/9
85°	7.25±0.46	20/9
80°	4.69±0.44	11/9
75°	1.33±0.49	20/9

[a] Averaged over $\cos\theta_{c.m.} \pm 0.1$.

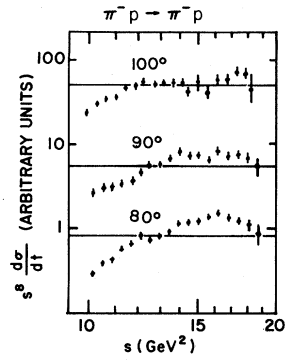

FIG. 18. $s^8 d\sigma/dt$ at constant c.m. angles for $\pi^- p$ scattering. The ordinate is logarithmic with decades indicated.

of n drops rather quickly for energies above $s = 14$ GeV^2, at angles away from 90°. This whole region is characterized by rapidly changing structure, and the s^{-8} rule can only possibly be true, over a large angular and energy range, in an average sense.

2. *Constituent-interchange model*

In Fig. 19 a number of angular-distribution ratios

$$R(z) = \frac{d\sigma}{dt}(z) \Big/ \frac{d\sigma}{dt}(0)$$

are given using high-energy $\pi^- p$ data. Qualitatively, they tend to show an energy-independent shape. Additional distributions are not shown, to retain clarity, but agree substantially with those plotted. Below a momentum of 6 GeV/c, the distributions do not agree. The prediction of Gunion *et al.* for $\alpha = 2$ and $\beta = 1$ is drawn on the graph, and it is seen to agree fairly well with the data.

With α and β fixed, the ratio of positive to negative elastic scattering at 90° c.m. is given by

$$R_{+-} = \frac{\frac{d\sigma}{dt}(\pi^+ p)}{\frac{d\sigma}{dt}(\pi^- p)} = \frac{(4\alpha + \beta)^2}{(\alpha + 4\beta)^2} .$$

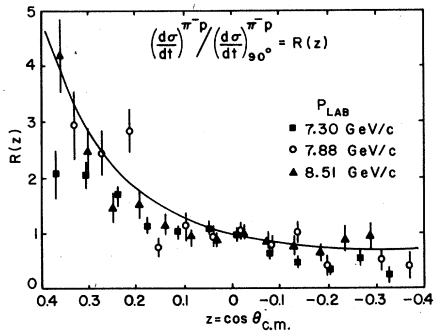

FIG. 19. Ratio of the differential cross section at $z = \cos\theta_{c.m.}$ to the 90° cross section, for several negative-pion–proton data sets. Curve is the prediction of Ref. 8.

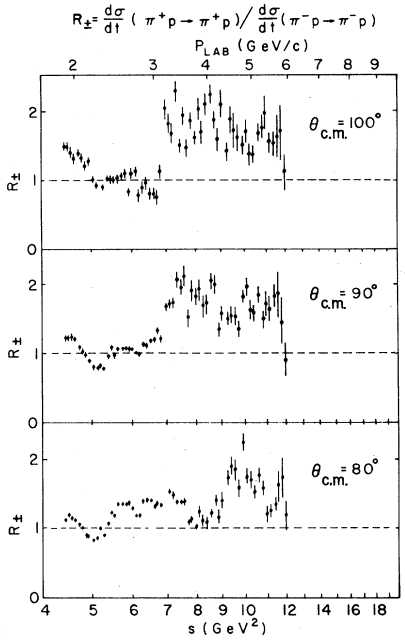

FIG. 20. Ratio R_{+-} of the positive-pion–proton cross section to the negative-pion–proton cross section, as a function of energy, for several angles.

Our positive-pion data do not go to high enough energy to call for serious comparison with the theory and the angular-distribution ratios computed do not agree well with the theoretical prediction. Nonetheless, we have computed the experimental ratio to see if it tends to the predicted value.

The experimental ratio R_{+-} for three angles is shown in Fig. 20. For each angle, the ratio has a low-energy part which oscillates around unity and a high-energy part of magnitude 1.6. (The CIM predicts $R_{+-} = 2.25$ for the usual quark configuration.) The division between these parts occurs at the same energy at which the distributions of cross sections at constant angles (Fig. 17) dip. A possible interpretation of these ratios is that below this minimum, the cross section is mainly diffractive and reflects the charge independence of the size of the proton. Departures from a ratio of unity can be attributed to the excitation of baryon resonances. In the region beyond the diffractive dip, the predominant process is constituent collision, so that the cross section reflects, instead of the pion-proton radius, the distribu-

tion of constituents of the particles.

The α and β parameters can be adjusted to give $R_{+-}=1.6$; the resulting angular distribution appears consistent with our data.

3. *Quark-rearrangement model*

Fishbane and Quigg predict the ratio of π^+p to π^-p wide-angle cross sections to be 1.5. This is in good agreement with our data. The Fishbane and Quigg argument is not meant to be rigorous, but a simple test of the validity of constituent ideas. The approximate agreement with the data, combined with some agreements in other experiments, should probably be considered encouraging

We now summarize our comparison with the constituent models.

(1) s^n dependence. We have good agreement s^{-10} for 90° pp scattering from $s=12$ to 19 GeV^2, but other parametrizations also give good fits. The $\pi^{\pm}p$ agree with s^{-8} only in an average sense.

(2) Angular dependence. The π^-p data agree fairly well with the constituent-interchange model, but the α and β parameters are not well determined.

(3) Ratio of positive- to negative-pion scattering. The prediction of the constituent-interchange model can be fitted if the parameters are adjusted. Agreement with the quark rearrangement scheme of Fishbane and Quigg is good.

(4) Additional structure. In $\pi^{\pm}p$ scattering, there is abundant evidence for a highly structured cross section in addition to the diffractive structure and approximate power-law dependence. Proton-proton scattering shows no such structure.

C. Comparison of statistical models with data

1. *Review of previous experiments*

Before examining our data for Ericson fluctuations, we briefly mention evidence from other experiments. The general technique used in looking for fluctuations is to inspect the cross sections for any narrow structure in energy or angle, where "narrow" means small compared to resonance widths or angular envelopes.

The data of two proton-proton elastic scattering experiments were examined this way with negative results.[23,28] In retrospect, this seems to have been a futile place to look since the reaction is "exotic"; that is, there are few if any observed direct-channel resonances and, therefore, no reason to expect fluctuations.

A dramatic effect, atrributed to Ericson fluctuations, has been reported in elastic π^+p scattering. The experiment of Eide *et al.*[20] measured the almost complete angular distribution of $\pi^{\pm}p$ elastic scattering at 5 GeV/c. Later Schmidt *et al.*[29]

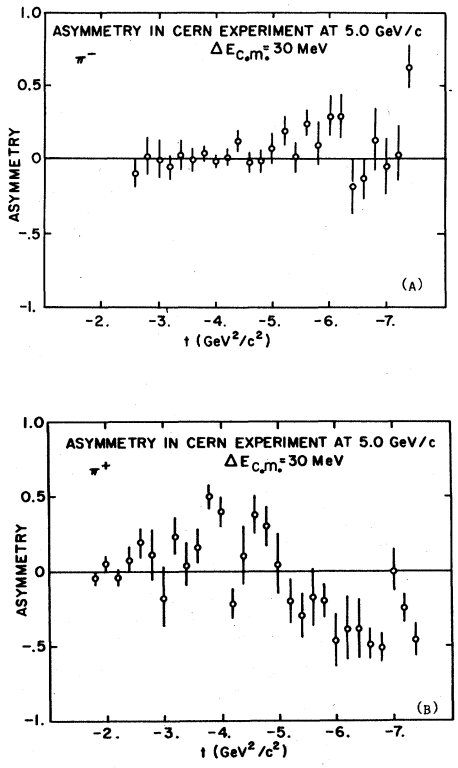

FIG. 21. Asymmetry measured by Schmidt *et al.*, (Ref. 29) in (a) negative-and (b) positive-pion–proton elastic scattering at 5 GeV/c. Asymmetry parameter is defined in text.

reexamined the data to look for fluctuations. Because the incident beam in the experiment had some momentum spread, Schmidt *et al.* were able to divide the data into angular distributions with two slightly different central momenta. From these distributions, they computed what they called the asymmetry parameter, defined as

$$A(t)=\frac{(d\sigma/dt)_u-(d\sigma/dt)_l}{(d\sigma/dt)_u+(d\sigma/dt)_l},$$

where u and l refer to cross sections at the upper and lower momenta. The difference in momentum corresponded to a 30-MeV c.m. energy difference. Their asymmetries are plotted in Fig. 21. In the π^+p data, there is a marked asymmetry indicating that the cross section changes by as much as a factor of 3 for the 30-MeV energy change. The π^-p asymmetries are consistent with zero except for a few points. The dramatic result for the positive data suggests that the cross section changes very rapidly in this region—perhaps faster than expected, given the resonance widths at lower energy.

Motivated by the results of Schmidt *et al.*, Michael *et al.*[30] examined their 3.7- and 7.1-GeV/c π^+p data in the same way and found no such effect.

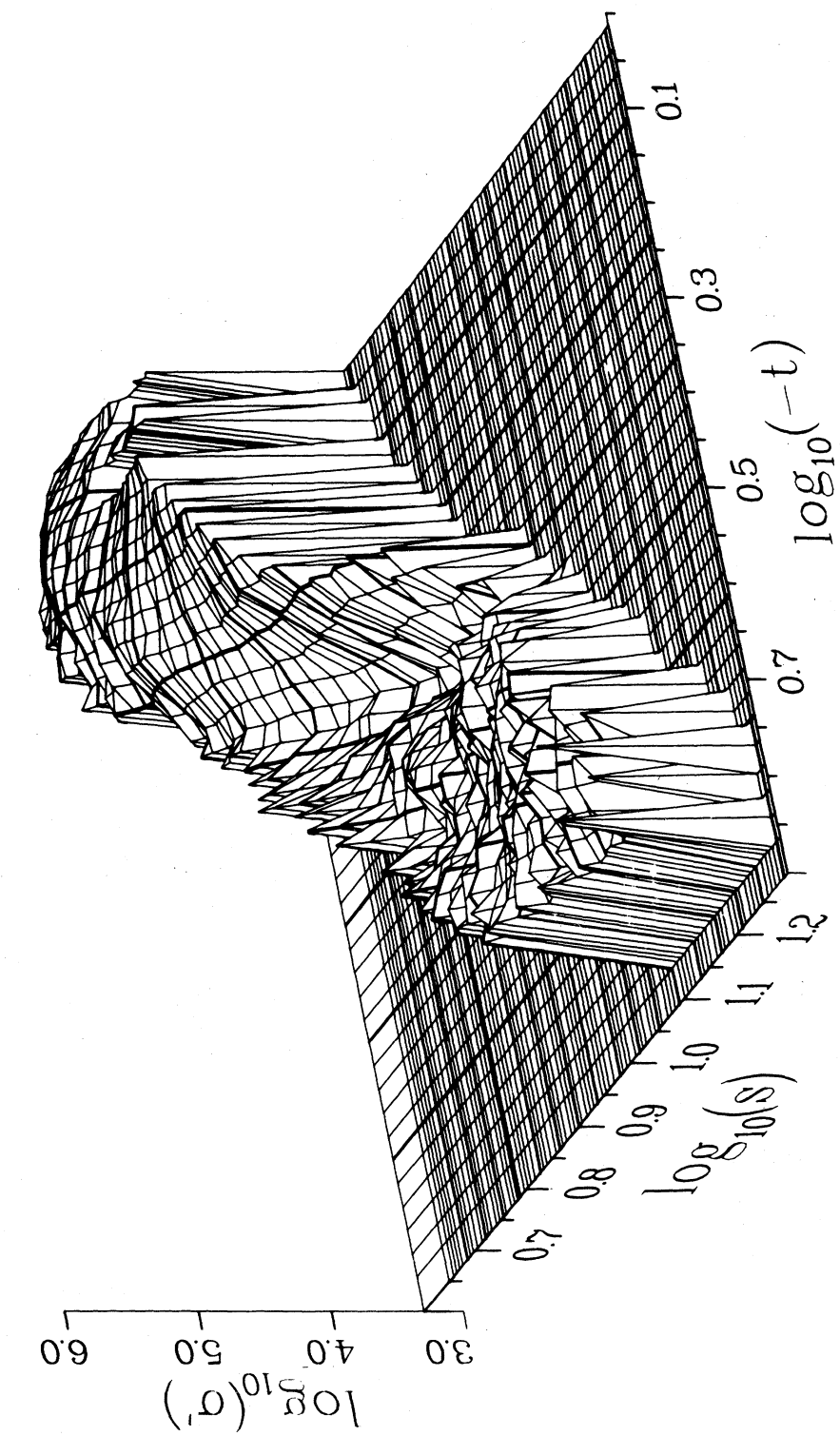

FIG. 22. Three-dimensional plots of $\log_{10}(\sigma')$ vs. $\log(s)$ and $\log(-t)$, where $\sigma' = s^3 t^3 \, d\sigma/dt$ and s and t are in GeV^2/c^2; σ is in μb. (a) $\pi^- p \to \pi^- p$; (b) $\pi^+ p \to \pi^+ p$ (c) $pp \to pp$.

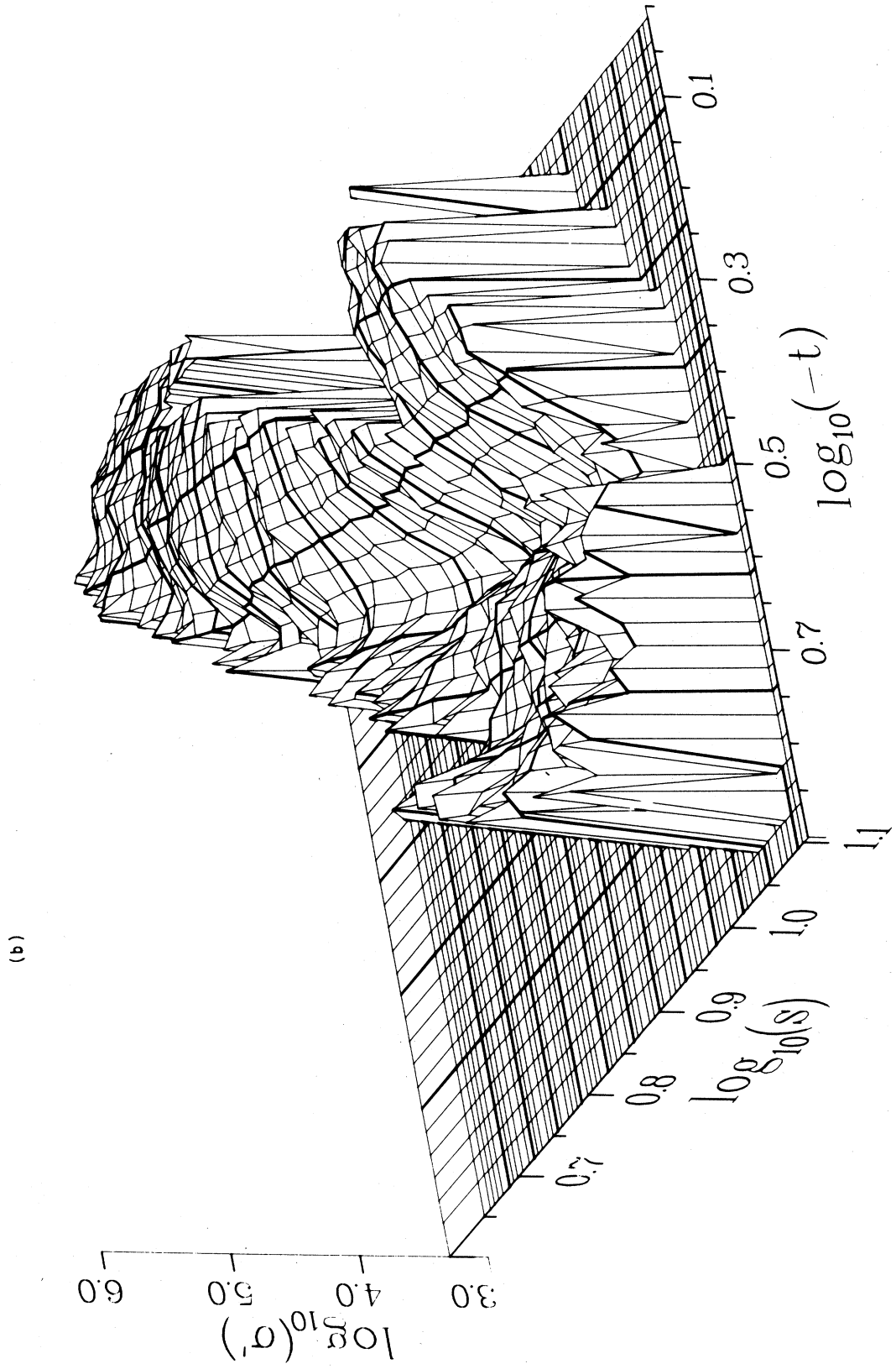

FIG. 22. *(Continued.)*

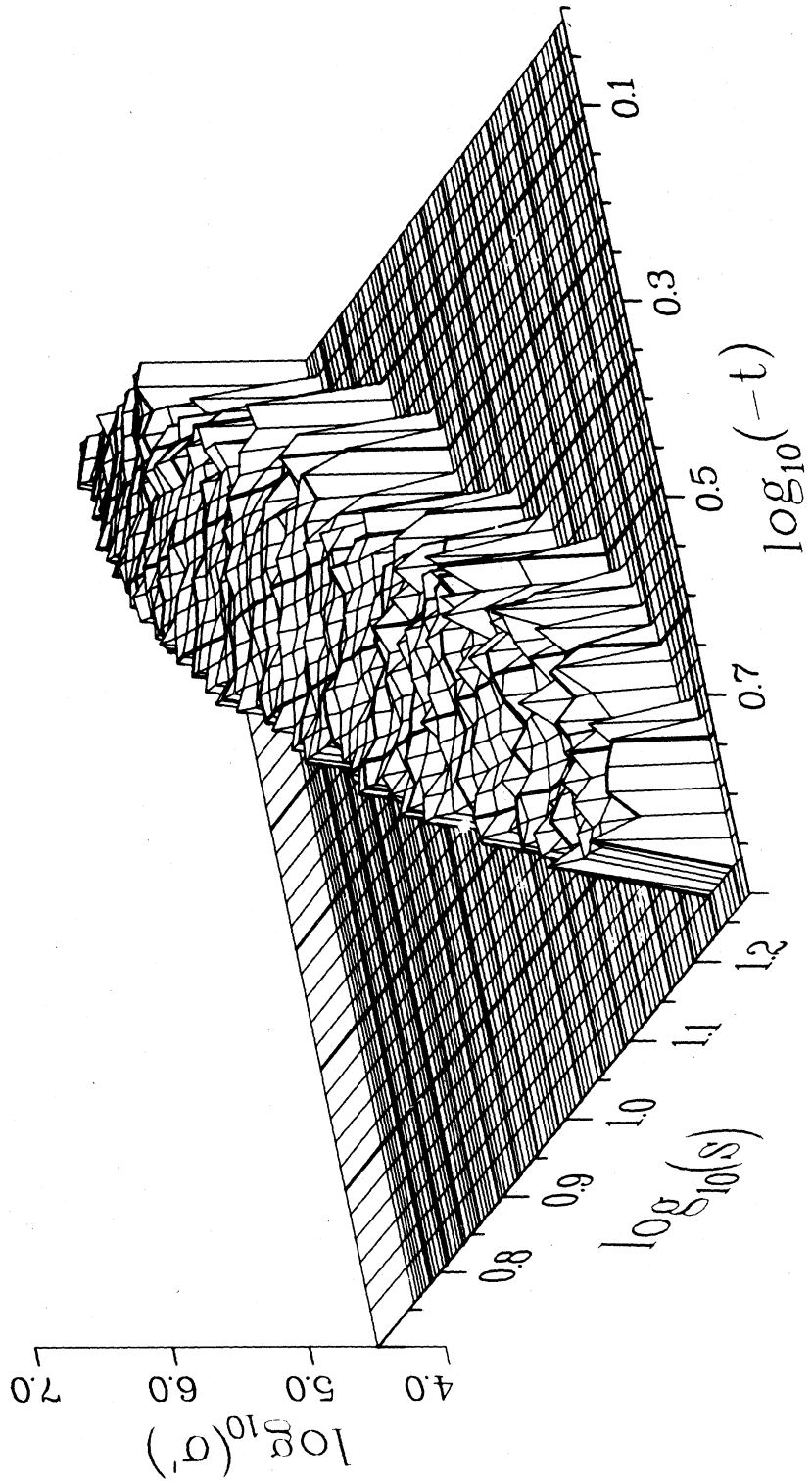

FIG. 22.*(Continued.)*

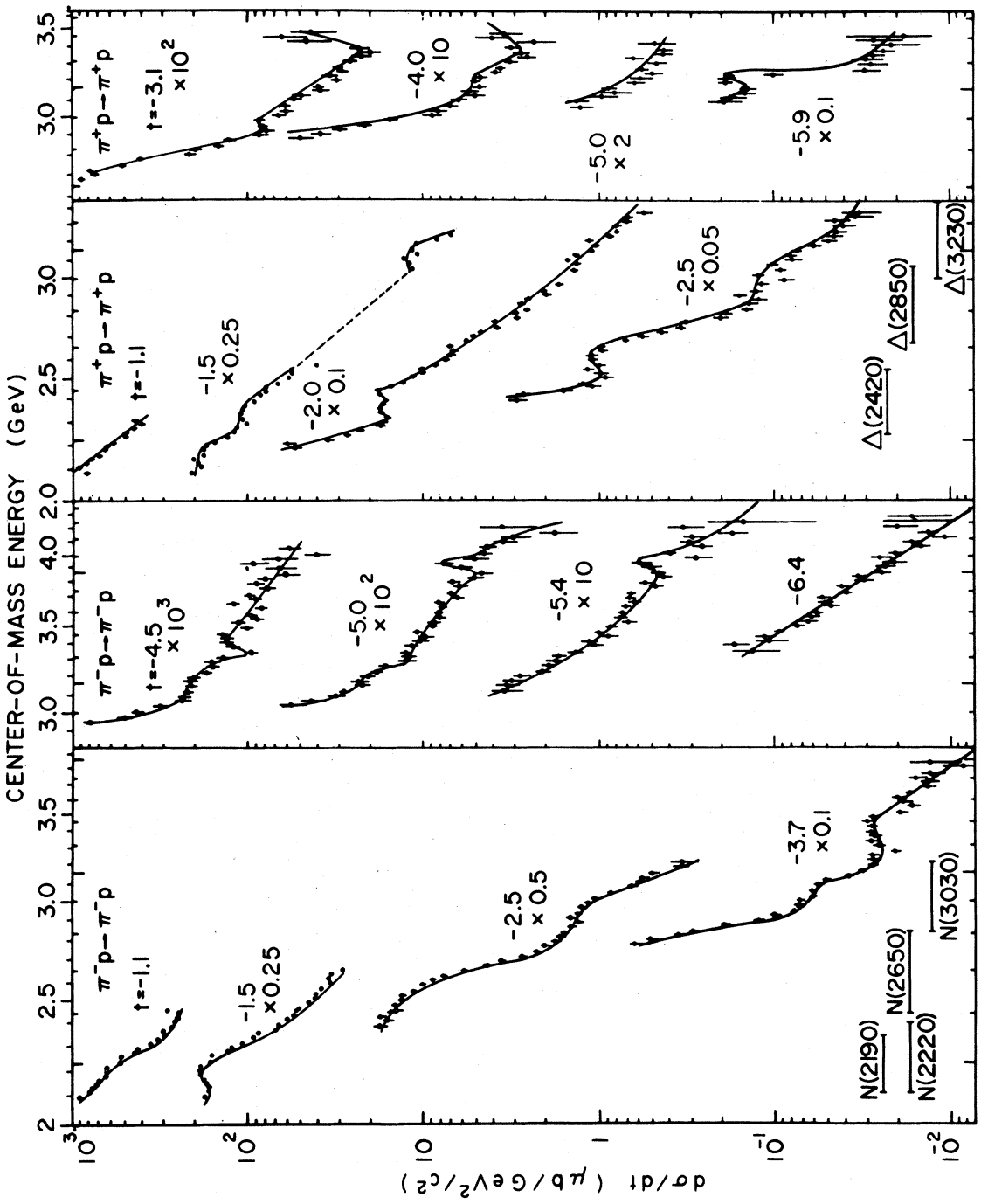

FIG. 23. Pion-proton cross sections at constant t values, plotted as functions of energy. The lines are drawn to guide the eye. The top number by each plot is t in GeV$^2/c^2$; the lower one, if present, is the scale factor by which $d\sigma/dt$ has been multiplied.

Dixon *et al.*[31] similarly examined their backward $\pi^- p$ data from 3 to 5.5 GeV/c, and they reported no narrow structure but they did see a large asymmetry when the c.m. energy difference was 140 MeV. Since they claim that resonances can be seen in their data, an asymmetry observed for this energy separation is presumably just a manifestation of the simple resonance structure.

2. *General properties of the new data*

Because our new data cover a very large energy and angular region in fine intervals (the 2% momentum increments correspond to intervals of 20 to 30 MeV in the center of mass), and because the fluctuating part of the cross section is expected to be relatively greater at wide angles, these data are the first to be really suitable for testing the theory and resolving the discrepancy of the earlier experiments.

To get an overall view of the data, we have plotted them, in Fig. 22, in a fashion similar to the plots made in nuclear scattering. Error bars are *not* drawn on this plot in order to prevent visual confusion. As in the nuclear scattering example, we see apparent rapid changes in the cross section for small changes in angle or energy. However, the statistical significance of these variations must be examined.

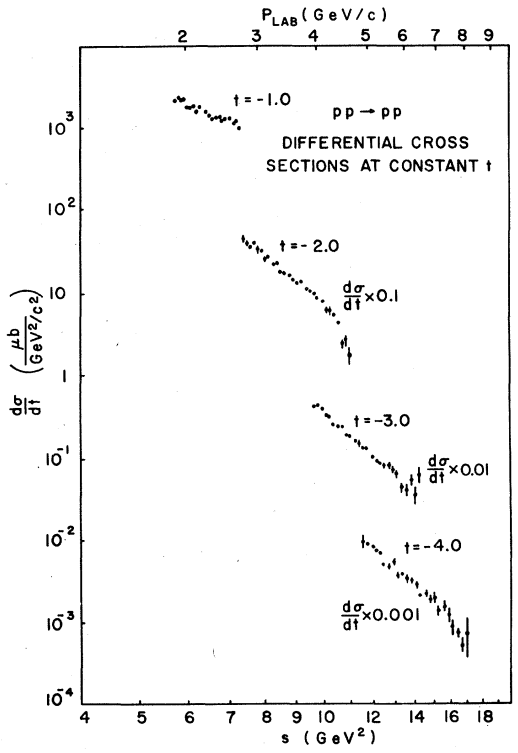

FIG. 24. Proton-proton cross sections at constant t values, plotted as functions of energy. t is in GeV$^2/c^2$.

We have thus taken constant t slices of the data and plotted them with their errors, a sample of which is shown in Fig. 23. This data cannot be simply characterized; a variety of shapes and slopes is seen. In contrast, the proton-proton data, plotted the same way in Fig. 24, show a simple and universal shape.

Looking at the pion data closely, one notes that for many of the t values a number of the points deviate significantly from a simple curve. At low energy we might expect some of these departures to be due to known resonances. The mass and widths of the well-established resonances in the energy range are indicated in Fig. 23. A particularly clear example is the bump found in the $\pi^- p$ cross section at $t = -1.5$ GeV$^2/c^2$, corresponding to the $N(2190)$ and $N(2220)$ resonances. At 30° (c.m.) to either side (not shown on this graph), the bump is absent, as expected for resonances with angular momentum 3 or 4. We take this as evidence that this method of displaying the data reveals known resonant structure. It can be seen in the cross sections plotted here, and in the rest of the data, that there is a structure—a bump or a dip—within the width of each of the known resonances. In general, the structures are significantly narrower than the known resonances and are not centered on them, so it is likely that they are new phenomena. Further, we can see structures at higher energies where there are no known nucleon resonances.

To get a quantitative measure of the departures from simple curves, we have fitted the constant t cross sections to several different functions of s. These attempts have met with the same obstacle: We have no *a priori* knowledge of the functional form of the background curve. However, two different types of fits yield substantially the same result. The first type of fit is of the logarithm of the cross section to a polynomial in the logarithm of s. Fits generally converge with three or four powers, but give bad fits in the χ^2 sense, where the cross section shows rapid structure. The fits generally act to average the irregularities, so deviations from fits are above and below the fit lines. The second fitting form is to $d\sigma/dt = as^b + cs^d$. This form is particularly amenable to demanding that the parameters vary slowly and continuously for adjacent t values. This constraint acts to emphasize different deviations than the polynomial fit, but gives generally similar numerical results. Examples of these fits are shown in Fig. 25.

We have found no parametrization of the data which gives good fits to all the constant t data. The weakest conclusion we can draw from this is that there is substantial s-channel structure at high energy. It has been generally believed that

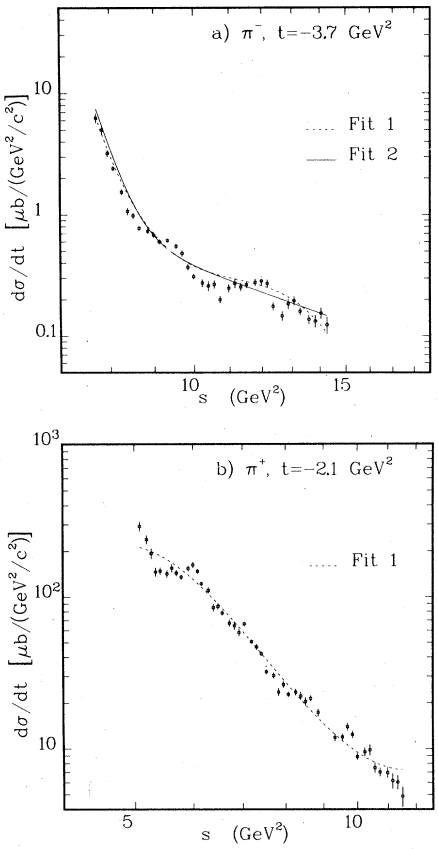

FIG. 25. Examples of fits to $\pi^{\pm}p \to \pi^{\pm}p$ differential cross sections at constant values of t. The two types of fit are described in the text.

t-channel processes dominate at high energies, leading to a smooth dependence on s. Our data show structure in s in pion-proton scattering up to the highest energies measured.

To make a stronger statement, we have noted that the deviations from simple curves tend to appear in bumps and dips that are fairly narrow—100 to 150 MeV. This is narrower than the widths of known high-mass resonances. It is also seen that structures persist over several adjacent t values, but not over all the angles.

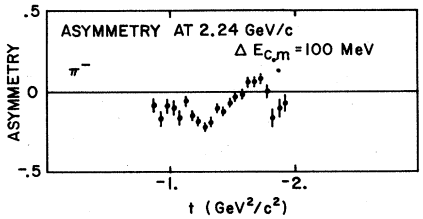

FIG. 26. Asymmetry for negative-pion–proton data at 2.24 GeV/c, with an energy separation of 100 MeV. See text for definition of asymmetry.

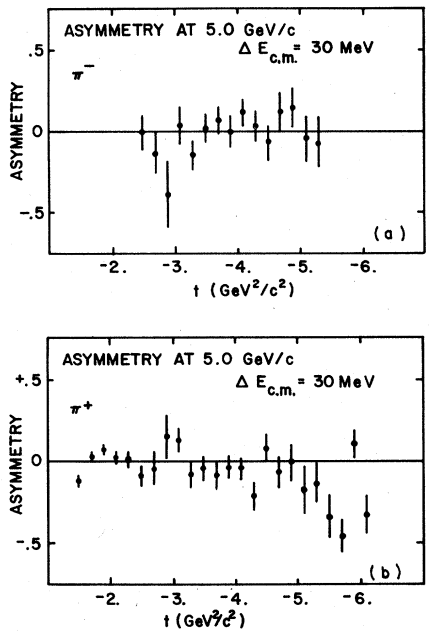

FIG. 27. Asymmetries for (a) negative- and (b) positive-pion–proton scattering at 5.0 GeV/c, with an energy separation of 30 MeV.

3. *Asymmetry analysis*

The data have also been examined using the method of Schmidt *et al.* The asymmetry in the region of the $N(2190)$ and $N(2220)$ in the π^-p data is shown in Fig. 26. For this asymmetry, the c.m. energy difference is about 100 MeV, and the large asymmetry seen is an indication of the resonance structure.

At 5 GeV/c the asymmetry has been calculated for each 2% momentum interval (30-MeV c.m. difference). The results differ from those of Schmidt *et al.* The asymmetries at 5.0 GeV/c for π^+p and π^-p are shown in Fig. 27. These correspond to the same energies as shown in Fig. 21. There is a clear disagreement. However, there is a partial agreement of the π^+p asymmetry at

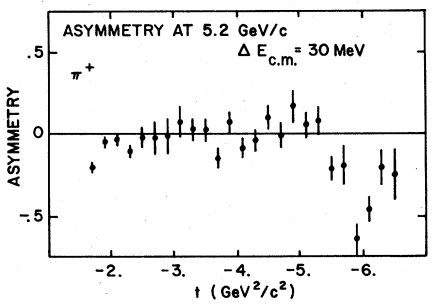

FIG. 28. Asymmetry for positive-pion–proton scattering at 5.2 GeV/c, with an energy separation of 30 MeV.

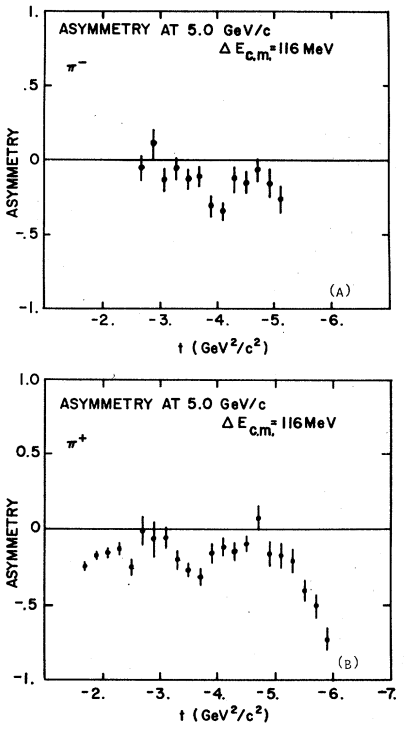

FIG. 29. Asymmetries for (a) negative- and (b) positive-pion–proton scattering at 5.0 GeV/c, with an energy separation of 116 MeV.

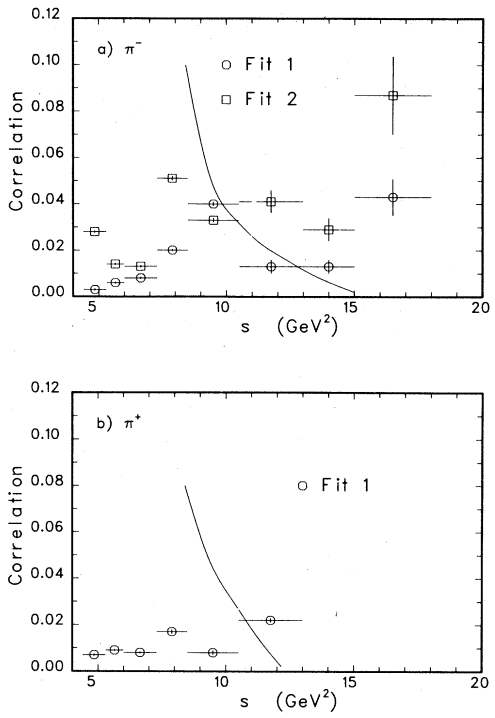

FIG. 30. Correlation functions for the (a) negative- and (b) positive-pion–proton data. See text for definition of the function. The solid lines are the predictions of Frautschi (Ref. 3), reduced by a factor of 10.

5.2 GeV/c (Fig. 28). Both our data and Schmidt's show a large negative asymmetry at $t = -6$ GeV$^2/c^2$, but we do not see a positive asymmetry at $t = -4$ GeV$^2/c^2$. At a larger energy separation (116 MeV), both positive and negative data show a structured asymmetry, as displayed in Fig. 29. This is a strong indication of structure of the type we have claimed above by a direct examination of the data.

Examining the rest of the data in this way, we have seen that throughout all the positive- and negative-pion data, there are significant asymmetries when the c.m. energy interval is about 100 MeV. In contrast, there is no asymmetry in any of the proton-proton data.

4. *Correlation-function analysis*

We have calculated the correlation functions for our data. The procedure used was to make fits to the constant-t data, use these data and fits to compute correlation functions, and then for each energy interval, average the correlation function of each t value. For the $\pi^- p$ data, we used both fitting methods mentioned previously to estimate the smooth part of the cross section, whereas for the $\pi^+ p$ and pp data, we used only the polynomial method. The pion-proton results are shown in Fig. 30 and the pp data in Fig. 31.

We see that both positive- and negative-pion–proton data show significant correlations, while the proton data do not.[32] The curves in the figures are Frautschi's predictions, calculated for a density of states larger by a factor of 100. The serious disagreement between the model and experiment depends primarily on the density of states; in the theory, the strong exponential increase of states forces a strong decrease in the correlation function. The normalization of the density is presumably adjustable.

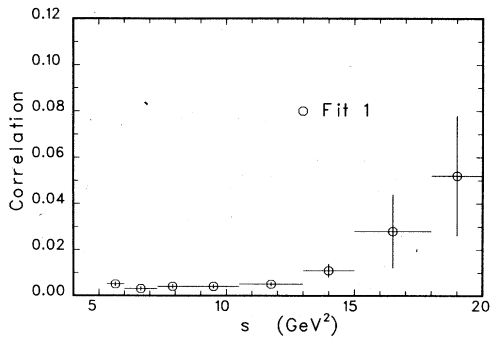

FIG. 31. Correlation function for the proton-proton data. See text for definition of function.

TABLE VI. Values of T_0 in fits of (a) $\pi^- p \to \pi^- p$ and (b) $\pi^+ p \to \pi^+ p$. Data to form $\ln(d\sigma/dt) = b - \sqrt{s}/T_0$.

(a) $\pi^- p$

$\theta_{c.m.}$	T_0(GeV^2) ($10 \leq s \leq 19$ GeV^2)	χ^2/DF	T_0(GeV^2) ($12 \leq s \leq 19$ GeV^2)	χ^2/DF	T_0(GeV^2) ($14 \leq s \leq 19$ GeV^2)	χ^2/DF
100°	0.262±0.006	60/32	0.250±0.009	38/22	0.292±0.021	22/14
90°	0.317±0.007	64/33	0.285±0.010	39/22	0.238±0.009	24/15
80°	0.337±0.007	72/33	0.314±0.010	43/23	0.269±0.010	34/15

(b) $\pi^+ p$

$\theta_{c.m.}$	T_0(GeV^2) ($10 \leq s \leq 13$ GeV^2)	χ^2/DF
100°	0.344±0.047	5/9
90°	0.257±0.020	11/9
80°	0.352±0.033	11/9

5. *Comparison with predictions of Eilam et al.*

We have also compared our data with the prediction of Eilam *et al.* that $d\sigma/dt \propto \exp(-\sqrt{s}/T_0)$, and the constant T_0 is on the order of 140 to 160 MeV. We get a not dissimilar result if we fit the 90° data above $s = 4$ GeV^2. For $\pi^+ p$, $T_0 = 132$ MeV ±1%; for $\pi^- p$, $T_0 = 142$ MeV ± 1%. However, the fits are very poor in the χ^2 sense. It is argued, though, that the $\exp(-\sqrt{s}/T_0)$ energy dependence is the average behavior, around which there should be statistical fluctuations which would result in a poor fit. On the other hand, the major reason for the bad fit quality is the large "diffractive" dip. There is no evidence that this is statistical, so the theory should either include this coherent structure or be applied in energy regions where it is not present.

Choosing the latter approach, we have fitted the pion-proton data to the form $d\sigma/dt = \alpha \exp(-\sqrt{s}/T_0)$ for several energies and angles. The binning is the same as used in part A of this section in the comparison with the dimensional-counting rule. The results are given in Table VI.

We note three points: (1) Only in the highest-energy range of the $\pi^- p$ data are the cross sections symmetric around 90°. The statistical model predicts a symmetric cross section. (2) There is only a hint, again in the $\pi^- p$ case, that the temperature T_0 is tending to a constant independent of energy. (3) The temperature at the highest energy is quite different from the prediction of Eilam *et al.*,; they relate T_0 to the hadronic interaction radius, obtaining for $1.1F$, $T_0 = 160$ MeV. Thus we must conclude that if the model is correct, and there is a statistical component of the cross section, the component is small.

In contrast to the πp case, the pp data agree fairly well with an exponential energy dependence, even though the theory is *not* supposed to apply to exotic reactions. As pointed out in part A of this section, several exponential forms fit the proton data moderately well over the entire energy range measured in this experiment. In sharp contrast to the pion data, the value for T_0(200 MeV) for $s > 14$ GeV^2 is not very different from the value (185 MeV) obtained by fitting the range $5.5 \leq s \leq 20$ GeV^2. Thus we have a confusing picture: The predicted energy dependence is found to agree where it is not supposed to apply, but does not describe the data it is designed to explain.

6. *Summary*

We summarize our comparison with statistical models:

(1) The structures seen in pion-proton data are probably caused by s-channel resonance production.

(2) The structures are not due to isolated resonances unless they have relatively narrow widths. The structures do not appear to have pure J angular distributions.

(3) There are no structures, apart from the $t = -2.8$ GeV$^2/c^2$ dip, which are present in all the data. There is no evidence that there are structures fixed in s, t, u, or $\cos\theta_{c.m.}$ which mimic fluctuations. There is structure visible in all displays of the cross sections.

(4) We believe that the structure we see is qualitatively consistent with the mechanism of Ericson fluctuations—that is, multiple overlapping resonances.

(5) The explicit prediction of Frautschi's model that there should be an exponential increase in the number of states does not describe the data. Hence, the observation of high-mass structures does not lead directly to the density of resonant states.

(6) There is no evidence that scattering at 90° has a predominantly statistical exponential energy dependence.

ACKNOWLEDGMENTS

We are grateful for the support and hard work of the staff of the Zero Gradient Synchrotron. E. Pell, W. Peterson, and M. Sabau assisted with apparatus and analysis for the experiment. This research was supported by the U. S. Department of Energy and the National Science Foundation.

---

*Present address: Department of Physics, The Rockefeller University, New York, New York 10021.
†Present address: Argonne National Laboratory, 9700 S. Cass Avenue, Argonne, Illinois 60439.
‡Present address: Department of Physics, Michigan State University, East Lansing, Michigan 48823.

[1]S. J. Brodsky and G. R. Farrar, Phys. Rev. Lett. 31, 1153 (1973).
[2]V. A. Matveev, R. M. Muradyan, A. N. Tavkhelidze, Lett. Nuovo Cimento 7, 719 (1973).
[3]S. Frautschi, Nuovo Cimento 12A, 133 (1972).
[4]K. A. Jenkins *et al.*, Phys. Rev. Lett. 40, 425 (1978); 40, 429 (1978).
[5]D. Sivers, Ann. Phys. (N.Y.) 90, 71 (1975).
[6]D. P. Owens *et al.*, Phys. Rev. 181, 1794 (1974).
[7]A. W. Hendry, Phys. Rev. D 10, 2300 (1974).
[8]J. F. Gunion, S. J. Brodsky, and R. Blankenbecler, Phys. Rev. D 8, 287 (1973).
[9]P. Fishbane and C. Quigg, Nucl. Phys. B61, 469 (1973).
[10]S. Frautschi, in *New Directions in Hadron Spectroscopy*, proceedings of the Summer Symposium, Argonne, Illinois, 1975, edited by S. L. Kramer and E. L. Berger (ANL, Argonne, 1975), p. 115; lecture at Workshop on Hadronic Matter at Extreme Energy Density, Erice, 1978, Caltech Report No. CALT-68-705 (unpublished).
[11]T. Ericson and T. Mayer-Kuckuk, Annu. Rev. Nucl. Sci. 16, 183 (1966).
[12]J. Ernst, P. von Brentano, and T. Mayer-Kuckuk, Phys. Lett. 19, 41 (1965). We thank J. Ernst for permission to reproduce the figure.
[13]G. Eilam, Y. Gell, B. Margolis, and W. J. Meggs, Phys. Rev. D 8, 2871 (1973).
[14]R. D. Klem *et al.*, Phys. Rev. D 15, 602 (1977).
[15]C. T. Coffin *et al.*, Phys. Rev. 159, 1169 (1967).
[16]D. R. Rust *et al.*, Phys. Rev. Lett. 24, 1361 (1970).
[17]R. C. Kammerud *et al.*, Phys. Rev. D 4, 1309 (1971).
[18]G. Cocconi *et al.*, Phys. Rev. 138, B165 (1965).
[19]H. DeKerrett *et al.*, Phys. Lett. 62B, 363 (1976).
[20]A. Eide *et al.*, Nucl. Phys. B60, 173 (1973).
[21]P. S. Aplin *et al.*, Nucl. Phys. B32, 253 (1971).
[22]B. Schrempp and F. Schrempp, Phys. Lett. 55B, 303 (1975).
[23]C. W. Akerlof *et al.*, Phys. Rev. 159, 1138 (1967).
[24]V. Barger, F. Halzen, and J. Luthe, Phys. Lett. 42B, 428 (1972).
[25]J. Orear, Phys. Lett. 13, 190 (1964). Other forms were suggested in the discussion of Akerlof *et al.*, Ref. 23.
[26]J. V. Allaby *et al.*, Phys. Lett. 25B, 156 (1967).
[27]Data above 3 GeV/c, from Refs. 6, 15, 16, 20, and 21, and from C. W. Akerlof *et al.*, Phys. Rev. Lett. 27, 219 (1971); P. L. Bastian *et al.*, Phys. Rev. D 3, 2047 (1971).
[28]J. V. Allaby *et al.*, Phys. Lett. 23, 389 (1966).
[29]F. H. Schmidt *et al.*, Phys. Lett. 45B, 157 (1973).
[30]W. Michael, in *New Directions in Hadron Spectroscopy* (Ref. 10), p. 130.
[31]R. L. Dixon *et al.*, in *New Directions in Hadron Spectroscopy* (Ref. 10), p. 137.
[32]The slight rise in the pp case is necessary, since the function is positive definite and the errors increase with energy. Apparently, the calculation of errors is not quite suitable, since the function is, at one point, as much as three standard deviations from zero. The pion data, however, are substantially different from zero.